Sustainability of Cutoff Walls for Environmental Containment: A Review

Manikanta Devarangadi,[1] Uma Shankar M.,[2] & Praveen Barmavatu[3]

[1]*Department of Civil Engineering, Ballari Institute of Technology & Management, Ballari, India;* [2]*School of Civil Engineering, Vellore Institute of Technology, Vellore, India;* [3]*Department of Mechanical Engineering, Shri Jagdish Prasad Jhabarmal Tibrewala University, Rajasthan, India*

4.1 INTRODUCTION

Sites polluted or contaminated by various industrial wastes and domestic wastes cause a menace to human health and the environment. Leachates generated through these wastes pollute land and groundwater. Various remedial measures, such as slurry walls or cutoff walls, are used to control leachate migration. One of the conventional methods is using vertical barriers made of cement–bentonite slurry trench cutoff walls, soil–bentonite (SB) slurry trench walls, and plastic concrete slurry walls, which works at a relatively low cost. Usually, high-density polyethylene is also frequently integrated into these barriers.

This chapter reviews the following:

1. The effect of low hydraulic conductivity of the several organic and inorganic effluents on vertical barriers made with bentonite and modified bentonites.

2. Investigation of the materials used and updating of their specification.

3. The effects of the addition of dredged sediments, sawdust, cementitious materials [ground granulated blast furnace slag (GGBS), cement bypass mixtures, pulverized fuel ash (PFA), and fly ash] to slurry walls.

4. The factors governing durability, permeability, and chemical compatibility.

5. Construction techniques adopted for slurry walls and their seismic performance.

6. Various consolidation tests, leaching behavior of radioactive elements, case studies, quality assessments/quality control, and immersion tests with bentonite and other materials.

ISBN: 978–1–56700–525–7

Chapter 6
Suitability of Bauxite Residue as a Landfill Liner Material—An Overview

Narala Gangadhara Reddy, Tayyaba Siddiqua, Manikanta Devarangadi, and Chandra Bogireddy

6.1 Introduction

As development progresses, the need for sustainable materials and better management of solid wastes also increases. Industries, which play a major role in the development of a nation produce tons of waste/byproducts and its disposal is a major concern. The byproducts disposed of pollute land, water and the surrounding environment. To overcome such problems utilization of waste materials according to their properties is a major solution. Aluminium ranks third among the most abundant elements on the Earth and its extraction has highly increased over a period of time. Among the largely produced byproducts, bauxite residue (BR) is a byproduct formed after the production of alumina by Bayer's or sintered process. In Bayer's process bauxite is digested in NaOH at high temperature and high pressure of 250 °C and 52 kg/cm^2 respectively.

It is estimated that BR produced across the globe is more than 120 million tonnes annually. BR is highly alkaline (pH > 10) due to the addition of caustic soda (NaOH) to bauxite ore during the extraction of alumina [1]. The major chemical constituents of BR are Fe_2O_3, SiO_2, Al_2O_3, Na_2O, and CaO. The chemical composition of BR

N. G. Reddy (✉) · T. Siddiqua
Kakatiya Institute of Technology and Science, Warangal 506015, India
e-mail: gn11@iitbbs.ac.in

N. G. Reddy
School of Building and Civil Engineering, Fiji National University, Samabula, Suva 3722, Fiji

M. Devarangadi
Ballari Institute of Technology and Management, Ballari 583104, India

C. Bogireddy
Shantou University, Shantou 515063, Guangdong, China

S. K. Das et al. (eds.), *Geoenvironmental and Geotechnical Issues of Coal Mine Overburden and Mine Tailings*, Springer Transactions in Civil and Environmental Engineering, https://doi.org/10.1007/978-981-99-6294-5_6

4 Spatio-Temporal Agricultural Drought Monitoring Using Remote Sensing Indices

Syed Sadath Ali, Koyel Mukherjee, Papia Kundu, and Piu Saha

Abstract

Drought is an intricate weather phenomenon; it directly affects food security and agricultural productivity. Accurate prediction of agricultural drought helps to take mitigation steps for reducing production losses. In the present study, agricultural drought was assessed by using the Normalized Difference Vegetation Index (NDVI), Vegetation Condition Index (VCI), Temperature Condition Index (TCI), and Vegetation Health Index (VHI) based on Landsat 8 and 9 data from 2013–2022. The LULC maps were also prepared using the supervised classification based on the maximum likelihood algorithm by the semi-automatic classification plugin (SCP) in QGIS from Sentinel-2 images. The remote sensing indices were calculated using a raster calculator in ArcGIS software. The results of VCI indicate that 2014 and 2017 years were highly affected by drought, whereas 2016 was the most vulnerable year according to TCI. In 2017, the entire district was badly affected by VCI and TCI. The VHI results showed that 2015, 2016, and 2018 were the most drought-prone years. The spatial agricultural drought result shows that Chattna, Bankura I, Onda, and Ranibudh were extreme drought-affected blocks. Drought greatly impacts agriculture, so satellite-based drought data would benefit the understanding of the drought of Bankura district risk within the entire geographical area.

Keywords

Agricultural drought · Temperature Condition Index · Vegetation Condition Index · Vegetation Health Index · Bankura

4.1 Introduction

Drought is a recurrent natural hazard that adversely affects the ecosystem, livelihoods, cultivation, and livestock farming (Alam et al. 2023; Ayugi et al. 2022), causing huge economic loss throughout the world (Guo et al. 2021; Zeng et al. 2022). It grows very slowly in the beginning but later it affects a large area with its severity (Liu et al. 2021). Based on physical

S. S. Ali
Civil Engineering Department, Ballari Institute of Technology and Management, Ballari, Karnataka, India

K. Mukherjee
Department of Geography, Rampurhat College, PO. Rampurhat, Dist. Birbhum, Rampurhat, West Bengal 731224, India

P. Kundu · P. Saha (✉)
Department of Geography and Applied Geography, University of North Bengal, PO. North Bengal University, Dist. Darjeeling, Siliguri, West Bengal 734013, India
e-mail: piusaha.nbu@gmail.com

J. Das and S. Halder (eds.), *Advancement of GI-Science and Sustainable Agriculture*, GIScience and Geo-environmental Modelling, https://doi.org/10.1007/978-3-031-36825-7_4

aspects, drought is classified as a meteorological, hydrological, and agricultural drought, among which 'agricultural drought' is characterized by insufficient moisture in the soil for cultivation at a particular time (Basak et al. 2022; Das et al. 2020). The intensity of 'agricultural drought' changes with space and time, and it is more challenging than other kinds of drought because it adversely degrades a particular region's agricultural activity. In India, especially in the western part of West Bengal, agricultural drought has a crucial effect on agricultural production and productivity by disturbing the balance between food supply and demand (Gidey et al. 2018). Between 1900 and 2020, a drought event in India had a significant impact on over 1.4 billion people, resulting in a threatening situation for water resources and food security. This event has revealed that agricultural drought affects more than 68% of India's land area (Nath et al. 2017), largely due to the rising trend of mean temperature, geo-environmental conditions, and climate change.

Under this critical situation, appraisal of agricultural drought could be helpful by using different spatio-temporal data from different sources like vegetation, hydrology, meteorology, etc. The spatial and non-spatial datasets are used for drought risk assessment (Apurv and Cai 2021; Hoque et al. 2021a; Kim et al., 2021). Remote sensing techniques are used in spatial analysis to support all the procedures (Hoque et al. 2021b; Zeng et al. 2022). The most popular remote sensing-based vegetation indices, such as Normalized Difference Vegetation Index (NDVI), Temperature Condition Index (TCI), Vegetation Condition Index (VCI), and Vegetation Health Index (VHI) have been used for the drought monitoring system (Hadri et al. 2021; Kogan 1997). The VHI is the most helpful satellite index to monitor agricultural drought (Wang and Yu 2021; Zhang et al. 2013). The Vegetation Health Index correlates with crop yield, the problem of crop health, and crop growth (Alahacoon et al. 2021; Zhao et al. 2022).

NDVI is one of the most popular vegetation health indices that analyze activities like respiration, transpiration productivity, temperature variability, etc. (Pei et al. 2018). For instance, Nejadrekabi et al. (2022) observed the moisture period using NDVI in the Khuzestan province. Vegetation growth in China from 1982 to 2010 was evaluated using NDVI (Peng & Gitelson 2011). Agricultural drought monitoring for three months was calculated using NDVI in Raya of northern Ethiopia (Gidey et al. 2018). This chapter states that VCI and TCI can be used to delineate the seasonal and inter-annual drought, while Sultana et al. (2021) assessed agricultural drought severity in the northwestern part of Bangladesh from 1990 to 2018 by applying TCI, VCI, and VHI. Zambrano et al. (2016) measured the agricultural drought in the cropland of the Biobio region in Chile from 2000 to 2015 by analyzing the temporal and spatial variation of vegetation conditions with stress due to scarcity of rainfall with VCI.

The novelty of this current endeavor is to identify and monitor agricultural drought in the Bankura district of West Bengal using remote sensing data. Evaluation of drought indices, calculation intensity, severity, and duration of drought are the prime concern of this chapter which helps make a proper plan for mitigation and irrigation practice in drought-vulnerable areas through establishing an integrated relationship among NDVI, LST, VCI, TCI, and VHI methods which provide a guideline for future drought.

4.2 Study Area

Bankura is the fourth largest district of West Bengal, located between 22°30′N to 23°30′N latitudes and 87°00′E to 87°30′E longitudes, having a 6,882 km^2 area. The total population of the Bankura district is 3,992,309 persons, and the population density is 523 persons/km^2 (Census 2011). Bankura is a connecting link between the plain of West Bengal and the Plateau of Chotanagpur. The Purulia district in the west surrounds it, Purba Bardhhaman and Paschim Bardhhaman districts in the north, Jhargram and Paschim Medinipur in the south, and the Hugli district in the southeast. Darakeswar, Damodar,

Kangsabati, Silabati, and Gandhewari rivers drain the district. Geomorphologically, the Bankura district is a part of the Chotanagpur plateau (Fig. 4.1). There are three types of topographical terrain; i.e., the western part is a hilly region characterized by large granite rock covered by natural vegetation, the central part is undulating and characterized by red lateritic, and the eastern part is an alluvial plain covered by loamy soil. Following the topographic terrain, land use pattern of this area is also changing from east to west, and the low-lying alluvial plain of the northeast is mainly used for paddy cultivation. The western surface is undulating and gradually rising, so most of the land is covered by jungle. Bankura is part of Rarh, and agriculture is the main economic activity of this concerned study area, but it is challenged by low water availability, climatic change, and reduced annual rainfall. In the last few years, drought incidents and intensity have been increasing (Bhunia et al. 2020; Das et al. 2013). The changing patterns of annual rainfall and 80% rainfall received during four months result in poor moisture in subsoil, which becomes a threat to crops and seriously affects the yields in the study area. The farmers of this area face some socio-economic problems; they lose their job and are forced to migrate. In recent times, Bankura district has become a geographer's attraction due to excessive drought proneness and its relation with the economy, poverty, mitigation, and migration-related scenarios (Raha and Gayen 2020).

4.3 Database and Methods

4.3.1 Database

In the present study, remote sensing data has been utilized from authenticated sources, and therefore, various drought indices are displayed by ESRI ArcGIS (Version 10.4.1) software.

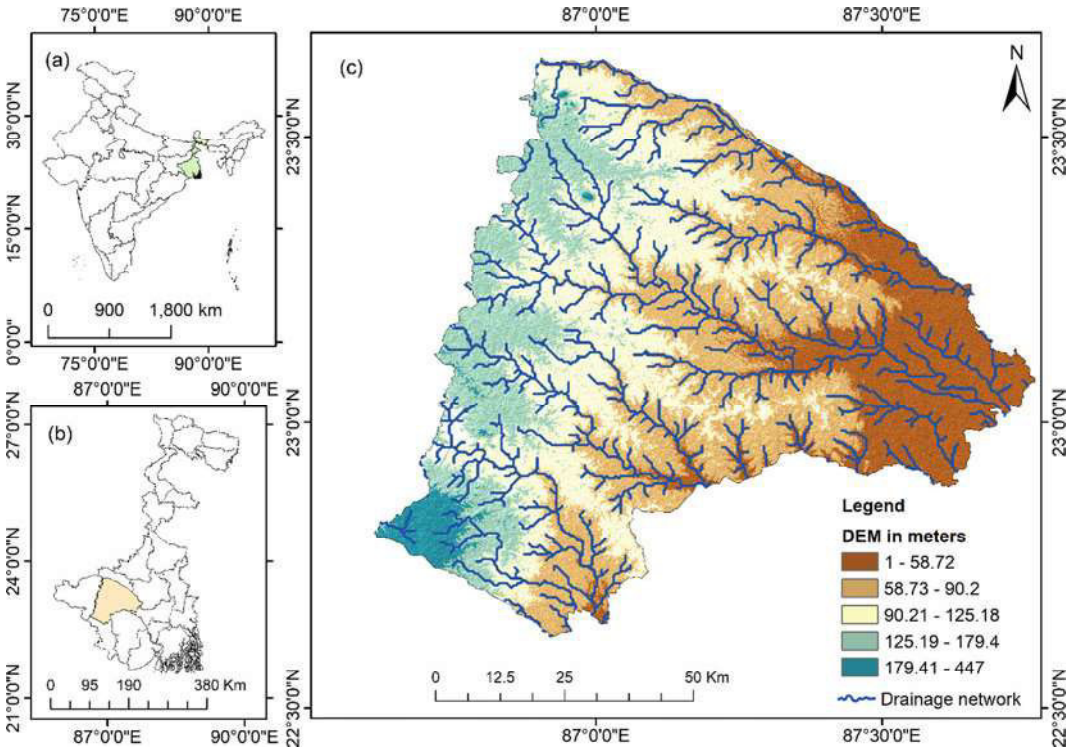

Fig. 4.1 Location map of the study area; **a** India, **b** West Bengal, and **c** Bankura

Landsat 8, Landsat 9 OLI/TIRS collection 2, level 1 images (Path: 139, Row: 044) were used for NDVI, VCI, LST, TCI, and VHI indices, obtained from the USGS Earth explorer website (https://earthexplorer.usgs.gov). The land use/land cover maps were prepared from Sentinel 2 images downloaded from https://scihub.copernicus.eu using a training sample and the maximum likelihood method in a QGIS semi-automatic classification plugin (SCP).

4.3.2 Methods

4.3.2.1 Normalized Difference Vegetation Index (NDVI)

The Normalized Difference Vegetation Index (NDVI) is a widely used remote sensing index to assess vegetation density and health. NDVI measures the difference between the reflectance of near-infrared (NIR) and visible red (VIS) light, which is correlated with the amount of vegetation present in an area (Glenn and Tabb 2019). NDVI can be used to monitor vegetation growth and health over time, detect changes in land use, and assess the impact of environmental factors on vegetation. It is commonly used in agriculture to assess crop health and yield potential and in forestry to monitor forest health and detect changes due to natural or man-made disturbances (Nejadrekabi et al. 2022).

Every geographical space has some carrying capacity (Kogan 1995). For estimating carrying capacity, we used NDVI. The maximum NDVI represents the highest carrying capacity, and the minimum NDVI represents a geographical area's lowest carrying capacity (ecosystem potential). NDVI also helps monitor crop yields, crop growth conditions, the health status of vegetation, and drought (Kogan 1995; Liu et al. 2021). The main concept of NDVI is that the healthy green leaves' internal mesophyll reflects near-infrared (NIR), whereas a large proportion of visible red radiation (VIS) is absorbed by leaf chlorophyll and other pigments. But in the case of water stress and unhealthy vegetation, the internal structure reacts reverse (Moisa et al. 2022).

$$\mathrm{NDVI} = (\mathrm{NIR} - \mathrm{RED})/(\mathrm{NIR} + \mathrm{RED}).$$

NDVI is calculated between the difference between near-infrared (NIR) and visible red bands of the electromagnetic spectrum. The index ranges from -1 to $+1$, with values closer to $+1$ indicating higher levels of healthy vegetation and values closer to -1 indicating little to no vegetation. In tropical and temperate rain forests, the value of NDVI ranges between 0.6 to 0.8, and in barren rock, sand, or snow area, it is below 0.1 (Dutta et al. 2015). There are some noise problems in NDVI. Sensor degradation, satellite change, change of satellite orbital drift, cloud, and aerosol are the sources of error (Kogan 1995). These weather-related NDVI problems must be overcome, and thus why Kogan (1995) suggested the Vegetation Condition Index (VCI).

4.3.2.2 Vegetation Condition Index (VCI)

The Vegetation Condition Index (VCI) is derived from remote sensing data developed for monitoring drought characteristics such as duration, intensity, spatial extent, and severity assessment. In this present chapter, VCI was used to monitor the Bankura district's agricultural drought by this equation.

$$\mathrm{VCI} = (\mathrm{NDVI} - \mathrm{NDVI_{MIN}})/(\mathrm{NDVI_{MAX}} - \mathrm{NDVI_{MIN}}) * 100,$$

whereas NDVI, $\mathrm{NDVI_{MIN}}$, $\mathrm{NDVI_{MAX}}$ are multiyear maximum and minimum values of NDVI. According to Kogan (1995), the VCI value is measured in percentile ranges from 0 to 100. The classification of VCI is shown in Table 4.2. When the value is near 100, it defines favorable condition for crop, but the value 0 or near 0 indicate bad crop condition.

4.3.2.3 Land Surface Temperature (LST)

Land surface temperature (LST) was calculated from the thermal infrared sensor (TIRS) band of Landsat 8 and 9 images from 2013 to 2022. The LST value ranges between 7500 and 65,535

Table 4.2 Detailing the threshold value of VCI, TCI, and VHI

Range	Dryness level
0–10	Extreme drought
10–20	Severe drought
20–30	Moderate drought
30–40	Light drought
> 40	No drought

(Wan 2006), and it was reclosed by 0.02 to convert into Kelvin unit. It represents the radiative skin temperature of the land surface from solar radiation. In this chapter, LST was converted and rescaled into degree Celsius.

LST is gained by these equations.

$$\mathrm{LST} = (\mathrm{BT}/(1 + (\lambda * \mathrm{BT}/\rho) * Ln(\varepsilon))) - 273.15,$$

where LST = Land surface temperature in Celsius (°C).

BT = Sensor brightness temperature in (°C).

λ = Wavelength of thermal band of various Landsat satellite.

ε = Emissivity of the land surface.

$\rho = (h \times (c/\sigma))$, which is equal to 1.438×10^{-2} mK.

In which, σ is the Boltzmann constant (1.380649×10^{-23} J/K), h is Plank's constant ($6.62607015 \times 10^{-34}$ J.s), and c is the velocity of light (3×108 m/s).

4.3.2.4 Temperature Condition Index (TCI)

The Temperature Condition Index (TCI) is a remote sensing index that provides an estimation of the vegetation's response to temperature stress. It measures the deviation of land surface temperature (LST) from its long-term average value and is based on the assumption that vegetation is sensitive to temperature anomalies (Swain et al. 2011). TCI is obtained by this equation.

$$\mathrm{TCI} = (\mathrm{LST}_{\mathrm{MAX}} - \mathrm{LST})/(\mathrm{LST} - \mathrm{LST}_{\mathrm{MIN}}) * 100,$$

where LST is the value of the land surface temperature of a particular month, and $\mathrm{LST}_{\mathrm{MAX}}$ and $\mathrm{LST}_{\mathrm{MIN}}$ is the temperature of the studying period. LST provides information about the vegetation of the area. If LST increases, then the evapotranspiration of plants also increases, and surface soil moisture also reduces, which is a good indicator of vegetation stress (Kogan 1995; Seiler et al. 1998). The TCI value ranges between 0 and 100. A high value of TCI indicates a favorable condition for a crop, whereas a low value of TCI indicates an adverse effect on vegetation or drought conditions.

4.3.2.5 Vegetation Health Index (VHI)

Vegetation Health Index (VHI) is the outcome of the combination of products extracted from vegetation signals, namely NDVI. It combines VCI and TCI (Orlovsky et al. 2011).

$$\mathrm{VHI} = a \times \mathrm{VCI} + (1 - a) \times \mathrm{TCI},$$

where VHI represents the vegetation health index, $a = 0.5$ similar contribution of VCI and TCI, VCI is the vegetation condition index, and TCI is the temperature condition index.

4.4 Results and Discussion

4.4.1 Land Use and Land Cover (LULC) Changes

The supervised classification with maximum algorithm method was employed to prepare land use and land cover (LULC) maps using Sentinel 2 images in the QGIS SCP plugin (Patil et al.

2012). The maps were categorized into six major types, including water body, vegetation cover, agricultural land, build-up area, bare ground, and range land, for the years 2018, 2019, 2020, 2021, and 2022, as depicted in Fig. 4.2 and Table 4.3.

The areal coverage or extension and areal changes from 2018 to 2022 have been detected through ArcGIS software, and it has been summarized in (Table 4.3). The LULC classification in 2018 (Fig. 4.2a) depicts that the majority of the area in Bankura district was under agricultural land (64.28%), the rest 18.24, 8.04, 2.72, and 1.10% areas are under vegetation cover, range land, build-up area, water body, and bare ground, respectively. Similarly, in 2019, the greatest share of land was occupied by also agricultural land (64.21%), and the trend of occupancy remained the same, i.e., land under vegetation cover (18.53%), range land (8.04%), build-up area (5.62%), water body (2.72%), and bare ground (1.02%) individually. Considering the trend of extension and rate (in %) of changes of each LULC from 2018 to 2022, vegetation cover and build-up areas increased by 3.90%, partly in Barjora, Sonamukhi, Taldangra, Onda, Vishnupur, Ranibundh blocks of this district and 27.21% in some parts of blocks like Indus, Kotalpur, Patrasayar, Jaypur, Vishnupur, Bankura I sequentially, whereas percentage of land occupancy in bare ground, range of land, and water body decreased by − 32.555 and − 19.75% partly in Mejhia, Gangajalghati, Chhatna, and − 9.84% at Ranibundh and Hirbundh blocks in the same period. Taking into consideration the overall study period, vegetation cover and build-up areas have shown their areal increment. In contrast, water bodies, agricultural land, bare ground, and range land have harshly diminished in the same period due to many unscientific activities like unplanned settlement, massive grazing, and resultant soil degradation. Unlike build-up areas and vegetation cover, the land share of water bodies, agricultural land, bare ground, and range land has been increased. It is also a remarkable point that build-up areas has increased in a far larger percentage than vegetation cover, proving that most of the bare ground, range land, water body, and agricultural land are

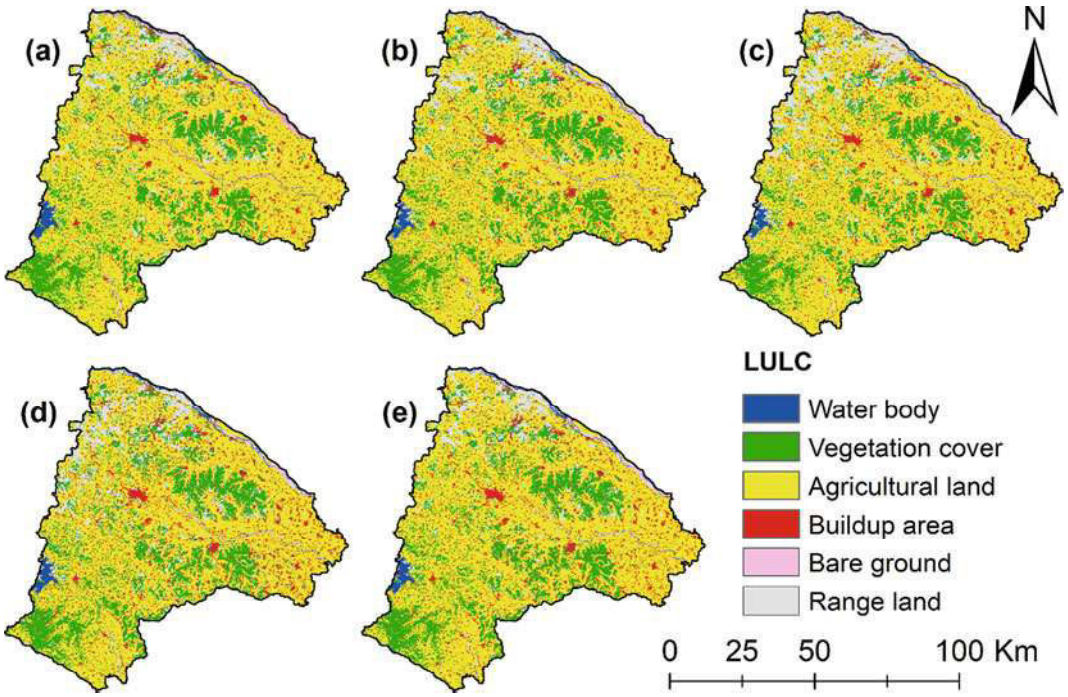

Fig. 4.2 Land use and land cover (LULC); **a** 2018, **b** 2019, **c** 2020, **d** 2021, and **e** 2022

Table 4.3 Land use and land cover (LULC) extent and change detection between 2018 and 2022

Sl No	Land use	2018	2019	2020	2021	2022	% of change
1	Water body	2.72	2.36	1.98	2.72	2.45	− 9.84
2	Vegetation cover	18.24	18.53	17.22	19.64	18.95	3.90
3	Agricultural land	64.28	64.21	63.04	59.82	64.25	− 0.04
4	Build-up area	5.62	6.71	6.86	7.88	7.15	27.21
5	Bare ground	1.10	1.02	0.91	0.79	0.74	− 32.55
6	Range land	8.04	7.17	10.00	9.16	6.46	− 19.75

converted to build-up areas but rationally maintains the vegetation-covered area by not unscientifically destruction of trees and continue the afforestation program. Considering the overall study period, the pattern of land use changes demonstrates that land occupancy of water body was increased from 2018 to 2019, then decreased in 2020, and again increased in 2021, but a little bit decreased in 2022. Land share of vegetation cover increased from 2018 to 2019, then decreased and continue to increase in 2021 which decreased in 2022. Agricultural land area decreased from 2018 to 2019, 2020, and 2021 but increased in 2022. In the build-up area, the land occupancy increased from 2018 to 2021 but decreased in 2022. The area under bare and range land has gradually reduced from 2018 to 2019, and so on. Generally, the result has revealed that a series of LULC changes in the study area for five years (2018–2022) shows the fact that build-up areas are most dominating in this area, indicating the continuous increment of human residence by maintaining green areas, whereas other land use pattern shows declining nature.

4.4.2 Normalized Difference Vegetation Index (NDVI)

It measures the photosynthetic activities of vegetation by indicating favorable vegetation conditions with high value and unfavorable vegetation conditions associated with low NDVI value (Cunha et al 2015). Five principal changes in vegetation (significant vegetation loss, vegetation loss, no vegetation change, vegetation gain, significant vegetation gain) have been detected from 2013 to 2022. Significant vegetation loss, which accounts for 5.42% of the total area, has been partially detected from 2013 to 2022 in Barjora, Sonamukhi, Patrasayar, Indus, Vishnupur, Sarenga, Raipur, Khatra blocks. The most worrying fact is that 48.17% vegetation loss in Mejhia, Gangajalpati, Barjora, Sonamukhi, Patrasayar, and Indus in the northeastern part of Bankura District, Bankura I and II, Onda in the middle part and Ranibundh, Raipur, Serenga in the southern part of this district is registered due to different unscientific construction work. In the meantime, about 12.64% area of the southwestern part is marked as an unchanged vegetation-covered area. Interestingly, 33.45% area has gained vegetation, whereas only 0.32% area has gained significant vegetation (Fig. 4.3 and Table 4.4).

This chapter has monitored the agricultural drought of the Bankura district from the year 2013 to 2022 by using the VCI technique. Figure 4.4 and Table 4.5 depict area-wise extreme, severe, moderate, and no drought conditions for ten years. Meanwhile, 79.65% (most of the area) area of this district was under extreme drought conditions in 2017 due to erratic rainfall and the low water-holding capacity of the soil. Community development blocks like Indus, Kotulpur, Jaypur, and Serenga accounted for extreme drought in 2014, 2015, and 2018. The maximum area (14.37%) under severe drought was in 2014,

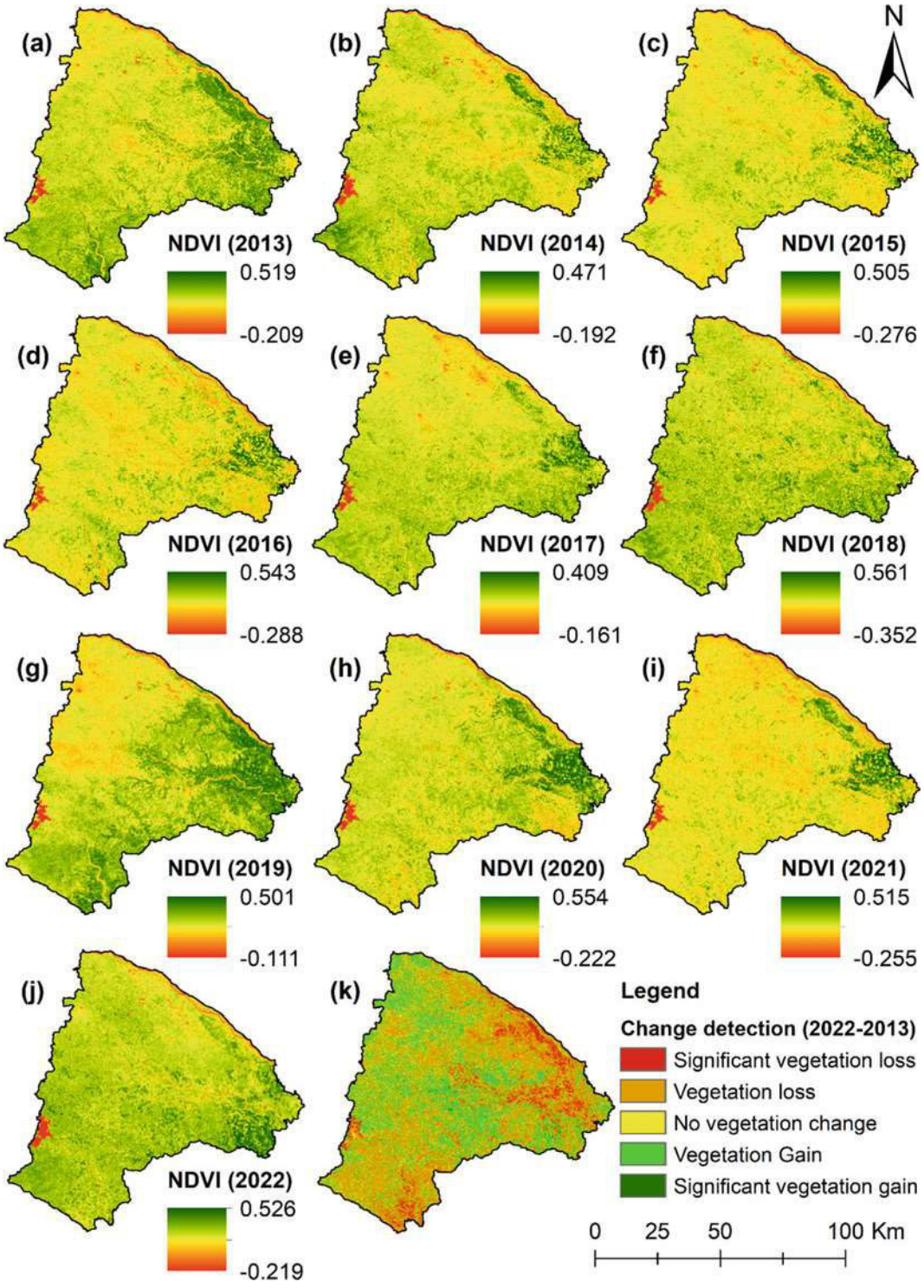

Fig. 4.3 Normalized Difference Vegetation Index (NDVI); **a** 2013, **b** 2014, **c** 2015, **d**, 2016, **e** 2017, **f** 2018, **g** 2019, **h** 2020, **i** 2021, **j** 2022, and **k** Change detection

Table 4.4 Vegetation change detection between 2013 and 2022

Sl. No	Level	Area in sq km	Area in %
1	Significant vegetation loss	373.75	5.42
2	Vegetation loss	3319.68	48.17
3	No vegetation change	871.00	12.64
4	Vegetation gain	2305.29	33.45
5	Significant vegetation gain	21.79	0.32

whereas 18.58 and 18.24% areas of the total were affected by moderate and light drought, respectively, in 2014, and a large area (95.50%) was registered as no drought-affected area in 2019 due to a sufficient amount of rainfall.

Figure 4.5 and Table 4.6 have assessed descriptive statistics (minimum, maximum, and mean temperature in °C) and standard deviation by considering ten years from 2013 to 2022 with the association of the LST technique. It illustrates that the lowest minimum temperature was recorded as 4.95 °C in 2014 and 25.40 °C in 2019. On the other hand, the maximum land surface temperature was 53.83 °C in 2018 and 35.43 °C in 2014. Low land surface temperature indicates dense vegetation cover and a low infiltration rate with minimum soil moisture, whereas high land surface temperature reveals no or thin vegetation cover with a high infiltration rate and maximum soil moisture. The highest mean temperature was recorded as 34.13 in 2016, and the lowest was 22.46 in 2014, respectively. The highest SD was recorded as 3.65 in 2014 and 1.79 in 2019, respectively. Their mean value shows the average fluctuation of temperature throughout ten years by calculating the average value for each year separately, whereas standard deviation shows the consistency among the distribution of mean temperature delicately.

In this chapter, TCI was calculated from Landsat 8, 9, and TIRS band 10 to categorize agricultural drought in five categories, i.e., extreme, severe, moderate, light, and no drought for the above said ten years. In 2016, 7.92% area of Bankura district was under extreme drought, the intensity of which reduced through rest years and remarkably in 2017 to 0.01%. While community development blocks like Chattna, Bankura I, and II, Taldangra, Simlapal, Khatra, Ranibundh, etc., were affected. On the other hand, 32.33% of the area in 2015 was identified as a severely drought-affected area, the areal extent of which was lowered to 0.01% in 2014. 29.65% area, including Chattna, Indpur, Bankura I, and Onda blocks, were under moderate drought-affected areas. 25.98 and 0.05% areas were recognized as the highest and lowest light drought-prone areas, respectively. 99.89% area of the Bankura district was not faced with drought in 2014, but it was reduced to 2.39% in 2017 (Fig. 4.6 and Table 4.7).

VHI, a combined indicator of vegetation health, depicts spatio-temporal drought variation in the Bankura district from 2013 to 2022 and is classified into five types. Figure 4.7 and Table 4.8 demonstrate that 18.96% area, including Chattna, Bankura I, Onda, and Ranibudh blocks, was extremely drought in 2016. This condition improved in 2014 by showing a 0.02% area under this adverse condition. The severe drought area was 27.92% in 2018 and gradually reduced to 0.04% in 2014. This fact clearly shows the improvement of drought conditions by applying canal irrigation, drilling irrigation, submersible

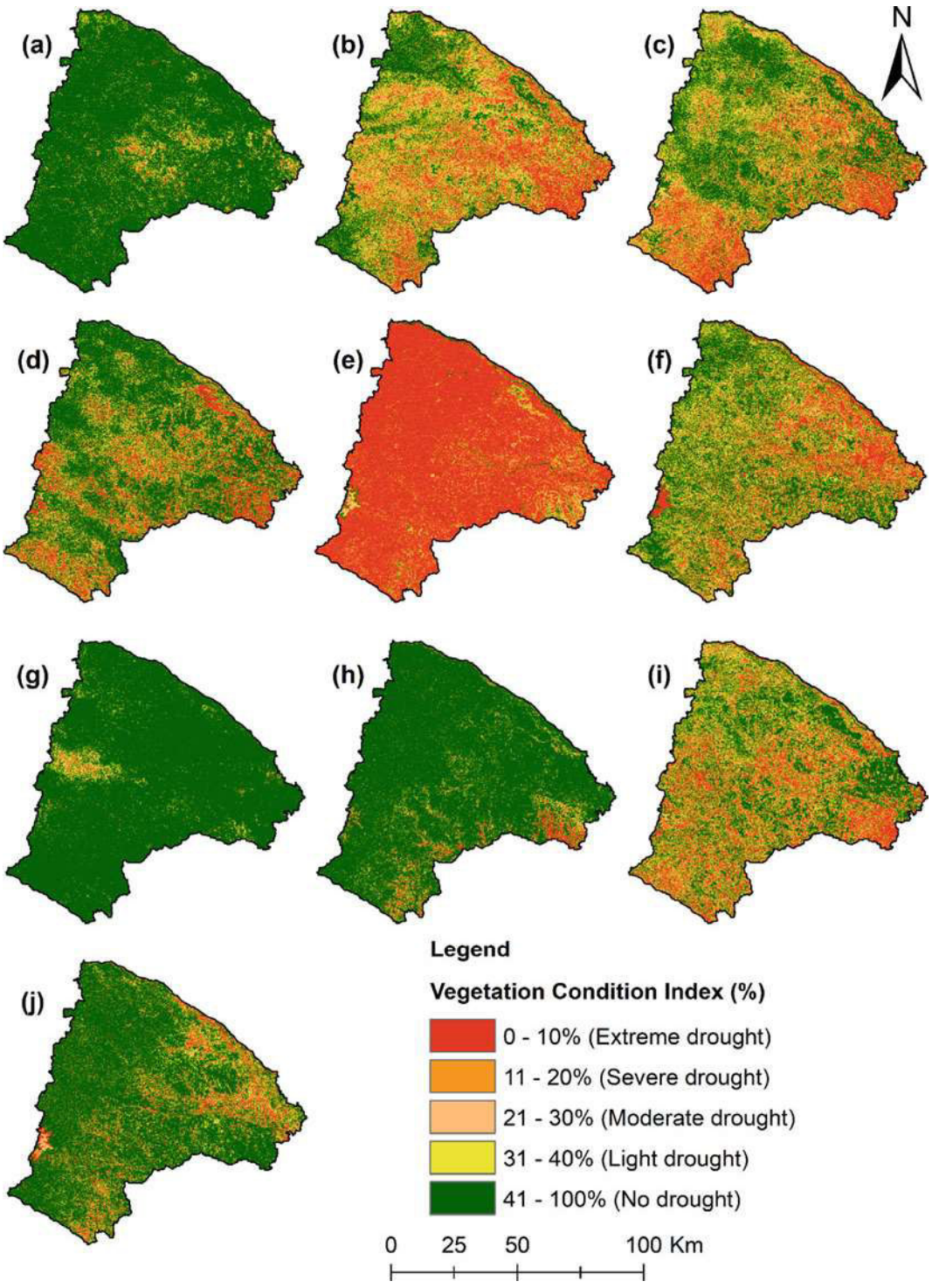

Fig. 4.4 Drought monitoring using Vegetation Condition Index (VCI); **a** 2013, **b** 2014, **c** 2015, **d** 2016, **e** 2017, **f** 2018, **g** 2019, **h** 2020, **i** 2021, and **j** 2022

Table 4.5 Spatio-temporal drought variation using Vegetation Condition Index (VCI)

Year	Extreme drought		Severe drought		Moderate drought		Light drought		No drought	
	Area		Area		Area		Area		Area	
	Sq. km	(%)	Sq. km	(%)	Sq. km	(%)	Sq. km	(%)	Sq. km	(%)
2013	55.51	0.81	90.77	1.32	198.65	2.88	356.79	5.18	6189.79	89.82
2014	1249.24	18.13	990.33	14.37	1280.26	18.58	1257.33	18.24	2114.34	30.68
2015	1075.03	15.60	920.88	13.36	1058.05	15.35	1128.15	16.37	2709.39	39.31
2016	833.95	12.10	631.40	9.16	712.77	10.34	777.86	11.29	3935.53	57.11
2017	5489.40	79.65	628.74	9.12	380.27	5.52	201.14	2.92	191.96	2.79
2018	1028.42	14.92	748.81	10.87	1070.95	15.54	1207.80	17.53	2835.52	41.15
2019	16.42	0.24	36.16	0.52	88.92	1.29	168.66	2.45	6581.36	95.50
2020	146.08	2.12	173.31	2.51	203.32	2.95	246.33	3.57	6122.48	88.84
2021	1086.36	15.76	980.26	14.22	1097.40	15.92	1034.36	15.01	2693.13	39.08
2022	427.40	6.20	344.26	5.00	466.24	6.77	611.26	8.87	5042.35	73.17

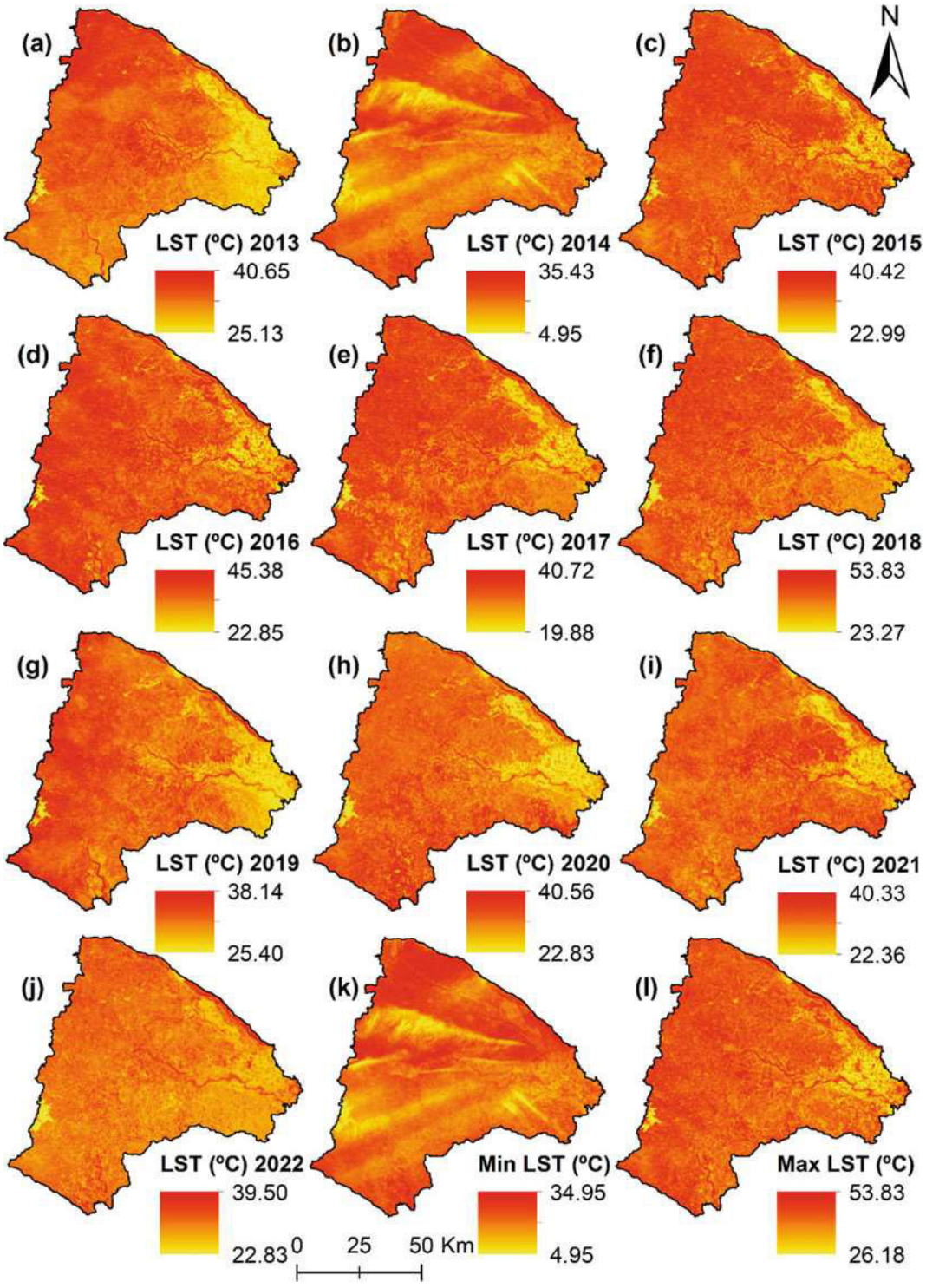

Fig. 4.5 Land surface temperature (LST); **a** 2013, **b** 2014, **c** 2015, **d** 2016, **e** 2017, **f** 2018, **g** 2019, **h** 2020, **i** 2021, **j** 2022, **k** minimum temperature, and **j** maximum temperature

Table 4.6 Descriptive statistics of land surface temperature from 2013 to 2022

Year	Minimum	Maximum	Mean	SD
2013	25.13	40.65	31.56	2.26
2014	4.95	35.43	22.46	3.65
2015	22.99	40.42	32.34	2.37
2016	22.85	45.38	34.13	2.78
2017	19.88	40.72	28.44	2.08
2018	23.27	53.83	33.36	2.88
2019	25.40	38.14	31.44	1.79
2020	22.83	40.56	29.84	2.22
2021	22.36	40.33	31.34	2.22
2022	22.84	39.50	29.19	1.83

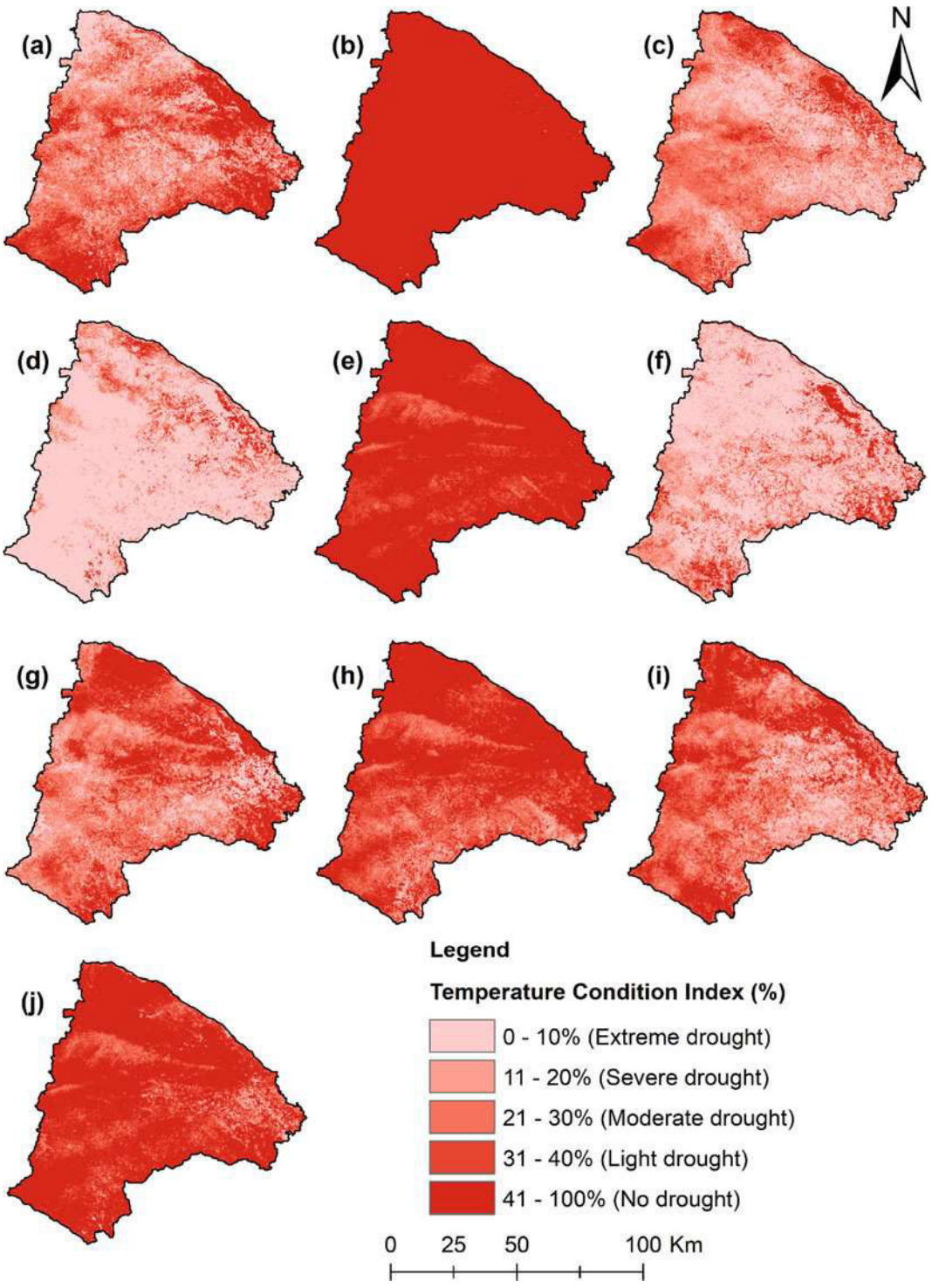

Fig. 4.6 Drought monitoring using Temperature Condition Index (TCI); **a** 2013, **b** 2014, **c** 2015, **d** 2016, **e** 2017, **f** 2018, **g** 2019, **h** 2020, **i** 2021, and **j** 2022

Table 4.7 Spatio-temporal drought variation using temperature condition index (TCI)

Year	Extreme drought		Severe drought		Moderate drought		Light drought		No drought	
	Area		Area		Area		Area		Area	
	Sq. km	(%)	Sq. km	(%)	Sq. km	(%)	Sq. km	(%)	Sq. km	(%)
2013	1070.19	15.53	1629.41	23.64	1749.54	25.39	1137.66	16.51	1304.71	18.93
2014	1.06	0.02	0.91	0.01	1.83	0.03	3.48	0.05	6884.23	99.89
2015	1363.97	19.79	2228.30	32.33	2043.04	29.65	783.74	11.37	472.47	6.86
2016	5232.01	75.92	881.13	12.79	428.21	6.21	185.25	2.69	164.90	2.39
2017	0.86	0.01	4.25	0.06	201.21	2.92	1208.40	17.53	5476.80	79.47
2018	4031.84	58.50	1462.82	21.23	699.42	10.15	317.08	4.60	380.35	5.52
2019	634.80	9.21	1515.30	21.99	1932.91	28.05	1315.07	19.08	1493.43	21.67
2020	97.43	1.41	359.93	5.22	1352.10	19.62	1790.62	25.98	3291.43	47.76
2021	709.47	10.29	1382.04	20.05	1906.45	27.66	1417.24	20.57	1476.30	21.42
2022	64.33	0.93	175.87	2.55	619.79	8.99	1502.11	21.80	4529.42	65.72

irrigation, etc. While, 39.73% area in 2017, including partly Indpur, Onda, Vishnupur, Taldangra, Khatra, Simlapal, the northern part of Ranibundh, Raipur blocks were recognized as the highest percentage of moderate drought-affected area and reduced at 0.16% in 2014. 24.84% area and was accounted for light drought-affected area in 2017. Most areas in this district faced no drought in 2014, which (positively) increased substantial water sources for agriculture.

4.5 Conclusion

In conclusion, the study presents a comprehensive analysis of spatio-temporal agricultural drought monitoring using remote sensing indices in Bankura district of West Bengal. The results show that severe drought conditions have affected various parts of the study area, leading to the abandonment of agricultural lands due to water and soil moisture scarcity. The study identifies specific areas that require urgent attention, including Chattna, Bankura I, Onda, Ranibudh, Indus, Kotulpur, Jaypur, and Serenga blocks, where water shortage is a significant concern for sustainable agricultural practices. The findings suggest that strengthening water resource infrastructure, adopting agricultural water-saving technologies, and promoting seasonal rainwater harvesting could mitigate the impacts of drought in the region. Moreover, the study recommends the implementation of sustainable drought policies, including alteration of sowing and planting times, preservation agriculture, and zero tillage, modification of agricultural practices, to improve resilience toward the effects of drought. The study's results could inform policymakers, farmers, and other stakeholders in addressing local and regional drought issues, and prospective researchers could use them to advance knowledge in the field. Overall, the study provides valuable insights into the spatio-temporal dynamics of agricultural droughts and underscores the need for a comprehensive approach toward managing drought risks.

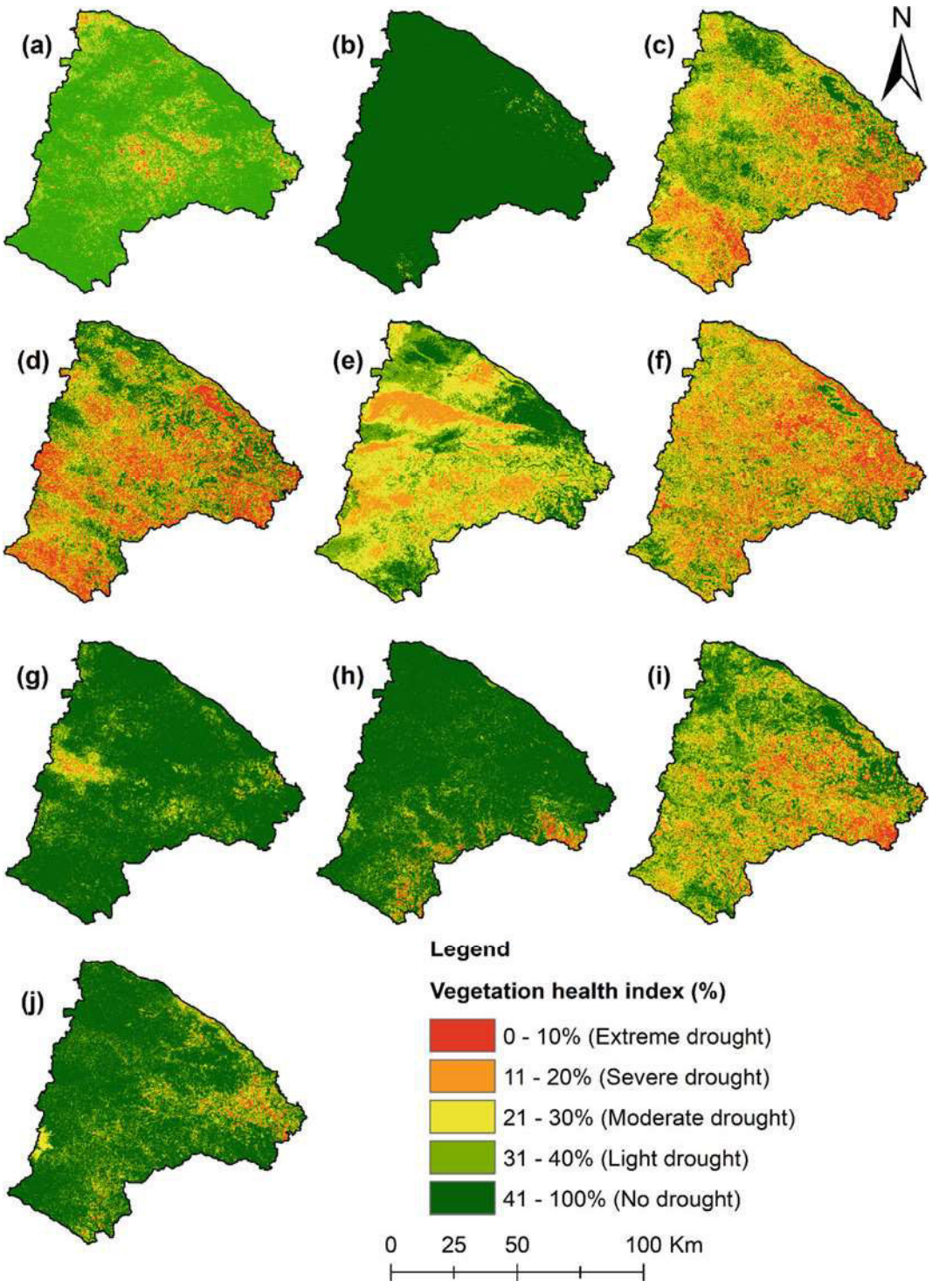

Fig. 4.7 Drought monitoring using Vegetation Health Index (VHI) **a** 2013, **b** 2014, **c** 2015, **d** 2016, **e** 2017, **f** 2018, **g** 2019, **h** 2020, **i** 2021 and **j** 2022

Table 4.8 Spatio-temporal drought variation using Vegetation Health Index (VHI)

Year	Extreme drought		Severe drought		Moderate drought		Light drought		No drought	
	Area		Area		Area		Area		Area	
	Sq. km	(%)	Sq. km	(%)	Sq. km	(%)	Sq. km	(%)	Sq. km	(%)
2013	51.87	0.75	201.21	2.92	556.18	8.07	1104.93	16.03	4977.32	72.22
2014	1.62	0.02	2.96	0.04	10.77	0.16	33.51	0.49	6842.65	99.29
2015	690.57	10.02	1477.71	21.44	1916.88	27.82	1570.98	22.80	1235.37	17.93
2016	1306.43	18.96	1382.12	20.06	1430.71	20.76	1186.07	17.21	1586.17	23.02
2017	3.73	0.05	1167.35	16.94	2737.72	39.73	1711.64	24.84	1271.07	18.44
2018	1051.92	15.26	1923.97	27.92	1922.39	27.90	1078.19	15.65	915.04	13.28
2019	13.90	0.20	72.76	1.06	256.25	3.72	674.78	9.79	5873.82	85.23
2020	68.91	1.00	153.92	2.23	252.58	3.67	454.08	6.59	5962.02	86.51
2021	447.32	6.49	1153.87	16.74	1681.43	24.40	1605.22	23.29	2003.67	29.07
2022	59.99	0.87	202.81	2.94	527.86	7.66	855.45	12.41	5245.41	76.11

References

Alahacoon N, Edirisinghe M, Ranagalage M (2021) Satellite-based meteorological and agricultural drought monitoring for agricultural sustainability in Sri Lanka. Sustainability 13(6):3427. https://doi.org/10.3390/su13063427

Alam J, Saha P, Mitra R, Das J (2023) Investigation of spatio-temporal variability of meteorological drought in the Luni River Basin, Rajasthan, India. Arab J Geosci 16(3):201. https://doi.org/10.1007/s12517-023-11290-8

Apurv T, Cai X (2021) Regional drought risk in the contiguous United States. Geophys Res Lett 48(5): e2020GL092200-1–e2020GL092200-12. https://doi.org/10.1029/2020GL092200

Ayugi B, Eresanya EO, Onyango AO, Ogou FK, Okoro EC, Okoye CO, Ongoma V et al (2022) Review of meteorological drought in Africa: historical trends, impacts, mitigation measures, and prospects. Pure Appl Geophys 179(4):1365–1386

Basak A, Rahman ATMS, Das J, Hosonod T, Kisi O (2022) Drought forecasting using the Prophet Model in semi-arid climate region of western India. Hydrol Sci J 67(9):1397–1417. https://doi.org/10.1080/02626667.2022.2082876

Bhunia P, Das P, Maiti R (2020) Meteorological drought study through SPI in three drought prone districts of West Bengal, India. Earth Syst Environ 4(1):43–55. https://doi.org/10.1007/s41748-019-00137-6

Census of India (2011) District census handbook, Bankura, Government of India

Cunha APM, Alvalá RC, Nobre CA, Carvalho MA (2015) Monitoring vegetative drought dynamics in the Brazilian semiarid region. Agric for Meteorol 214–215:494–505

Das S, Choudhury MR, Nanda S (2013) Geospatial assessment of agricultural drought (a case study of Bankura District, West Bengal). Int J Agric Sci Res (IJASR) 3(2):1–27

Das J, Gayen A, Saha P, Bhattacharya SK (2020) Meteorological drought analysis using Standardized Precipitation Index over Luni River Basin in Rajasthan, India. SN Appl Sci 2(9):1–17. https://doi.org/10.1007/s42452-020-03321-w

Dutta D, Kundu A, Patel NR, Saha SK, Siddiqui AR (2015) Assessment of agricultural drought in Rajasthan (India) using remote sensing derived Vegetation Condition Index (VCI) and Standardized Precipitation Index (SPI). Egypt J Remote Sens Space Sci 18(1):53–63. https://doi.org/10.1016/j.ejrs.2015.03.006

Gidey E, Dikinya O, Sebego R, Segosebe E, Zenebe A (2018) Analysis of the long-term agricultural drought onset, cessation, duration, frequency, severity and spatial extent using Vegetation Health Index (VHI) in Raya and its environs, Northern Ethiopia. Environ Syst Res 7(1):1–18

Glenn DM, Tabb A (2019) Evaluation of five methods to measure normalized difference vegetation index (NDVI) in apple and citrus. Int J Fruit Sci 19(2):191–210

Guo H, Wang R, Garfin GM, Zhang A, Lin D (2021) Rice drought risk assessment under climate change: based on physical vulnerability a quantitative assessment method. Sci Total Environ 751:141481. https://doi.org/10.1016/j.scitotenv.2020.141481

Hadri A, Saidi MEM, Boudhar A (2021) Multiscale drought monitoring and comparison using remote sensing in a Mediterranean arid region: a case study from west-central Morocco. Arab J Geosci 14(2):1–18. https://doi.org/10.1007/s12517-021-06493-w

Hoque M, Pradhan B, Ahmed N, Alamri A (2021a) Drought vulnerability assessment using geospatial techniques in Southern Queensland, Australia. Sensors 21(20):6896. https://doi.org/10.3390/s21206896

Hoque MAA, Pradhan B, Ahmed N, Sohel MSI (2021b) Agricultural drought risk assessment of Northern New South Wales, Australia using geospatial techniques. Sci Total Environ 756:143600. https://doi.org/10.1016/j.scitotenv.2020.143600

Kim JE, Yu J, Ryu JH, Lee JH, Kim TW (2021) Assessment of regional drought vulnerability and risk using principal component analysis and a Gaussian mixture model. Nat Hazards 109(1):707–724. https://doi.org/10.1007/s11069-021-04854-y

Kogan FN (1995) Application of vegetation index and brightness temperature for drought detection. Adv Space Res 15(11):91–100. https://doi.org/10.1016/0273-1177(95)00079-T

Kogan FN (1997) Global drought watch from space. Bull Am Meteor Soc 78(4):621–636

Liu Q, Zhang J, Zhang H, Yao F, Bai Y, Zhang S, Liu Q (2021) Evaluating the performance of eight drought indices for capturing soil moisture dynamics in various vegetation regions over China. Sci Total Environ 789:147803. https://doi.org/10.1016/j.scitotenv.2021.147803

Moisa MB, Merga BB, Gemeda DO (2022) Multiple indices-based assessment of agricultural drought: a case study in Gilgel Gibe Sub-basin, Southern Ethiopia. Theor Appl Climatol 148(1):455–464. https://doi.org/10.1007/s00704-022-03962-4

Nath R, Nath D, Li Q, Chen W, Cui X (2017) Impact of drought on agriculture in the Indo-Gangetic Plain, India. Adv Atmos Sci 34(3):335–346

Nejadrekabi M, Eslamian S, Zareian MJ (2022) Spatial statistics techniques for SPEI and NDVI drought indices: a case study of Khuzestan Province. Int J Environ Sci Technol 19:6573–6594

Orlovsky L, Kogan F, Eshed E, Dugarjav C (2011) Monitoring droughts and pastures productivity in Mongolia using NOAA-AVHRR data. In: Use of satellite and in-situ data to improve sustainability. Springer, Dordrecht, pp 69–79

Patil MB, Desai CG, Umrikar BN (2012) Image classification tool for land use/land cover analysis: a comparative study of maximum likelihood and minimum distance method. Int J Geol Earth Environ Sci 2(3):189–196

Pei F, Wu C, Liu X, Li X, Yang K, Zhou Y, Wang K, Xu L, Xia G (2018) Monitoring the vegetation activity in China using vegetation health indices. Agric for Meteorol 248:215–227

Peng Y, Gitelson AA (2011) Application of chlorophyll-related vegetation indices for remote estimation of maize productivity. Agric For Meteorol 151(9):1267–1276. https://doi.org/10.1016/j.agrformet.2011.05.005

Raha S, Gayen SK (2020) Simulation of meteorological drought using exponential smoothing models: a study on Bankura District, West Bengal, India. SN Appl Sci 2(5):909

Seiler RA, Kogan F, Sullivan J (1998) AVHRR-based vegetation and temperature condition indices for drought detection in Argentina. Adv Space Res 21(3):481–484

Sultana MS, Gazi MY, Mia MB (2021) Multiple indices based agricultural drought assessment in the northwestern part of Bangladesh using geospatial techniques. Environ Challenges 4:100120-1–100120-17

Swain S, Wardlow BD, Narumalani S, Tadesse T, Callahan K (2011) Assessment of vegetation response to drought in Nebraska using Terra-MODIS land surface temperature and normalized difference vegetation index. Gisci Remote Sens 48(3):432–455

Wan Z (2006) MODIS land surface temperature products users'guide. Institute for Computational Earth System Science, University of California, SantaBarbara

Wang JL, Yu YH (2021) Comprehensive drought monitoring in Yunnan Province, China using multisource remote sensing data. J Mt Sci 18(6):1537–1549. https://doi.org/10.1007/s11629-020-6333-7

Zambrano F, Lillo-Saavedra M, Verbist K, Lagos O (2016) Sixteen years of agricultural drought assessment of the BioBío region in Chile using a 250 m resolution Vegetation Condition Index (VCI). Remote Sens 8(6):530

Zeng J, Zhang R, Qu Y, Bento VA, Zhou T, Lin Y, Wang Q (2022) Improving the drought monitoring capability of VHI at the global scale via ensemble indices for various vegetation types from 2001 to 2018. Weather Clim Extremes 35:100412. https://doi.org/10.1016/j.wace.2022.100412

Zhang B, Wu P, Zhao X, Wang Y, Gao X, Cao X (2013) A drought hazard assessment index based on the VIC–PDSI model and its application on the Loess Plateau, China. Theor Appl Climatol 114(1):125–138. https://doi.org/10.1007/s00704-012-0826-4

Zhao X, Xia H, Liu B, Jiao W (2022) Spatiotemporal comparison of drought in Shaanxi–Gansu–Ningxia from 2003 to 2020 using various drought indices in Google Earth Engine. Remote Sens 14(7):1570. https://doi.org/10.3390/rs14071570

5 Recent Trends of Meteorological Variables and Impacts on Agriculture in Northwest Bangladesh

J. M. Adeeb Salman Chowdhury,
Md. Abdul Khalek, and Md. Kamruzzaman

Abstract

The study focused on two meteorological variables (rainfall and temperature) and their trend variations from 1960 to 2021. The recorded data was extracted from five regional weather stations in northwest area under Bangladesh Meteorological Department (BMD). By trend analysis, Rajshahi station found the lowest annual average rainfall (1460 mm) and the highest annual average temperature (25.30 °C). The precipitation concentration index (PCI) in the study area described that most of the stations carried varying precipitation concentration (16–20) except Dinajpur station. Linear trend analysis, the nonparametric Mann–Kendall (MK) test, Kendall's tau, Sen's slope estimator, and Spearman's rho (SR) test were used to define whether there were any trend fluctuations and calculate the magnitude of changes at the selected stations. Further, the Sequential Mann–Kendall test was executed to distinguish trend differences and abrupt deviations over time. During the study, Rajshahi station showed the highest significant decreasing trend with the degree of change assessed by Sen's slope estimator which was − 5.50 mm/year. Through cropping seasonal rainfall analysis, it had been observed that only the *Rabi* season (80%) found a declining trend across all stations. According to temperature trend analysis, except for Dinajpur station, all stations showed increasing trends in the annual and seasonal analysis by MK test and SR test. On the other hand, only Bogura and Syedpur stations were found significant at 5% level of significance. The magnitude of change discovered by the Sen's slope estimates varied from − 0.003 to 0.017 °C/year. The *Kharif* season temperature was significantly observed with a positive trend in all stations; however, the *Rabi* and pre-*Kharif* seasons temperature continued to show both increasing and decreasing trends. Furthermore, we checked the time series properties of meteorological data and constructed an appropriate model to forecast next five years based on the previous 60 years' recorded data. The research outcomes will be valuable for the sustainable agronomic growth of the country and reduce agricultural crop vulnerability during drought in the northwest region.

J. M. Adeeb Salman Chowdhury · Md.Kamruzzaman (✉)
Institute of Bangladesh Studies,
University of Rajshahi, Rajshahi, Bangladesh
e-mail: mkzaman@ru.ac.bd

J. M. Adeeb Salman Chowdhury
e-mail: asc_2010@cou.ac.bd

Md.Abdul Khalek
Department of Statistics, University of Rajshahi,
Rajshahi, Bangladesh
e-mail: mak.stat09@gmail.com

J. Das and S. Halder (eds.), *Advancement of GI-Science and Sustainable Agriculture*,
GIScience and Geo-environmental Modelling, https://doi.org/10.1007/978-3-031-36825-7_5

ISBN 978-81-976997-6-4

ADVANCED CONCRETE TECHNOLOGY

SCICRAFTHUB
Publication

Mr. Anil Kumar H. M

Dr. Tanu H.M.

Mr Basavaraja R

Shrujal J. Barvaliya

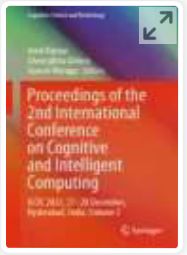

International Conference on Information and Management Engineering

ICCIC 2022: **Proceedings of the 2nd International Conference on Cognitive and Intelligent Computing** pp 197–204

Novel Approach to Identify and Eliminate Deadlocks in the ‘C’ Program

R. N. Kulkarni, Pratibha Mishra, J. Vedavyas & Arun Biradar

Conference paper | First Online: 02 October 2023

Part of the Cognitive Science and Technology book series (CSAT)

Abstract

The programming system of any organization comprises various types of interrelationships, like period dependency, sequence dependency, called-calling in-hierarchy dependency, and other types of application-dependent dependencies. The functionalities in the ‘C’ program are normally un-modular and may scatter in number of

interdependent programs group. The control flow graph of the C program helps in identifying the navigational paths within the interdependent programs groups. A deadlock is a situation in which two programs, functional units, or modules that share the same resource effectively prevent each other from accessing the resource. Different techniques are available to detect potential deadlocks in the programming system. Analyzing and comprehending each potential deadlock in order to determine whether the deadlock is viable in a real-world execution requires significant programmer effort. In this paper, a novel approach is proposed to detect deadlock and also eliminate deadlock, which is designed by considering the control flow of the program. In the beginning, the control flow of the entire program is abstracted, and then the entries of each called and calling function are entered in a four-column program dependency table. After performing the entry for the entire program, scan the entire table from left to right and top to bottom. If any row in the program dependency table appears more than once, then there is a possibility of deadlock. After identifying the repeated row, find out the functions that are repeated, and then, the deadlock is resolved by copying the functions in the appropriate place without modifying the functionality.

Keywords

Deadlock

Deadlock resolution algorithm (DRA)

Dependency table (DT)

References

1. Cai Y, Zhai K, Wu S, Chan WK (2013) Synchronizing threads globally to detect real deadlocks for multithreaded programs 3(7), ISSN 2250-3153

2. Terekhov I, Camp T (1999) Time efficient deadlock resolution algorithms. 69(3):149–154

3. Chahar P, Dalal S, Deadlock resolution techniques: an overview. Int J Sci Res Publ 3(7), ISSN 2250-3153

4. Buhler JD, Agrawal K, Li P, Chamberlain RD (2012) Efficient deadlock avoidance for streaming computation with filtering. 2012 ACM

5. Vaisla KS, Goswami M, Singh A, VGS algorithm—an efficient deadlock resolution method. Int J Comput Appl 44(1) (0975-8887)

6. Malhotra D (2016) Different deadlock handling strategies in distributed environment. Int J Adv Res Comput Sci Softw Eng 6(2), ISSN: 2277 128X

7. Reema Thareja ,”data structure using C”, Second Edition. Publisher: Oxford, SBN: 9780198099307, 0198099304.

8. Cormen TH, Eleiserson C, Revert RL, Introduction to algorithm, 2nd edn. England McGraw-Hill Book Company, Cambridge, Massachusetts London

9. Kulkarni RN, Patil P (2017) Abstraction of information flow and functional dependency from a restructured legacy ‘C’ program for parallelization. In: International conference on smart technologies for smart nation (SmartTechCon)—2017, ISBN978-1-5386-0569-1

10. Kulkarni R, Handigund SM (2007) Moulding the legacy C programs for reengineering. In: Proceeding of the international conference on Advances on computer vision and information technology ACVIT-2007 held on November 28–30, 2007, pp 1531–1537 at Aurangabad, Maharashtra, India, ISBN-978-81-89866-74-7

11. Giebas D, Wojszczyk R (2020) Deadlocks detection in multithreaded applications based on source code analysis, Appl Sci 2020, 10(2):532. https://doi.org/10.3390/app10020532

12. Tang F, You I, Yu S, Wang C-L, Guo M, Liu W (2012) An efficient deadlock prevention approach for service oriented transaction processing 63(2):458–468, https://doi.org/10.1016/j.camwa.2011.07.063

13. El-Tamimi AM, Al-Ahmari A, Kaid H (2015) Comparison and evaluation of deadlock prevention methods for different size

automated manufacturing systems. Math Prob Eng 2015, Article ID 537893 | https://doi.org/10.1155/2015/537893

14. Tafa I, Jonuzaj R, Deadlocks: manipulating threads to detect and avoid them. Int J Comput Sci Manag Stud (IJCSMS) 42(04)

15. Publishing Date: 16th November, 2021 An Indexed, Referred, Peer Reviewed and Impact Factor Journal ISSN (Online): 2231-5268, www.ijcsms.comIJCSMSwww.ijcsms.com

16. Detecting deadlock in programs with data-centric synchronization, May 2018. In: Proceedings—international conference on software engineering. https://doi.org/10.1109/ICSE.2013.6606578

17. Deadlock detection in distributed system. Indonesian J Electric Eng Comput Sci 24(3):1596. https://doi.org/10.11591/ijeecs.v24.i3.pp1596-1603

Author information

Authors and Affiliations

Department of Computer Science and Engineering, Ballari Institute of Technology and

Management, Ballari, India

R. N. Kulkarni, Pratibha Mishra & J. Vedavyas

School of CSE, Reva University, Bangalore, India

Arun Biradar

Corresponding author

Correspondence to J. Vedavyas .

Editor information

Editors and Affiliations

BioAxis DNA Research Centre Private Limited, Hyderabad, Andhra Pradesh, India

Amit Kumar

Department of Computer Science, Brunel University, Uxbridge, UK

Gheorghita Ghinea

CMR College of Engineering and Technology, Hyderabad, India

Suresh Merugu

Rights and permissions

Copyright information

About this paper

Cite this paper

Kulkarni, R.N., Mishra, P., Vedavyas, J., Biradar, A. (2023). Novel Approach to Identify and Eliminate Deadlocks in the ‘C’ Program. In: Kumar, A., Ghinea, G., Merugu, S. (eds) Proceedings of the 2nd International Conference on Cognitive and Intelligent Computing. ICCIC 2022. Cognitive Science and Technology. Springer, Singapore. https://doi.org/10.1007/978-981-99-2746-3_21

.RIS .ENW .BIB

DOI	Published	Publisher Name
https://doi.org/10.1007/978-981-99-2746-3_21	02 October 2023	Springer, Singapore

Print ISBN	Online ISBN	eBook Packages
978-981-99-2745-6	978-981-99-2746-3	Intelligent Technologies and Robotics Intelligent Technologies and Robotics (R0)

Publish with us

Policies and ethics

International Conference on Information and Management Engineering

ICCIC 2022: **Proceedings of the 2nd International Conference on Cognitive and Intelligent Computing** pp 205–212

Novel Approach to Abstract Object Features from Java Program

R. N. Kulkarni & P. Pani Rama Prasad

Conference paper | First Online: 02 October 2023

Part of the Cognitive Science and Technology book series (CSAT)

Abstract

Nowadays, the software developers use unified modeling language tool (UML) to design the application software for an organization. The present UML tool available in the market supports thirteen different diagrams, which represents the static behavior and dynamic behavior of the software. In this paper, an automated tool is proposed that abstracts the object features from the Java program. To abstract these object features,

initially the tool extracts all the necessary components related to the class such as class name, attributes associated with the class, methods, and visibility information like private, public, and protected. Finally, all the extracted features are stored in the form of a table called class table. Further, the information available in the class table, and input Java program is used to abstract the features of object such as object name, attributes, methods used by the object, visibility, and associations.

Keywords

UML Restructuring Class table

Object table Java program

References

1. Kulkarni R N, Pani Rama Prasad P (2021) Abstraction of UML class diagram from the input Java program. Int J Adv Netw Appl 12(04):4644–4649

2. Kulkarni R N, Patil P (2020) Abstraction of functional modules from a Legacy 'C' Program using program slicing, perspectives in communication, embedded-systems and signal-processing 4(4):39–44

3. Mazumder SF, Latulipe C, Are variable, array and object diagrams in Java textbooks explanative? In: Proceedings of the 2020 ACM conference on innovation and technology in computer science education, 2020, pp 425–431

4. Sharaff A, Rath SK (2020) Formalization of UML class diagram using colored Petri Nets. In: IEEE 1st International conference on power, control and computing technologies (ICPC2T), Raipur, 2020, pp 256–261

5. Sabir U, Azam F et al (2019) A model driven reverse engineering framework for generating

high level UML models from Java source code. IEEE Access 2019, pp 312–318

6. Kulkarni R N, Pani Rama Prasad P (2019) Restructuring of Java program to be amenable for reengineering. J Eng Sci Technol 02(06):45–51

7. Mahanto P, Barisal SK, Mohapatra DP (2019) Achieving MC/DC using UML object diagram. In: IEEE International conference on information technology (ICIT), Bhubaneswar, 2019, pp 182–189

8. Kästner A, Gogolla M, Selic B (2018) From (imperfect) object diagrams to (imperfect) class diagrams: new ideas and vision paper. In: Proceedings of the 21th ACM/IEEE international conference on model driven engineering languages and systems, 2018, pp 71–80

9. Kästner A, Gogolla M, Selic B (2018) Towards flexible object and class modeling tools: an experience report. In: MODELS'18: Proceedings of the 21th ACM/IEEE international conference on model driven engineering languages and systems, 2018, pp 13–22

10. Singh D (2018) A scrutiny study of various unified modeling language (UML) diagrams,

software metrics tool and program slicing technique. J Emerg Technol Innov Res (JETIR) 5(6)

11. Singh D, Sidhu HJS (2018) A scrutiny study of various unified modeling language (uml) diagrams, software metrics tool and program slicing technique 5(6), 254–262

12. Handigund SM, Sajjanar S, Arunakumari BN (2015) Resuscitation of syllogism within unified modeling language levels through the renovation of object diagram. In: IEEE International conference on advances in computing, communications and informatics (ICACCI), pp 114–121

13. Torchiano M, Torchiano M, Ricca F, Leotta M (2017) Do UML object diagrams affect design comprehensibility? Results from a family of four controlled experiments. J Vis Lang Comput, pp 135–143

14. Duc BM (2015) Uniform object modeling methodology and reuse of real-time system using UML. In: Proceedings of the 5th ACM international conference on Embedded software, 5(2), pp 44–47

15. Zeaaraoui A, Ettifouri EH, Bouchentouf T (2015) An automated object-based approach to transforming requirements to class diagrams. In: IEEE Second world conference on complex systems (WCCS), 2(1), pp 69–75

16. Parada AG, Siegert E, de Brisolara LB (2014) Generating Java code from UML class and sequence diagrams. IEEE Explore, 33–38

Author information

Authors and Affiliations

Department of Computer Science & Engineering, Ballari Institute of Technology and Management, Ballari, India

R. N. Kulkarni & P. Pani Rama Prasad

Corresponding author

Correspondence to R. N. Kulkarni .

Editor information

Editors and Affiliations

BioAxis DNA Research Centre Private Limited, Hyderabad, Andhra Pradesh, India

Amit Kumar

Department of Computer Science, Brunel University, Uxbridge, UK

Gheorghita Ghinea

CMR College of Engineering and Technology, Hyderabad, India

Suresh Merugu

Rights and permissions

Reprints and permissions

Copyright information

About this paper

Cite this paper

Kulkarni, R.N., Pani Rama Prasad, P. (2023). Novel Approach to Abstract Object Features from Java Program. In: Kumar, A., Ghinea, G., Merugu, S. (eds) Proceedings of the 2nd International Conference on Cognitive and Intelligent Computing. ICCIC 2022. Cognitive Science and Technology. Springer, Singapore. https://doi.org/10.1007/978-981-99-2746-3_22

.RIS .ENW .BIB

DOI	Published	Publisher Name
https://doi.org/10.1007/978-981-99-2746-3_22	02 October 2023	Springer, Singapore

Print ISBN	Online ISBN	eBook Packages
978-981-99-2745-6	978-981-99-2746-3	Intelligent Technologies and Robotics Intelligent Technologies and Robotics (R0)

Publish with us

Policies and ethics

Congress on Smart Computing Technologies

CSCT 2022: **Congress on Smart Computing Technologies** pp 419–434

Real-Time Flood Prediction System Using Machine Learning Algorithms

K. S. Raghu Kumar & Rajashree V. Biradar

Conference paper | First Online: 11 July 2023

Part of the Smart Innovation, Systems and Technologies book series (SIST,volume 351)

Abstract

As computing power rises and machine learning algorithms improve, new options for flood detection are opened up using machine learning methodologies. Machine learning has become a popular tool for studying nonlinear systems, such as floods and for making flood predictions. Traditional techniques of flood forecasting use a link of hydraulic and hydrologic models to represent the physical activities. Such models help us understand systems better, but they're computationally and

data-intensive. Methods based on machine learning offer the potential to improve accuracy while also cutting down on calculation time and model development costs. In this paper, six different machine learning algorithms like artificial neural networks (ANN), KNeighbors classifier, logistic regression, support vector classifier (SVC), decision tree and random forest classifiers have been implemented individually to evaluate and compare the performances while predicting the possibilities of floods. Among the five algorithms, the logistic regression has performed well during the prediction of floods with an accuracy of 99.39%, recall value of 93.91% and ROC value of 96.98%. During the evaluation of predicting the floods in an individual state, the random forest algorithm has performed well by obtaining 97.33% of accuracy. It would be fascinating to study other aspects of machine learning-based flood prediction. Collecting future forecasts and rainfall levels using sensors could detect air pressure, humidity, and temperature to increase the prediction ability of algorithms and improve model performance in anticipating floods further in time.

Keywords

Artificial neural networks

Decision tree classifier

Flood prediction system

KNeighbours classifier **Logistic regression**

Machine learning algorithms

Random forest classifier

Support vector classifier

References

1. Mosavi, A., Ozturk, P., Chau, K.W.: Flood prediction using machine learning models: literature review. Water (Switzerland) **10**(11) (2018). https://doi.org/10.3390/w10111536

2. Wagenaar, D., Curran, A., Balbi, M., Bhardwaj, A., Soden, R., Hartato, E., MestavSarica, G., Ruangpan, L., Molinario, G., Lallemant, D.: Invited perspectives: how machine learning will change flood risk and impact assessment. Nat. Hazard. **20**(4), 1149–1161 (2020). https://doi.org/10.5194/nhess-20-1149-2020

3. Casella, G., Fienberg, S., Olkin, I.: An introduction to statistical learning. In: Design, vol. 102 (2006). https://doi.org/10.1016/j.peva.2007.06.006

4. Liu, Q., Wu, Y.: Supervised learning. Encyclopedia Sci. Learn. (2012). https://doi.org/10.1007/978-1-4419-1428-6

5. Jongman, B., Ward, P.J., Aerts, J.C.J.H.: Global exposure to river and coastal flooding: long term trends and changes. Glob. Environ. Chang. **22**, 823–835 (2012)

6. Liu, C., Guo, L., Ye, L., Zhang, S., Zhao, Y., Song, T.: A review of advances in China's flash flood early-warning system. Nat. Hazards **92**, 619–634 (2018)

7. Xie, K., Ozbay, K., Zhu, Y., Yang, H.: Evacuation zone modeling under climate change: a data-driven method. J. Infrastruct. Syst. **23**, 1–9 (2017)

8. Mosavi, A., Rabczuk, T., Varkonyi-Koczy, A.R.: Reviewing the novel machine learning tools for materials design. In: Recent Advances in Technology Research and Education, pp. 50–58. Springer, Cham, Switzerland (2017)

9. Choubin, B., Khalighi-Sigaroodi, S., Malekian, A., Ki¸si, Ö.: Multiple linear regression, multi-layer perceptron network, and adaptive neurofuzzy inference system for forecasting precipitation based on largescale climate signals. Hydrol. Sci. J. **61**, 1001–1009 (2016)

10. Kim, S., Matsumi, Y., Pan, S., Mase, H.: A real-time forecast model using artificial neural network for after-runner storm surges on the Tottori coast, Japan. Ocean Eng. **122**, 44–53 (2016)

11. Gizaw, M.S., Gan, T.Y.: Regional flood frequency analysis using support vector regression under historical and future climate. J. Hydrol. **538**, 387–398 (2016)

12. Kasiviswanathan, K., He, J., Sudheer, K., Tay, J.-H.: Potential application of wavelet neural network ensemble to forecast streamflow for flood management. J. Hydrol. **536**, 161–173 (2016)

13. Ravansalar, M., Rajaee, T., Kisi, O.: Wavelet-linear genetic programming: a new approach for modeling monthly streamflow. J. Hydrol. **549**, 461–475 (2017)

14. Tan, L., Li, X., Wang, Z., Guo, H., Wang, J.: Lightweight reduced graphene oxide@ mos2 interlayer as polysulfide barrier for high-performance lithium–sulfur batteries. ACS Appl. Mater. Interfaces. **10**, 3707–3713 (2018)

Author information

Authors and Affiliations

Department of CSE, RYM Engineering College, Ballari, Karnataka, India

K. S. Raghu Kumar

Professor, Department of CSE, Ballari Institute of Technology and Management, Ballari, Karnataka, India

Rajashree V. Biradar

Corresponding author

Correspondence to K. S. Raghu Kumar .

Editor information

Editors and Affiliations

South Asian University, New Delhi, Delhi, India

Jagdish Chand Bansal

Department of Computer Science and Engineering, Rajasthan Technical University, Kota, Rajasthan, India

Harish Sharma

Department of Computer Science and Electrical Engineering, University of Stavanger, Stavanger, Norway

Antorweep Chakravorty

Rights and permissions

Copyright information

About this paper

Cite this paper

Raghu Kumar, K.S., Biradar, R.V. (2023). Real-Time Flood Prediction System Using Machine Learning Algorithms. In: Bansal, J.C., Sharma, H., Chakravorty, A. (eds) Congress on Smart Computing Technologies. CSCT 2022. Smart Innovation, Systems and Technologies, vol 351. Springer, Singapore. https://doi.org/10.1007/978-981-99-2468-4_32

.RIS .ENW .BIB

DOI	Published	Publisher Name
https://doi.org/10.1007/978-981-99-2468-4_32	11 July 2023	Springer, Singapore

Print ISBN	Online ISBN	eBook Packages
978-981-99-2467-7	978-981-99-2468-4	Intelligent Technologies and Robotics Intelligent Technologies and Robotics (R0)

Publish with us

Policies and ethics

Location Based Energy Efficient Security Mechanism in Wireless Sensor Networks using Qlearning-PSO-AES Algorithm

Publisher: IEEE

Rajashree V Biradar ; Sudhakar Avareddy ; V.C. Patil **All Authors**

Abstract: Wireless Sensor Networks (WSNs) are gaining popularity in various applications, including environmental monitoring, healthcare, and security surveillance. However, ensuri... **View more**

Metadata

Abstract:

Wireless Sensor Networks (WSNs) are gaining popularity in various applications, including environmental monitoring, healthcare, and security surveillance. However, ensuring the security of WSNs is challenging due to resource limitations and dynamic nature of WSNs. Location-based security management has emerged as an effective approach to enhance WSN security by leveraging node location information to mitigate security threats. A hybrid Qlearning-PSO-AES technique for location-based security management in WSNs has been proposed in this paper. The proposed technique incorporates location information, dynamic trust evaluation, and advanced encryption algorithms to enhance WSN security. In this proposed work, the Qlearning algorithm is applied to learn the node's current state, including position and velocity, and to estimate trust values of nodes based on their past interactions. The PSO algorithm is used to determine the optimal placement of sensor nodes within the network, optimizing network lifetime, coverage, connectivity and energy consumption. Furthermore, the optimal solution obtained from PSO, represented by the best fitness value, is utilized for selecting encryption keys in the AES algorithm. The encryption keys are dynamically updated based on node movement to enhance WSN security. Simulation results clearly demonstrate that the proposed technique not only enhances the security of WSNs but also optimizes network performance, making it well-suited for real-world applications in various domains.

Published in: 2023 International Conference on Network, Multimedia and Information Technology (NMITCON)

Date of Conference: 01-02 September 2023

DOI: 10.1109/NMITCON58196.2023.10275874

Date Added to IEEE *Xplore*: 17 October 2023

Publisher: IEEE

ISBN Information:

Conference Location: Bengaluru, India

Contents

WSNs consist of small, low-cost, and low-power independent sensor nodes that communicate with each other to collectively gather and process data from the surrounding environment [1]. The Fig. 1 dipicts the architecture of WSN. Wireless sensor networks have gained significant attention in recent years due to their wide range of applications in various domains such as environmental monitoring, surveillance, healthcare, and industrial automation. Although WSNs play a crucial role in various applications, and their distributed and resource-constrained nature poses several challenges. Challenges in WSN include: Limited resources, Energy efficiency, Scalability, Communication reliability, Data aggregation and fusion, Localization and positioning, Network dynamics, Quality of Service (QoS) and integration with other networks etc. Addressing these challenges requires innovative solutions and careful trade-offs to optimize performance, energy efficiency and security in WSNs. The proposed algorithm mainly concentrate on two main challenges of WSNs i.e. localization and security. Localization [2] is an important issue in WSN, and accurate localization is essential for many applications like target tracking, object localization, environment monitoring etc. that rely on precise location information in WSNs. Security [3] of communication in WSN is a critical issue that needs to be addressed. Due to the limited computational resources of the sensors, it is a challenging to implement robust encryption algorithm. This paper proposes a hybrid approach that combines the Qlearning-PSO-AES algorithms to achieve enhanced location based energy efficient secured communication over WSNs. The proposed work can be effectively used in certain applications within the context of Wireless Sensor Networks (WSNs) like Intrusion Detection Systems (IDS), Environmental Monitoring, Target Tracking and Localization, Traffic Monitoring and Control etc. Section II describes Related Work, section III describes Proposed Work, section IV describes Simulation Setup and Results. Followed by Conclusion, Future Scope and References at the end.

Authors
Figures
References
Keywords
Metrics

Downl

PDF

Naive Bayes Classifier based Movie Recommendation System

Publisher: IEEE

Yeresime Suresh ; Br Rohit Kumar ; C Jahnavi Reddy ; P Sai Rohini ; K Sharath **All Authors**

Abstract: In 21st Century almost every single piece of data is available over the internet. All we need is to surf through the internet. User sometimes spend more time in surfing t... **View more**

Metadata

Abstract:
In 21st Century almost every single piece of data is available over the internet. All we need is to surf through the internet. User sometimes spend more time in surfing the internet to get information about a movie. So the emphasis is to make every piece of data available in a single page which will help user to surf faster. Our approach is to build a website with customized search engine for Hollywood movies. Initially, the movie database gathers data from IMDB and Kaggle movie dataset. When the user enters the movie title in the webpage. TMDB API gathers the data from the TMDB website. This provides the user with the simplistic and user-friendly environment. It also provides the basic information about the movie, classification of the movie review based on classifier algorithm and generates a list of top 10 similar movies based on cosine-similarity measure and content-based filtering approach.

Published in: 2023 International Conference on Sustainable Computing and Smart Systems (ICSCSS)

Date of Conference: 14-16 June 2023

DOI: 10.1109/ICSCSS57650.2023.10169718

Date Added to IEEE *Xplore*: 07 July 2023

Publisher: IEEE

ISBN Information:

Conference Location: Coimbatore, India

Contents

decision to launch this initiative. In daily life, recommendation algorithms are more important. Due to many works in our life, people are constantly pressed for time. Therefore, the suggestion systems are crucial because they recommend without too much human effort. A recommendation system essentially seeks out material that would be interesting for a particular person. These recommendation engines saves time for people in taking decisions. These recommendation systems use artificial intelligence, where they can predict what a person wants to view.

Authors

Figures

References

Keywords

Metrics

More Like This

Determination of SME Tax with Naïve Bayes Method
2023 International Conference On Cyber Management And Engineering (CyMaEn)
Published: 2023

Drug Review-based Diabetes Prediction by Using Naïve Bayes Method
2021 International Conference Advancement in Data Science, E-learning and Information Systems (ICADEIS)
Published: 2021

Show More

noQ: An Innovative Approach to Virtualize and Automate Queues

Publisher: IEEE

Mohammed Shafiulla ; Naveen S Math ; Akash B ; Aditi Naidu B T ; Shreya B M **All Authors**

Abstract: It has been observed that waiting has been a constant trouble in our increasingly fast-paced world where the traditional waiting in lines/queues is not a viable option as... **View more**

Metadata

Abstract:
It has been observed that waiting has been a constant trouble in our increasingly fast-paced world where the traditional waiting in lines/queues is not a viable option as it is statistically shown that 25% of people would only wait for a max of 2 mins, 59% would wait no longer than 4 mins and 73% would abandon their purchase or work if its more than 5 mins. So, to tackle this common issue, the proposed system incorporates an innovative solution by virtualizing the entire queuing system and creating a scheduling process with the help of advanced scheduling algorithms such as FCFS Scheduling and Priority Scheduling. This is a web application that will be developed using Full stack (Laravel, PHP, CSS, HTML, phpMyAdmin). With the help of this an ecosystem will be created where the work process can be monitored, altered, and improved that makes it efficient for both the parties, i.e., the workers and the people waiting in a queue, and allowing for further improvement by collecting workers statistics which can be used by the admin to further optimize the workflow. This system enables 'Virtual Queue Creation' by adapting functionalities such as 'Virtual Room Creation' used by famous organizations such as Google and Microsoft. The work statistics get stored in the backend with the help of SQL-based technology i.e., phpMyAdmin and a user-friendly UI will be developed for ease of use for all the end users of this proposed virtual system. The web application as mentioned above uses scheduling algorithms for the automation of queue management and will also have the functionality for manual management making it more flexible for the end users. This web application will incorporate several APIs for data collection and storage for statistics handling. The APIs and frameworks that will be used are Laravel, Excel JS API, and user-created APIs. This new system will be able to reduce the waiting times to a great extent and will be able to facilitate the needs that are necessary for th...

(Show More)

Published in: 2023 3rd International Conference on Intelligent Technologies (CONIT)

Date of Conference: 23-25 June 2023 **DOI:** 10.1109/CONIT59222.2023.10205919

Date Added to IEEE *Xplore*: 07 August 2023 **Publisher:** IEEE

ISBN Information: **Conference Location:** Hubli, India

Contents

With the population upsurge in the past few years, there has hardly been any place without a lengthy queue. In some instances, like paying the bill at the hospital or the booking counter at the railway counter or bus stand, waiting in a queue cannot be avoided. As we are accustomed to queues everywhere, we are delighted if we don't see a queue at the movie theatre or the booking counter. There is often pandemonium in queues with the crowd not following the proper etiquette. This leads to a total disruption of the queue and often increased waiting times or in the worst cases, it could result in losing your chance of getting the work done at the right time. As we now live in a world where everything is virtual and engaged with the internet, particularly businesses, there can be effective changes made to minimize the need for queues. noQ is a web application that focuses on diminishing the hassle that arises while dealing with queues. This system would help in reducing the time spent standing in long endless queues as it allows the user to utilize their time productively. This virtual system helps to maintain decorum and proper discipline in queues. noQ would also help in better queue maintenance by calculating the time spent at the counter by each person. noQ would comprise of an admin panel for the admin where they can organize the queues efficiently and minimize waiting times for the users.

An Innovative Approach for Delivering Food and Grocery

Chidananada ; C. K. Srinivasa ; P Panirama Prsad **All Authors**

Abstract:"ShopNest" is a mobile application which connects local customers to local retailers. Due to massive supermarkets most of the minute retail shops have taken a bad hit. Th... **View more**

Metadata

Abstract:
"ShopNest" is a mobile application which connects local customers to local retailers. Due to massive supermarkets most of the minute retail shops have taken a bad hit. This idea provides a great opportunity for small retail shops to increase their business and also a quick delivery saves time for customers. As we see, most parents and elder people depend on the caretaker of their family to get their essentials. So, the concept is to help the dependent, to reach out for their essentials. It was also observed that some people are emotionally connected with some specific shop(s) and people usually write down a list of their essentials on a piece of paper which has no use in online ordering. In this article a novel approach is proposed which provides the liberty to the people in the way they order, providing value to that piece of paper while placing the order and to connect people to their favorite shop(s) through the application and service and deliver the ordered products.

Published in: 2023 4th IEEE Global Conference for Advancement in Technology (GCAT)

Date of Conference: 06-08 October 2023

DOI: 10.1109/GCAT59970.2023.10353434

Date Added to IEEE *Xplore*: 19 December 2023

Publisher: IEEE

ISBN Information:

Conference Location: Bangalore, India

Contents

ways of placing orders. ShopNest" is a mobile application which connects local customers to local retailers. Due to massive supermarkets most of the minute retail shops have taken a bad hit. This idea provides a great opportunity for small retail shops to increase their business and also a quick delivery saves time for customers. As we see, most parents and elder people depend on the caretaker of their family to get their essentials. So, the concept is to help the dependent, to reach out for their essentials. It was observed that some people are emotionally connected with some specific shop(s) and people usually write down a list of their essentials on a piece of paper which has no use in online ordering. In this article a novel approach is proposed which provides the liberty to the people in the way they order, providing value to that piece of paper while placing the order and to connect people to their favorite shop(s) through the application and service and deliver the ordered products.

Authors

Figures

References

Keywords

Metrics

More Like This

The business power consumption manage model innovation of State Grid JIBEI Electric Power Company based on the mobile application
2020 International Conference on Electrical Engineering and Control Technologies (CEECT)
Published: 2020

Usability Evaluation on an Indonesian Mobile Application for Small Business Lending
2018 International Conference on Information Technology Systems and Innovation (ICITSI)
Published: 2018

Show More

MACHINE LEARNING

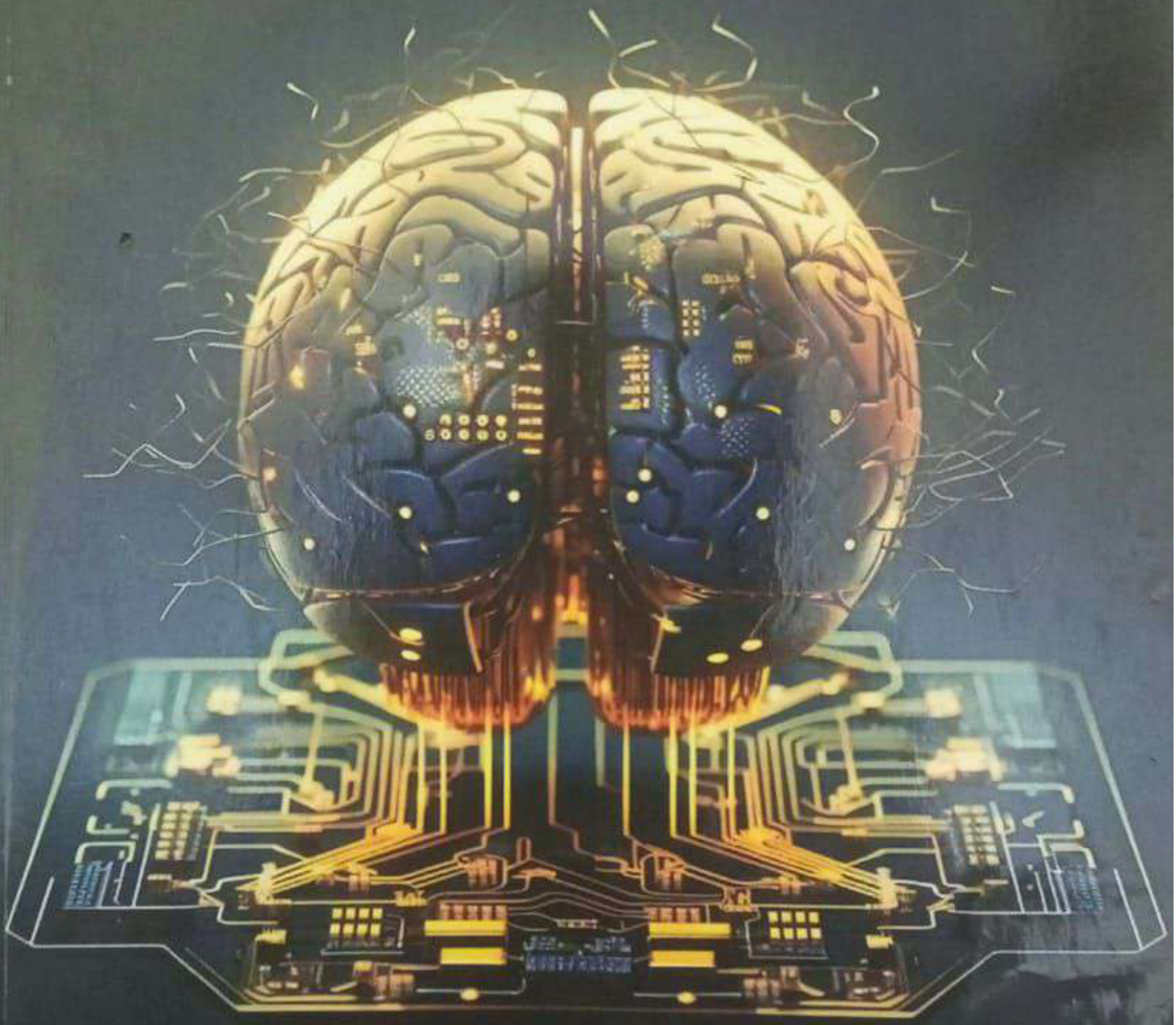

Milad Mohseni
Dr. Jagadish R M
Ravikiran Mahadasa
Dr. K Purushotam Naidu

Raja Rammohun Roy National Agency for ISBN

Department of Higher Education, Ministry of Education
Government of India

Search ISBN

From Date | To Date | Advance Search

Book Title | Email | Name of Author/Co-Author

BR | 2024 | 9788196544478

--Select Product Form-- | --Select Language--

Search

Export to Excel

Search:

#	Book Title	ISBN	Product Form	Language	Applicant Type	Name of Publishing Agency/Publisher	Name of Author/Editor	Publication Date
1	Machine Learning	978-81-965444-7-8	Paperback / softback	English	Publisher	BR International	Author : Milad Mohseni,Dr. Jagadish R M,Ravikiran Mahadasa,Dr. K Purushotam Naidu	08/02/2024

Showing 1 to 1 of 1 entries

Previous Next

CHAPTER 6

Design of nanostructured biosensors based on organic and other composite materials

B. Chethan Ph D[1,*], V. Prasad[1], A. Sunilkumar[2], S. Thomas[3], A. Sreeharsha[4,5]

[1]Department of Physics, Indian Institute of Science, Bangalore, Karnataka, India
[2]Department of Physics, Ballari Institute of Technology and Management, Ballari, Karnataka, India
[3]International and Inter University Centre for Nanoscience and Nanotechnology, Mahatma Gandhi University, Kottayam, Kerala, India
[4]Department of Pharmaceutical Sciences, College of Clinical Pharmacy, King Faisal University, Al-Ahsa, Saudi Arabia
[5]Department of Pharmaceutics, Vidya Siri College of Pharmacy, Bengaluru, Karnataka, India
[*]***Dr. CHETHAN B. e-mail address: chethanbchetu@gmail.com***

6.1 Introduction to sensors

A receptor–transducer sensor device is used to convert a biological response into an electrical signal. The design and development of biosensors have attained a greater interest nowadays because biosensors find widespread applications in the medical field, diagnosis of the disease, ecology monitoring, and maintaining the quality of food, drug, and water. The biosensing devices attained a greater demand and face many challenges to fabricate the sensing device with better sensitivity, a lower limit of detection, good stability, quick response time, reduced device size, and simple operation. These challenges can be fulfilled by the interphase of chemical and morphological properties of the nanomaterials with the sensor technology. The nanomaterials from zero to three dimensions are having advantageous properties like high surface area, enhanced conductivity, and tunable electrical and mechanical properties making these nanomaterials potential candidates to fabricate biosensors. Among the nanomaterials, nanoparticles, nanowires, and nanorods find advantageous properties because of their high stability, high carrier capacity, high detection limit, large surface area, active sites, and more thermal conductivity. The ferrites, polymers, metal, metal oxides, carbon-based materials, and their composites are widely used in the fabrication of

Novel Nanostructured Materials for Electrochemical Bio-sensing Applications

ISBN 978-0-443-15334-1, DOI: 10.1016/B978-0-443-15334-1.00006-7

biosensors. In this chapter, the evolution of the sensors, types of sensors, and biosensor types are discussed deliberately. This chapter provides different methods which have been used in the synthesis and fabrication of biosensors using nanomaterials.

In this modern world, as awareness of man increased to lead a sophisticated life, the need for science and technology has gained momentum (Amrutha et al., 2021; Chethan et al., 2019; Gleiter, 2000; Hareesha & Manjunatha, 2021; Hareesha et al., 2021; 2021; Manjunatha et al., 2014; Pal et al., 2011; Pushpanjali et al., 2021; Tigari & Manjunatha, 2019; Manjunatha, 2020). Nowadays civilized people depend more on the gadgets like computers, Xerox machines, air conditioning, cell phones, television, smoke detectors, and refrigerators. Many of these gadgets work with the help of sensors. The term sensor refers to a device or module that assists in detecting changes in physical quantities, such as pressure, heat, humidity, movement, force, and an electrical quantity like current, and then turns these physical quantities into signals that can be monitored and analyzed. Sensors are the brains of measuring systems. An ideal sensor should have the following qualities: high resolution, reproducibility, repeatability, range, drift, calibration, sensitivity, selectivity, and linearity (Chethan et al. 2022, 2023; Chethan et al., 2018; Chethan Ramana et al., 2019; El-Denglawey et al., 2021; El-Denglawey Manjunath et al., 2021; Manjunatha et al., 2019; Pratibha & Chethan, 2022; Pratibha et al., 2020; Ravikiran & Chethan, 2022; Rupashree et al., 2021; Shanawad Chethan et al., 2023; Shanawad et al., 2023; Sunilkumar et al., 2023).

Today, we benefit from science and technological advancements that make our lives run more smoothly. We frequently rely on various devices that help us to interact with the physical environment, such as television remote controls, smoke detectors, infrared (IR) thermometers, lamp switches, and fans. Due to numerous applications, including environmental and food quality monitoring, medical diagnostics and health care, automotive and industrial manufacture, as well as space, defense, and security, the advancement of sensor technology has assumed increasing significance (Dincer et al., 2019; Ensafi et al., 2011; Ensafi, 2019; Theavenot et al., 2001).

6.1.1 Classification of sensors

Depending on the physical quantity and analyte to be measured, sensors can be broadly categorized into a number of categories, which include: (1) energy source, (2) physical contact, (3) comparability, (4) analog and digital sensors, and (5) signal detection. Based on these quantities, sensors are broadly classified as follows (Khanna, 2012; White, 1987).

Energy source: Two types of sensors are employed based on energy sources:

1. **Active and passive sensors**: Active sensors, such as microphones, thermistors, strain gauges, and capacitive and inductive sensors, require an external energy source. These kinds of sensors are known as parametric sensors (the output depends on the parameter). Thermocouples, piezoelectric sensors, and photodiodes are examples of passive sensors that produce signals without requiring external energy. These sensors are referred to as self-generating sensors.
2. Physical contact: Based on physical contact, sensors can be classified as contact or noncontact.
3. **Contact and noncontact sensors:** Contact sensors, like temperature sensors, need to make physical touch with their stimulus, whereas noncontact sensors include optical, magnetic, and infrared (IR) thermometers.
4. Comparability **sensors can be either absolute or relative**.
5. **Absolute and relative sensors:** Thermistors and strain gauges are examples of absolute sensors. Relative sensors, such as a thermocouple that measures temperature differences and a pressure gauge that measures pressure, relative to atmospheric pressure, perceive the stimulus in relation to a fixed or changing reference.
6. **Analog and digital sensors:** Sensors come in two varieties: analog and digital. An analog sensor converts a measured physical quantity into an analog form (continuous in time). This group of analog sensors includes thermocouples, strain gauges, and resistance temperature detectors (RTDs). Pulses are the output that a digital sensor produces. Encoders fall under the category of digital sensors.
7. **Signal detection:**

The basic classification of sensors based on signal detection and transformation of information is as follows:

a. **Physical sensors:** A physical quantity is measured by a physical sensor, which then transforms into a signal that the user can recognize. The force, acceleration, rate of flow, mass, volume, density, and pressure are just a few of the environmental changes that these sensors can identify. The use of physical sensors has increased significantly in the biomedical industry, especially with the development of novel measurement technologies and the improvement of microelectromechanical system technology for the creation of more precise and smaller sensors.
b. **Thermal sensors:** A thermal sensor is a device that measures the temperature of an environment and converts the measured data into electronic data for recording or monitoring temperature change signals. Thermistors, RTDs, and thermocouples are a few types of temperature sensors.
c. **Biological sensors:** Biological sensors keep an eye on biomolecular interactions like those involving antibodies and antigens, DNA and enzymatic reactions, or cellular communication. The abbreviated form of the term "biosensors" refers to biological sensors.
d. **Chemical sensors:** The International Union of Pure and Applied Chemistry defines a chemical sensor as a device that converts chemical information into an analytically useful signal ranging from the concentration of a particular sample component to total composition analysis. Chemical sensors are used to keep an eye on the quantity or activity of the relevant chemical species in the gaseous or liquid phase. In addition, they are used to monitor assays for organophosphorus chemicals, food and drug analyses, and environmental pollution. They can be utilized for clinical diagnostic applications as well.

6.1.2 Biosensor

A biosensor is a tool or probe that combines an electronic component with a biological element, like an enzyme or antibody, to produce a quantifiable signal. Information about a physiological change or the presence of different chemical or biological components in the environment is detected, recorded, and transmitted by the electronic component. Biosensors are available in a variety of sizes and designs, and they have the ability to measure and detect even very low quantities of certain diseases, harmful chemicals, and pH values. Certain static and dynamic requirements are required to develop a highly effective and capable biosensor

system. These requirements allow for the optimization of the biosensors' performance for commercial applications.

6.1.2.1 Constituents of biosensors

The main constituents of biological sensors comprise of:

1. **Analyte:** A material of interest whose components are being determined or detected is an analyte. The biological constituents may be in the form of glucose, lactose, ammonia, and glucose (Bhalla et al., 2016).
2. **Transducer:** One crucial component of a biosensor is the transducer which is a device that converts energy from one form to another. It transforms the biorecognition event into an electrical signal that is quantifiable and connected to the quantity or the presence of a chemical or biological target.
3. **Bioreceptor:** Bioreceptors are biological components such as enzymes, cells, aptamers, deoxyribonucleic acid (DNA or RNA), and antibodies that are capable of recognizing the target substrate. Biorecognition is the process of producing a signal when a bioreceptor and an analyte interact.
4. **Electronics:** To get the signal ready for the display, it is processed. Amplification and digitalization take place on the electrical signals collected from the transducer. The display unit quantifies the signals that have been processed.
5. **Display:** The display unit is made up of a user interpretation system, such as a computer or a printer, that provides the output so that the user can read and understand the appropriate response according to the end-user requirement.

6.1.2.2 Evolution of biosensors

Leland Charles Clark Jr., the father of the biosensors, reported about the components of the biosensors in this work in the year 1956. He fabricated the electrode which is possible to determine the oxygen content in the blood. Later in 1962, Clark reported about the amperometric enzyme electrode for glucose detection. In the upcoming year 1967, Updike and Hicks modified the Clarks work and find out the first functional enzyme electrode for oxygen sensor. After, in 1969 Guilbault and Montalvo depicted the first urea detection sensor based on potentiometric enzyme electrode. In the year 1973, Guilbault and Lubrano fabricated the hydro-

gen peroxide detection sensor based on the lactate enzyme sensor. In this way, many researchers have fabricated many biosensors in these years.

6.1.2.3 Characteristics of biosensors

There are some static and dynamic conditions that must be met to create a highly effective and powerful biosensor system. These requirements allow for the performance of the biosensors to be enhanced for commercial applications which are as follows.

Selectivity: When choosing a bioreceptor for a biosensor, selectivity is an important attribute to be taken into account. A bioreceptor may identify a specific target analyte molecule in a sample that contains undesired pollutants and admixture compounds.

Sensitivity: It is defined as the smallest amount of analyte that can be accurately detected or recognized in the fewest steps at low concentrations (ng mL^{-1} or fg mL^{-1}) to confirm the presence of analyte traces in the sample.

Linearity: Linearity helps ensure that the findings of measurements are accurate. The substrate concentration can be detected at higher levels when linearity (straight line) is increased.

Reproducibility: Reproducibility is defined by precision (similar output when the sample is measured multiple times) and accuracy (the ability of a sensor to generate a mean value that is more closely related to the actual value when the sample is sampled multiple times). When the same sample is analyzed more than once, the biosensor's ability to produce the same results is what matters.

Stability: One essential quality in biosensor applications where ongoing monitoring is necessary is stability. Stability is the degree to which the biosensing equipment is vulnerable to environmental perturbations both inside and outside. The affinity of the bioreceptor (the degree of analyte binding to the bioreceptor) and bioreceptor degradation with time are the variables that determine stability.

Response period: It is playing a very crucial role in selecting the best sensor which is having short response time and recovery time factors which implies its effectiveness.

6.1.3 Classification of biosensors based on bioreceptors

Bioreceptors are regarded as the key element in the development of biosensors, as it was previously discussed. Enzymatic biosensors are the

most prevalent type of biosensor. Other types include immunosensors, which have high specificity and sensitivity and are particularly useful in diagnosis, aptamer- or nucleic acid-based biosensors, which have high specificity for microbial strains and nucleic acid-containing analytes, and microbial or whole-cell biosensors.

The second division is based on the transducer, and the sensors are divided into the following groups: electrochemical (which is further divided into potentiometric, amperometric, impedance, and conductometric groups), electronic biosensor, thermal biosensor, optical, and mass-based or gravimetric. Bioreceptor–analyte combinations fall under a different group and are few. Various classifications are made based on the technology (nano, surface plasmon resonance [SPR], biosensors-on-chip [lab-on-chip], electrometers, and deployable) and the detection sensor systems (optical, electrical, electronic, thermal, mechanical, and magnetic).

According to the quantity of interactions between analyte and bioreceptor, transducers produce visual or electrical signals. The working principle divides transducers into the following major categories: electrochemical, optical, thermal, electronic, and gravimetric transducers. Depending on the input, the output may take the form of a figure, numerical, graphic, or tabular result.

Catalytic and affinity/noncatalytic biosensors are two categories of biosensors that fall under the biorecognition principle. Analyte–bioreceptor interaction leads to the creation of a novel biochemical reaction product in a catalytic biosensor. Enzymes, microbes, tissues, and entire cells are all a part of this biosensor. An irreversible binding between the analyte and the receptor occurs in the case of affinity (noncatalytic) biosensors, and no new biochemical reaction product is produced as a result of the contact. The detection targets for this sort of sensor include antibodies, cell receptors, and nucleic acids.

6.1.3.1 Enzyme-based biosensors

Enzymes are typical biocatalysts that are effective at accelerating the rate of biological reaction. An enzyme-based biosensor's operation is based on the catalytic reaction and binding properties for detecting the target analyte. The process of recognizing analytes involves a number of potential mechanisms: analyte concentration is correlated with decreased enzymatic product formation because

1 The analyte is metabolized by the enzyme.

2 The analyte activates the enzyme.
3 The enzyme concentration is tracked by monitoring the change in enzyme characteristics.

Because enzyme-based biosensors have a long history, different biosensors can be created based on the specificity of the enzyme. Improving the sensitivity, stability, and flexibility of the enzyme structure is costly and difficult due to the exceedingly sensitive nature of the enzyme structure. For enzyme-based biosensors, electrochemical transducers are most frequently employed. Glucose and urea biosensors are the most used enzyme-based biosensors. Due to the long history of enzyme-based biosensors, many biosensors can be developed depending on the specificity of the enzyme (Schroeder & Cavacini, 2010).

6.1.3.2 Antibody-based biosensors

Affinity biorecognition elements like antibodies have been in use for more than 20 years due to their broad variety of applications and potent antigen–antibody interactions. Immunoglobulins (Ig) have a "Y" shape with two heavy and two light polypeptide chains joined by disulfide bonds, and antibodies have this structure as well. Immunosensors are biosensors that rely on the interaction between an antibody and an antigen or that incorporate antibodies as ligands.

There are two types of immunosensors:
1 Nonlabeled and
2 Labeled.

To precisely identify the antigen–antibody complex, nonlabeled immunosensors are built by calculating the physical alterations brought on by the formation of the complex. An easily detectable label is added in the case of labeled immunosensors (Bhardwaj et al., 2021).

6.1.3.3 Aptamer-based biosensors

The synthetic single-stranded nucleic acids known as aptamers can fold into two-dimensional (2D) and three-dimensional (3D) structures and can bind to target molecules in a selective manner. Because there is less spatial blocking and more surface area on the targets in 2D or 3D structures, their binding efficiency is high. Aptamers are nucleic acid molecules, which makes them physically and functionally stable throughout a wide variety of temperatures and storage conditions. Aptamers may be chemically synthesized, are stable in the pH range of 2–12, and have some

thermal refolding properties, in contrast to antibodies, which must be produced by biological systems. Aptamers also have the advantage of being chemically altered to meet the detection requirements for the target molecule. Fluorescent nanoparticles, like QDs, offer significant advantages over conventional fluorescent dyes for tracking biological systems in real time. Aptamer–QD conjugates were employed to pinpoint targets, including cancer cells, bacterial spores, and proteins (He et al., 2021).

6.1.3.4 Whole-cell-based biosensors

Since microbes (bacteria, fungi, algae, protozoa, and viruses) have the potential to serve as biorecognition components, they are used in the construction of whole-cell-based biosensors. They can manufacture recognition components, such as antibodies, on their own and without the need of extraction and purification. Whole-cell-based biosensors are simple to use and are developing quickly compared to animal or plant cells.

The whole-cell-based biosensor principle states that the cells may interact with a wide range of analytes, display the electrochemical response that a transducer can detect, and communicate. These biosensors were effectively used in environmental monitoring, food analysis, pharmacology, heavy metals, pesticides, detection of organic pollutants, and drug screening due to their high selectivity, good sensitivity, and capability of detection (Riangrungroj et al., 2019).

6.1.3.5 Nanoparticle-based biosensors

A new class of bioreceptor nanomaterials have recently been proposed in addition to the ones mentioned above. Numerous nanomaterials have been used as bioreceptors as a result of advances in nanotechnology and nanoscience. In terms of biosensing applications, nanoparticles offer a wider variety in both transducers and bioreceptors. For instance, nanomaterials based on cerium oxide show catalytic activity that is bioreceptor-friendly and mimics biological processes. Many inorganic materials, including graphene- and CNT-based nanomaterials, noble metal nanoparticles, and quantum dots, have been successfully used as transducers because of their effective transduction capabilities.

6.1.4 Emerging nanomaterials used in the fabrication of biosensors

Through specific self-assembly techniques nanomaterials are synthesized. These nanomaterials have many distinct properties including elec-

trical, mechanical, optical, and magnetic. Nowadays, many nanomaterials are used in drug delivery, bloodless surgery, multifunctional device fabrication, and the fabrication of biosensors. Nanomaterial-based biosensors have attained advanced properties compared to conventional biosensors. These nanobiosensors got epitome sensitivity, stability, and selectivity for the detection of various biomolecules.

Advanced nanomaterials are broadly classified into two types: 2D transition metals and 2D organic polymers.

6.1.4.1 Two-dimensional transition metals

Transition metals are those elements in groups 4–11 in the periodic table. Due to its intriguing characteristics, including a significant surface area and an ultrathin planar structure, transition metal nanomaterials can be used to create biosensors.

6.1.4.1.1 Transition metal chalcogenides

The transition metal dichalcogenides (TMDCs) are a class of 2D graphene cognate/nanosheets that are considered to be advanced. They are typically represented by the formula MX2, which stands for a hexagonal layer of a transition metal (M) and two layers of chalcogen (X). They can be made using a variety of techniques, such as mechanical cleavage, epitaxial growth, and chemical vapor deposition (CVD).

Recently, a hybrid structure of blue phosphorene (BlueP)/TMDCs, graphene, and Ag–Au bimetallic sheets was used to create a surface plasmon resonance (SPR)-based biosensor. The study's findings showed that compared to traditional biosensors, the monolayer BlueP/MoS2 and graphene structure significantly increase the biosensor's sensitivity by 19.73%.

A photoelectrochemical immunosensor for the detection of carcinoembryonic antigen was made using tungsten disulfide (WS2) nanosheets in a different investigation. The development of a gold nanoparticle (GNP)/WS2 nanocomposite. According to the performed investigation, the photoelectrochemical responses of WS2 combined with GNPs were improved (Singh et al., 2020). To achieve photoelectrical immune sensing of the antigen in clinical samples, the nanocomposite was coated onto a glass surface, and then, antibodies specific to carcinoembryonic antigens were immobilized. Additionally, 2D TMDC-de-

rived quantum dots have demonstrated their value in the optical detection of neurotransmitters without the use of antibodies.

6.1.4.1.2 Advanced transition metal oxides

Comparable to TMDCs, transition metal oxide displays a variety of distinctive qualities, such as electrocatalytic and magnetic capabilities, which make them a fantastic choice for use in the construction of biosensors. Due to their distinctive electrical, optical, and chemical properties in comparison to other transition metal oxides (TMOs), manganese oxides are the most widely employed advanced materials in sensing applications. TMOs and 2D transition metal carbides were combined in a recent work to create a biosensor.

For the separation and purification of proteins, a biosensor based on molecularly imprinted polymers has been developed. In this study, the surface of tubular carbon fibers with carboxyl modifications was grown with MnO_2 nanosheets. The outcomes demonstrated that the development of MnO_2 shells increases the quantity of protein-imprinting sites. An electrochemical biosensor was created to detect hydrogen peroxide using a MnO_2–graphene nanosheet nanocomposite on a glassy electrode. The findings of this study showed that TMOs' electrocatalytic activity is beneficial in the oxidation of H_2O_2, which results in the catalytic activity of the biosensor at extremely low concentrations. Metal–organic gels were utilized to create copper oxide nanoparticles, another TMO that can mimic peroxidase activity and be used to detect cholesterol and glucose. To create diverse nanostructures for drug delivery, therapy, and the monitoring of various diseases, 2D organic polymers are utilized. These polymers have the ability to mimic a wide range of biomolecules. These sensors have promising applications in clinical medicine, food analysis, environmental analysis, and other fields.

6.1.4.2 Two-dimensional organic polymers

Due to their exceptional qualities, including great flexibility and tunability, ultrathin structure, and adaptability, organic polymers have been employed extensively which are still in demand. Modified metal–organic frameworks and polypeptides are the two organic polymers in this group that are most frequently employed, and they have become the preferred materials for making biosensors.

6.1.4.2.1 Metal–organic frameworks

Inorganic and organic crystalline porous hybrid materials are arranged in metal–organic frameworks (MOFs) to form a cage-like structure. Typically, positively charged metal ions are surrounded by organic linker molecules. A MOF's hollow structure provides an incredibly large internal surface area which greatly increases its utility. Photodynamic treatment for tumors can be performed with organic polymer-based MOFs. By using platinum nanoparticles to magnify the signals, a MOF-based biosensing device has also been created for the detection of neurotransmitters. A MOF containing 2D palladium nanosheets, doxorubicin, and polydopamine was used to create a theranostic nanoplatform to improve biocompatibility. The application of this mixture as a medication delivery component resulted from its impressive photothermal conversion and optoacoustic properties. As a result, these nanoparticles can be used successfully in applications for sensing, imaging, and drug delivery when combined with other materials. They can also be employed for both treatment and bacterial eradication. A biosensor for augmented anti-infective therapy has been created using 2D carbon nanosheets generated from MOFs.

6.1.4.2.2 Black phosphorous

The most thermodynamically stable form of phosphorus is called black phosphorous (BP). Phosphorene, also known as BP, offers important characteristics as a nanomaterial, including strong electroconductivity, an ambipolar field effect, high carrier mobility, and an adjustable bandgap. For the purpose of creating biosensors for the diagnosis and treatment of various diseases in recent years, numerous researchers have employed BP. The application of a 3D BP nanoscaffold for recovering neurogenesis was the subject of a revolutionary work which is presented in the year 2020.

For instance, cellulose hydrogels were used in the construction of 2D BP nanosheets (BPNSs) for photothermal therapy against cancer. These hydrogels and BPNS 3D networks have improved stability, strong photothermal responsiveness, and flexibility. The clinical study demonstrates the unique applications of this nanoplatform which is also 100% safe and biocompatible. In another fascinating study, BP was used to construct a 3D-printed scaffold that participates in bone regeneration and is intended to be used in the photothermal ablation therapy of osteosarcoma. As a re-

sult, researchers frequently use BP to create nanodevices for the treatment of diseases due to their photothermal characteristics. A 2D fingerprint nanoprobe based on BP has been used to demonstrate an enhanced fabrication method for biological surface-enhanced Raman scattering (SERS) characterization. This work created flake-shaped BP–gold nanoparticle nanohybrid theranostic nanoplatforms for phototherapy, bioimaging, and drug delivery. Genome editing, antibacterial effectiveness, photodynamic anticancer therapy, imaging, and cancer theranostics have all utilized BP-containing biosensors.

6.1.5 Distinct platforms in the fabrication of advanced biosensor devices

In these decades, more advanced biosensing devices are fabricated using different device fabrication techniques. These biosensors are fabricated by many more techniques, viz., ion beams, microfluidics, near-field electrospinning, lab-on-a-chip, and chip calorimetry. Fabrication of the integrated biosensing device for local and real-time sensing applications got epitome scope. Micro- and nanoscale patterning on the surface of the sensor enhances the sensing performances by getting over the surface-based limitations. Miniaturization in device fabrication has helped to get remarkable sensing performances in biosensors. Several types of biosensors based on the different fabrication techniques are made, and they depicted better sensitivity and little limit of detection. Nowadays, versatile biosensors are being fabricated to detect various biomarkers or diseases, namely, cancer, cholesterol, bacterial infection, and exosomes.

6.1.5.1 Focused ion beam technique

This technique is usually used for the deposition of nanomaterials. These days, this technique has got widened the scope for the fabrication of the biosensing device. The probe attached to the ion beam is used for the fabrication of the biosensing devices. This technique is the more consistent way of preparing biosensing devices. Many more modifications are applied to the focused ion beam (FIB) technique to fabricate more reliable nanobiosensor devices. The FIB-made biosensors are compact, less costly, and can be used as a refractive index for various chemical and biological sensing applications (Erdman et al., 2019).

Principle: High- and low-gallium ion-beam focusing is used for site-specific sputtering in this technique.

Advantages: Multiple specimens are formed in a small area and are time efficient, and beam strength can be adjusted.

Disadvantages: The use of gallium may contaminate the samples, and physical and electrical properties can be affected.

6.1.5.2 Electrospinning

This is the oldest technique used by researchers for many decades. According to their convenience, the researchers have made many modifications to this technique for the fabrication of biosensors. By decreasing the electrode gap distance, one can successfully deposit the nanomaterials on the sensing device. Through the electrospray technique, this technique has evolved. M13 bacteriophage microfabrication has been achieved with this technique (He et al., 2017).

Principle: By decreasing the spinning gap, controllable deposition can be achieved.

Advantages: This method is simple and cost-effective, and large-scale processing is possible. All polymers (high molecular weight) can be easily processed by this method.

Disadvantages: This method is not suitable for 3D structures, and synergistic porosity for achieving good biosensing is unable to be achieved by this method.

6.1.5.3 Paper-based microfluidics

This technique is based on the principle of fluid action. The paper-based devices are easy to fabricate and of less cost. Usually, cellulose paper is used for the fabrication of the device followed by computer-based printing. The printing can be performed through different methods, namely, wax printing, laser printing, and conducting inkjet printing. Among these printing techniques, wax printing is widely used because it is effective, easier, and cost-effective. These paper-based microfluid devices will perform better sensitivity than other techniques. The paper-based CMOS photodiode biosensor is used to detect and diagnose sepsis (Hu et al., 2020). By using this paper-based sensing device, biomarkers are formed to detect glucose and lactate in human serum. A 3D paper-based sensing device with glucose detection has been developed to detect silver ions (Xiao et al., 2019).

Principle: This method is mainly based on fluidic actuation.

Advantages: This method is of low cost, easily desirable, simple, possibility of rapid detection, flexible substrate, easily degradable, and eco-friendly.

Disadvantages: This method is limited to multiple detections, it is not operable at room temperature, and extra heating is very much necessary for proper sensing.

6.1.5.4 Microelectromechanical systems

Microelectromechanical systems (MEMSs), nanoelectromechanical systems (NEMSs), and bio-nano-electromechanical systems (bio-NEMS) are the major biosensing fabrication techniques used for micro- and nanoscale device fabrication. For the detection of biochemical components, MEMS fabrication techniques are widely used (Bryzek, 2005). Bio-NEMS technique is majorly used to detect highly complex biochemical components. Moreover, the MEMS techniques are used in biosensors for diagnosis of diseases, therapeutics, and monitoring ecosystem and human health. To detect genome bacteria and viruses, a miniaturized silicon-chip biosensor has been fabricated by the MEMS technique (Battaglia et al., 2019).

Principle: This method is mainly based on capacitive piezoresistive resonant thermoelectric principle.

Advantages: Industrial production is possible, cost-effective, and low power consumption is possible for device fabrication.

Disadvantages: For the production of a single unit, it is too expensive, especially during the initial developmental stage.

6.1.5.5 Surface plasmon resonance-based biosensor

Using incident light to stimulate the electrons at the interfaces of the material is the basic technique of the SPR technique. An SPR biosensor is used to detect the gluten in the urine samples of people to detect celiac disease. A highly sensitive biosensor to detect microRNA was developed (Wei et al., 2020).

Principle: The incident polarized light falls on the metal film at the interface of the media with varying refractive index (RI).

Advantages: Miniaturized devices can be prepared with this method, and the devices prepared through this method are highly sensitive.

Disadvantages: Calibration has to be done for a long time.

6.1.5.6 Whispering-gallery-mode biosensors

Whispering-gallery-mode (WGM) biosensing devices are very much sensitive to biomolecules and chemical ions. Usually, this technique is used for the examination of the modifications occurring on the surface of the material. For the ultrasensitive detection of the biomolecules, this method is preferable. For the detection of the grapevine virus, an optical immunosensor device was fabricated using the WGM resonator technique (Fu et al., 2020; Tereshchenko et al., 2020).

Principle: It works on the principle of the wave that travels on the concave surface.

Advantages: Q-factor is high, low mode volumes, small size, easy to integrate with the chip, and high tenability.

Disadvantages: Bending loss and evanescent coupling loss are observed.

6.2 Conclusion

In these decades, tremendous improvements happened in the fabrication of biosensor devices for better management of health. These days, many more opportunities are opening for the development, implementation, and acquisition of versatile properties of nanomaterials in the fabrication of biosensors. The use of advanced 2D transitional materials and organic polymers has attained better sensitivity, selectivity, and stability in biosensors. The biocompatible nature, enhanced conductivity, and good sensing response of the nanomaterials and their composites made it easier to develop biosensing devices. Using nanomaterial composites leads to fabricating the sensing devices with less detection limit. These types of quick-responding, lower-LOD biosensing devices are used for health monitoring applications. The recently flourished SERS and WGM techniques have remarkable advantages for device fabrication, miniaturization, and possible easy handling. With the use of the new fabrication technology, using advanced nanomaterials finds a way to develop versatile devices for biosensing (Table 6.1).

Table 6.1 Timeline of the biosensors developed in these years.

Sl. no.	Researchers name	Year	Biosensor	References
1.	M. Cramer	1906	Electric potential arising between parts of the fluid	Cremer (1906)
2.	Soren Sorensen	1909	Concept of pH and pH scale	Sörensen and Mitteilung (1909)
3.	Griffin and Nelson	1909–22	First to demonstrate the immobilization of the enzyme invertase on aluminum hydroxide and charcoal	Griffin and Nelson (1916)
4.	W.S. Hughes	1922	Discovered a pH measurement electrode	Hughes (1922)
5.	Leland C. Clark	1956	Invented the first oxygen electrode	Heineman et al. (2006)
6.	Leland C. Clark et al	1962	Experimentally demonstrated an amperometric enzyme electrode for detecting glucose	Clark and Lyons (1962)
7.	Updike and Hicks	1967	First functional enzyme electrode based on glucose oxidase immobilized onto an oxygen sensor	Updike and Hicks (1967)
8.	Guilbault and Montalvo	1969	Reported the first potentiometric enzyme electrode-based sensor for detecting urea	Guilbault and Montalvo (1969)
9.	Bergveld	1970	Discovery of ion-sensitive field-effect transistor	Bergveld (1970)
10.	Guilbault and Lubrano	1973	Defined glucose and a lactate enzyme sensor based on hydrogen peroxide detection at a platinum electrode	Bergveld (1970)

Sl. no.	Researchers name	Year	Biosensor	References
11.	K. Mosbach and B. Danielsson	1974	Developed enzyme thermistor	Mosbach and Danielsson (1974)
12.	D.W. Lubbers and N. Opitz	1975	Demonstrated fiber-optic biosensor for carbon dioxide and oxygen detection	Lübbers and Opitz (1975)
13.	Suzuki et al.	1975	First demonstrated microbe-based immunosensor	Suzuki et al. (1975)
14.	Clemens et al.	1976	First bedside artificial pancreas	Clemens et al. (1976)
15.	Peterson	1980	Demonstrated the first fiber-optic pH sensor for in vivo blood gases	Yoo and Lee (2010)
16.	Schultz	1982	Fiber-optic biosensor for glucose detection	Schultz (1982)
17.	Liedberg et al.	1983	Surface plasmon resonance (SPR) immunosensor	Liedberg et al. (1983)
18.	Roederer and Bastiaans	1983	Developed the first immunosensor based on piezoelectric detection	Roederer and Bastiaans (1983)
19.	Cass. A. E	1984	First mediated amperometric biosensor	Cass et al. (1984)
20.	Pharmacia Biacore	1990	SPR-based biosensor	Mun'delanji and Tamiya. (2015)
21.	Poncharal et al.	1999	First nanobiosensor	Poncharal et al. (1999)
22.	S. Girbi et al.	2018	Nerve-on-chip-type biosensor for assessment of nerve impulse conduction	Gribi et al. (2018)

References

Amrutha, B.M., Manjunatha, J.G., Aarti, S.B., & Nagarajappa, H. (2021). Sensitive and selective electrochemical detection of vanillin at graphene-based poly (methyl orange) modified electrode. *Journal of Science: Advanced Materials and Devices*, *6*, 415-424. https://doi.org/10.1016/j.jsamd.2021.05.002.

Battaglia, S., Petralia, S., & Vicario, N., et al. (2019). An innovative silicon-chip for sensitive real time PCR improvement in pathogen detection. *Analyst*, *144*(7), 2353-2358.

Bergveld, P. (1970). Development of an ion-sensitive solid-state device for neurophysiological measurements. *IEEE Transactions on bio-medical Engineering*, *17*, 70-71.

Bhalla, N., Jolly, P., Formisano, N., & Estrela, P. (2016). Introduction to biosensors. *Essays in Biochemistry*, *60*, 1-8.

Bhardwaj, H., Sumana, G., & Marquette, C.A. (2021). Gold nanobipyramids integrated ultrasensitive optical and electrochemical biosensor for Aflatoxin B1 detection. *Talanta*, *222*, Article 121578.

Bryzek, J. (2005). Principles of MEMS. In *Handbook of measuring system design*. John Wiley & Sons, Ltd.

Cass, A.E., Davis, G., Francis, G.D., Hill, H.A., Aston, W.J., Higgins, I.J., Plotkin, E.V., Scott, L.D., & Turner, A.P. (1984). Ferrocene-mediated enzyme electrode for amperometric determination of glucose. *Analytical Chemistry*, *56*, 667-671.

Chethan, B., Ravikiran, Y.T., Vijayakumari, S.C., Rajprakash, H.G., & Thomas, S. (2018). Nickel substituted cadmium ferrite as room temperature operable humidity sensor. *Sensors and Actuators A: Physical*, *280*, 466-474.

Chethan, B., RajPrakash, H.G., Ravikiran, Y.T., Vijayakumari, S.C., & Thomas, S. (2019). Polypyyrole based core-shell structured composite based humidity sensor operable at room temperature. *Sensors and Actuators B: Chemical*, *296*, Article 126639.

Chethan, B., Raj Prakash, H.G., Ravikiran, Y.T., Vijayakumari, S.C., Ramana, C.H.V.V., Thomas, S., & Kim, D. (2019). Enhancing humidity sensing performance of polyaniline/water soluble graphene oxide composite. *Talanta*, *196*, 337-344.

Chethan, B., Prasad, V., & Thomas, S. (2022). Graphene-based sensing devices for soil moisture analysis. In *Electrochemical sensors based on carbon composite materials* (pp. 4-1-4–20). IOP Publishing. https://doi.org/10.1088/978-0-7503-5127-0ch4.

Chethan, B., Prasad, V., Sunilkumar, A., Veena, V.S., & Thomas, S. (2023). *Trends in development of nanomaterial-based sensing devices* (pp. 287-305). ACS Publishers. https://doi.org/10.1021/bk-2023-1437.ch012.

Clark, L.C., & Lyons, C. (1962). Electrode systems for continuous monitoring in cardiovascular surgery. *Annals of the New York Academy of Sciences*, *102*, 29-45.

Clemens, A.H., Chang, P.H., & Myers, R.W. (1976). Le développement d'un système automatique d'infusion d'insuline controle par laglycemie, son système de dosage du glucose et ses algorithmes de controle. *Journées annuelles de diabétologie de l'Hôtel-Dieu*, 269-278.

Cremer, M. (1906). Über die Ursache der elektromotorischen Eigenschaften der Gewebe, zugleich ein Beitrag zur Lehre von den polyphasischen Elektrolytketten. *Zeitschrift fur Biologie*, *47*, 562-608.

Dincer, C., Bruch, R., Costa-Rama, E., Fernández-Abedul, M.T., Merkoçi, A., Manz, A., Urban, G.A., & Güder, F. (2019). Disposable sensors in diagnostics, food, and environmental monitoring. *Advanced Materials.*, *31*, Article 1806739.

El-Denglawey, A., Angadi, V.J., Manjunatha, K., Chethan, B., & Somvanshi, S.B. (2021). Role of dysprosium in enhancing the humidity sensing performance in manganese zinc ferrites for sensor applications. *Journal of Materials Science: Materials in Electronics*, *32*, 23554-23565. https://doi.org/10.1007/s10854-021-06842-1.

El-Denglawey, A., Manjunatha, K., Vijay Sekhar, E., Chethan, B., Zhuang, J., & Angadi, V.J. (2021). Rapid response in recovery time, humidity sensing behavior and magnetic properties of rare earth (Dy & Ho) doped Mn–Zn ceramics. *Ceramics International*, *47*, 28614-28622. https://doi.org/10.1016/j.ceramint.2021.07.020.

Ensafi, A.A. (2019). An introduction to sensors and biosensors. In Ensafi A.A. (Ed.), *Electrochemical biosensors* (1st ed., pp. 1-10). Cambridge, MA, USA: Elsevier.

Ensafi, A.A., Karimi-Maleh, H., Ghiaci, M., & Arshadi, M. (2011). Characterization of Mn-nanoparticles decorated organo-functionalized SiO_2-Al_2O_3 mixed-oxide as a novel electrochemical sensor: Application for voltammetric determination of captopril. *Journal of Materials Chemistry*, *21*, 15022-15030.

Erdman, N., Bell, D.C., & Reichelt, R. (2019). Scanning electron microscopy. In *Springer handbook of microscopy* (pp. 229-318). Cham: Springer International Publishing.

Fu, L., Lu, Q., & Liu, X., et al. (2020). Combining whispering gallery mode optofluidic microbubble resonator sensor with GR-5 DNAzyme for ultra-sensitive lead ion detection. *Talanta*, *213*, Article 120815.

Gleiter, H. (2000). Nanostructured materials: Basic concepts and microstructure. *Acta Materialia*, *48*, 1-29.

Gribi, S., De Dunilac, S.B., Ghezzi, D., & Lacour, S.P. (2018). A microfabricated nerve-on-a-chip platform for rapid assessment of neural conduction in explanted peripheral nerve fibers. *Nature Communications*, *9*, 4403.

Griffin, E.G., & Nelson, J.M. (1916). The influence of certain substances on the activity of invertase. *Journal of the American Chemical Society*, *38*, 722-730.

Guilbault, G.G., & Montalvo, J.G., Jr. (1969). Urea-specific enzyme electrode. *Journal of the American Chemical Society*, *91*, 2164-2165.

Hareesha, N., & Manjunatha, J.G. (2021). Electro-oxidation of formoterol fumarate on the surface of novel poly (thiazole yellow-G) layered multi-walled carbon nanotube paste electrode. *Scientific Reports*, *11*, 12797. https://doi.org/10.1038/s41598-021-92099-x.

Hareesha, N., Manjunatha, J.G., Amrutha, B.M., Sreeharsha, N., Basheeruddin, A., Md, & Khalid, A. (2021). A fast and selective electrochemical detection of vanillin in food samples on the surface of poly (glutamic acid) functionalized multiwalled carbon nanotubes and graphite composite paste sensor. *Colloids and Surfaces A: Physicochemical and Engineering Aspects*, *626*, Article 127042.

Hareesha, N., Manjunatha, J.G., Pushpanjali, P.A., Prinith Subbaiah, N., Charithra, M.M., Sreeharsha, N., Basheeruddin Asdaq, S.M., & Md Khalid, A. (2021). Electrochemical sensing of antibiotic drug amoxicillin in the presence of dopamine at simple and selective carbon paste electrode activated with cetyltrimethylammonium bromide surfactant. *Monatshefte für Chemie*. https://doi.org/10.1007/s00706-021-02870-z.

He, X.X., Zheng, J., & Yu, G.F., et al. (2017). Near-field electrospinning: Progress and applications. *The Journal of Physical Chemistry C*, *121*(16), 8663-8678.

He, Y., Zhou, L., Deng, L., Feng, Z., Cao, Z., & Yin, Y. (2021). An electrochemical impedimetric sensing platform based on a peptide aptamer identified by high-throughput molecular docking for sensitive l-arginine detection. *Bioelectrochemistry (Amsterdam, Netherlands)*, *137*, Article 107634.

Heineman, W.R., Jensen, W.B., Leland, C., & Clark Jr (2006). (1918–2005). *Biosensors & Bioelectronics*, *21*, 1403-1404.

Hu, C.X., Annese, V.F., & Velugotla, S., et al. (2020). Disposable paper-on-CMOS platform for real-time simultaneous detection of metabolites. *IEEE Transactions on bio-medical Engineering*, *67*(9), 2417-2426.

Hughes, W.S. (1922). The potential difference between glass and electrolytes in contact with the glass. *Journal of the American Chemical Society*, *44*, 2860-2867.

Khanna, V.K. (2012). Introduction to nanosensors. In Khanna V.K. (Ed.), *Nanosensors: Physical, chemical, and biological* (1st ed., pp. 37-40). Boca Raton, FL, USA: CRC Press.

Liedberg, W., Nylander, C., & Lundstrm, I. (1983). Surface plasmon resonance for gas

detection and biosensing. *Sensors and Actuators. A, Physical*, *4*, 299-304.
Lübbers, D.W., & Opitz, N. (1975). The pCO_2-/pO_2-optode: A new probe for measurement of pCO2 or pO in fluids and gases (authors transl). *Zeitschrift für Naturforschung C*, *30*, 532-533.
Rupashree, M.P., Soppin, K., Pratibha, S., & Chethan, B. (2021). Cost effective photocatalytic and humidity sensing performance of green tea mediated copper oxide nanoparticles. *Inorganic Chemistry Communications*, *134*. https://doi.org/10.1016/j.inoche.2021.108974.
Manjunatha, J.G. (2020). A surfactant enhanced graphene paste electrode as an effective electrochemical sensor for the sensitive and simultaneous determination of catechol and resorcinol. *Chemical Data Collections.*, *25*, Article 100331.
Manjunatha, J.G., Deraman, M., Nur Hamizah, B., & Talib, I.A. (2014). Selective detection of dopamine in the presence of uric acid using polymerized phthalo blue film modified carbon paste electrode. *Advanced Materials Research*, *895*, 447-451.
Manjunatha, S., Machappa, T., Ravikiran, Y.T., Chethan, B., & Sunilkumar, A. (2019). Polyaniline based stable humidity sensor operable at room temperature. *Physica B: Condensed Matter*, *561*, 170-178.
Mosbach, K., & Danielsson, B. (1974). An enzyme thermistor. *Biochimica et Biophysica Acta*, *364*, 140-145.
Mun'delanji, C.V., & Tamiya, E. (2015). Nanobiosensors and nanobioanalyses: A review. In Mun'delanji C.V., Kerman K., Hsing I.M., & Tamiya E. (Eds.), *Nanobiosensors and nanobioanalyses* (1st ed., pp. 3-20). Tokyo, Japan: Springer.
Pal, S.L., Jana, U., Manna, P.K., Mohanta, G.P., & Manavalan, R. (2011). Nanoparticle: An overview of preparation and characterization. *Journal of Applied Pharmaceutical Science*, 06, 228-234.
Poncharal, P., Wang, Z.L., Ugarte, D., & De Heer, W.A. (1999). Electrostatic deflections and electromechanical resonances of carbon nanotubes. *Science (New York, N.Y.)*, *283*, 1513.
Pushpanjali, P.A., Manjunatha, J.G., Nagarajappa, H., D'Souza, E.S., Charithra, M.M., & Prinith, N.S. (2021). Voltammetric analysis of antihistamine drug cetirizine and paracetamol at poly (L-Leucine) layered carbon nanotube paste electrode. *Surfaces and Interfaces*, *24*, Article 101154.
Riangrungroj, P., Bever, C.S., Hammock, B.D., & Polizzi, K.M. (2019). A label-free optical whole-cell *Escherichia coli* biosensor for the detection of pyrethroid insecticide exposure. *Scientific Reports.*, *9*, 12466.
Ravikiran, Y.T., & Chethan, B. (2022). Humidity sensing studies on conducting polymers: Polyaniline and polypyrrole. *Inorganic Chemistry Communications*, *145*. https://doi.org/10.1016/j.inoche.2022.110019.
Roederer, J.E., & Bastiaans, G.J. (1983). Microgravimetric immunoassay with piezoelectric crystals. *Analytical Chemistry*, *55*, 2333-2336.
Pratibha, S., & Chethan, B. (2022). Carbon nanomaterial-based sensor safety in different fields. In *Carbon nanomaterials-based sensors* (pp. 315-332). Elsevier. https://doi.org/10.1016/B978-0-323-91174-0.00016-0.
Pratibha, S., Chethan, B., Ravikiran, Y.T., Dhananjaya, N., & Jagadeesh Angadi, V. (2020). Enhanced humidity sensing performance of Samarium doped Lanthanum Aluminate at room temperature. *Sensors and Actuators. A, Physical*, *304*. https://doi.org/10.1016/j.sna.2020.111903.
Shanawad, S.S., Sunilkumar, A., Khened, B.S., Chethan, B., Prasad, V., Kotresh, M.G., Sharanakumar, T.M., & Veena, V.S. (2023). Polyaniline/vanadium pentoxide/lead tetroxide ternary composite for LPG sensing. *Journal of Materials Science: Materials in Electronics*, *34*. https://doi.org/10.1007/s10854-023-09962-y.
Shanawad, S.S., Chethan, B., Prasad, V., Sunilkumar, A., & Veena, V.S. (2023). Humidity

sensing performance of the magnesium oxide nanoparticles. *Journal of Materials Science: Materials in Electronics*, *34*. https://doi.org/10.1007/s10854-022-09714-4.

Schroeder, W.H., & Cavacini, L. (2010). Structure and function of immunoglobulins. *The Journal of Allergy and Clinical Immunology*, *125*, S41-S52.

Schultz, J.S. (1982). *Oxygen Sensor of Plasma Constituents*. U.S. Patent No. 4,344,438A, 17 August 1982.

Singh, K.R.B., Nayak, V., Sarkar, T., & Singh, R.P. (2020). Cerium oxide nanoparticles: Properties, biosynthesis and biomedical application. *RSC Advances*, *10*, 27194-27214.

Sörensen, S.P.L., & Mitteilung, E., II (1909). Über die Messung und die Bedeutung der Wasserstoffionenkoncentration bei enzymatischen Prozessen [Enzyme studies. 2nd Report. On the measurement and the importance of hydrogen ion concentration during enzymatic processes]. *Biochemische Zeitschrift*, *21*, 131-304.

Suzuki, S., Takahashi, F., Satoh, I., & Sonobe, N. (1975). Ethanol and lactic acid sensors using electrodes coated with dehydrogenase–collagen membranes. *Bulletin of the Chemical Society of Japan.*, *48*, 3246-3249.

Sunilkumar, A., Khened, B.S., Chethan, B., Prasad, V., Kotresh, M.G., Sharanakumar, T.M., & Veena, V.S. (2023). Ultrahigh sensitive and selective room temperature operable poisonous carbon monoxide gas sensor based on polyaniline ternary composite. *Inorganic Chemistry Communications*, *150*. https://doi.org/10.1016/j.inoche.2023.110476.

Tereshchenko, A., Yazdi, G.R., & Konup, I., et al. (2020). Application of ZnO nanorods based whispering gallery mode resonator in optical immunosensors. *Colloids and Surfaces B*, *191*, Article 110999.

Theavenot, D.R., Toth, K., Durst, R.A., & Wilson, G.S. (2001). Electrochemical biosensors: Recommended definitions and classification. *Biosensors & Bioelectronics*, *16*, 121-131.

Tigari, G., & Manjunatha, J.G. (2019). Electrochemical preparation of poly(arginine)-modified carbon nanotube paste electrode and its application for the determination of pyridoxine in the presence of riboflavin: An electroanalytical approach. *Journal of Analysis and Testing*, *3*, 331. https://doi.org/10.1007/s41664-019-00116-w.

Updike, S.J., & Hicks, G.P. (1967). The enzyme electrode. *Nature*, *214*, 986-988.

Wei, X., Liu, D., & Zhao, M., et al. (2020). An enzyme-free surface plasmon resonance imaging biosensing method for highly sensitive detection of microRNA based on catalytic hairpin assembly and spherical nucleic acid. *Analytica Chimica Acta*, *1108*, 21-27.

White, R.M. (1987). A sensor classification scheme. *IEEE Transactions on Ultrasonics, Ferroelectrics, and Frequency Control*, *34*, 124-126.

Xiao, W., Gao, Y., & Zhang, Y., et al. (2019). Enhanced 3D paper-based devices with a personal glucose meter for highly sensitive and portable biosensing of silver ion. *Biosensors & Bioelectronics*, *137*, 154-160.

Yoo, E.-H., & Lee, S.-Y. (2010). Glucose biosensors: An overview of use in clinical practice. *Sensors*, *10*, 4558-4576.

CHAPTER 4

An Overview of Stability, Lifetime, and Reuse of Surfactant Sensors

A. SUNILKUMAR,*[a] B. CHETHAN,[b] V. PRASAD[b] AND S. MATTEPPANAVAR[c]

[a] Department of Physics, Ballari Institute of Technology and Management, Ballari-583104, Karnataka, India; [b] Department of Physics, Indian Institute of Science, Bangalore, Karnataka, India; [c] KLE Society's BasavaprabhuKore Arts, Science and Commerce College, Chikodi-591201, Karnataka, India
*Email: sunilanegundi@gmail.com

4.1 Introduction

The word surfactant is a contraction of surface active agents. These are chemical compounds that decrease the surface tension between liquid–gas, solid–liquid, and liquid–liquid. Surfactants behave as emulsifiers, detergents, foaming agents, and wetting agents. Every molecule comprises both hydrophilic and hydrophobic properties. Hydrophilic means the molecules have a quest for water molecules and hydrophobic relates to the exclusion of water molecules.[1] Surfactants in water form aggregates based on the chemical structure; these surfactants unite the hydrophilic head and hydrophobic tail. In general, for surfactants like foaming agents and emulsifiers, the dynamics at the interfaces play a significant role in their behavior. To achieve stabilization at an interface, the adsorption and desorption of surfactants, along with surface rheology, play an important role. Surfactants can be both toxic and non-toxic in nature.[2]

Detection Science Series No. 23
Surfactant-based Sensors in Chemical and Biochemical Detection
Edited by J. G. Manjunatha

Published by the Royal Society of Chemistry, www.rsc.org

Quats, also known as quaternary ammonium cations, are made by alkylating tertiary amines with halocarbons that have long alkyl chains. The charge of the quaternary ammonium compounds is independent of the pH of their solution. There are numerous quaternary ammonium compounds, including domiphen bromide, cetrimonium, cetrimide, didecyldimethyl ammonium chloride, benzethonium chloride, methyl benzothonium chloride, cetalkonium chloride, and dofaniumchloride. These quats have profound applications as antimicrobials in detergents and disinfectants. Based on the concentration level they can cause health problems to mankind, including mild skin and respiratory irritation.[3]

Surfactants uses in daily life are depicted in Figure 4.1. Human beings depend heavily on surfactants, which are used in a variety of processes such as cleaning, dispersion, wetting, foaming, and anti-foaming. Many surfactants are used in everyday applications, such as detergents, fabric softeners, motor oils, emulsions, soaps, adhesives, and inks. Surfactants are also used in formulations of agrochemicals like insecticides, spermicides and biocides. In personal care items like toothpaste, shampoo, shower gel, hair conditioners, and cosmetics, surfactants are also used. Oils in oil wells are mobilized using alkali surfactant polymers.[4] Bio-surfactants can be used in medicinal lotions and sprays on the surface of the skin and mucous membranes. Surfactants are used with quantum dots to control their growth. Surfactants have even brought a new era in the field of nanoscience.[5]

Chemical sensors are made of various sensory parts that have an additive effect on analyte detection. The classification of different chemical sensors

Figure 4.1 Surfactant usage in day-to-day life.

includes optical, electrical, acoustic wave, and potentiometric systems. Sensor components are chosen based on their preferred sensing characteristics, such as sensitivity, selectivity, method of detection, response and recovery time, specificity for a given class of analyte, and molecular interaction.[6] A multi-analyte test demonstrates the efficiency of the sensor, which employs various, unique sensor materials for targeted analyte detection in a mixture. Development of single-sensor technology for a target analyte based on physical, optical, and electrical characteristics comprises particular molecular targets to sustain strong and specific binding with the analyte. The performance of chemical sensors is frequently enhanced by inhibited sensing settings and changes in the ambient environment. In order to enable sensing in various combinations under all circumstances, chemical sensors work *via* an arrangement of conjunctional responses of cross-reactive sensors. A specific analyte's fingerprints are produced by combinatorial reactions to its various components. A complex mixture of phospholipids (PL) and proteins (SP) called pulmonary surfactant lowers surface tension at the air–liquid interface of the alveolus, preventing its collapse during end-expiration. Additionally, it helps the host's natural defenses against infections that are inhaled.[7]

Pneumocytes in human gestation secrete surfactant. It is mostly composed of cholesterol, phospholipids, protein, and neutral lipids. Dipalmitoylphosphatidylcholine (DPPC) phospholipid is the main surface-active agent of this surfactant. Surfactant proteins include SP-A, SP-B, SP-C, and SP-D. Surface tension is reduced and surface pressure is increased by surfactant. High surface pressure prevents the alveolar surface area from shrinking, whereas low surface tension maintains lung stability by lowering the pressure gradient of the surfactant.[8]

Olivera Galovic *et al.* have described a new graphene-based surfactant sensor for the detection of anionic surfactants in real samples. The dimethyldioctadecylammonium–tetraphenylborate (DDA–TPB) ion pair is used as a sensing material, and graphene is used as the supporting material, to create a new high-sensitivity potentiometric solid-state sensor for the measurement of anionic surfactants.[1] Dubravka Madunic *et al.* have shown the detection of cationic surfactants employing a novel sensitive potentiometric sensor in pharmaceutical disinfectants. A novel, sensitive potentiometric surfactant sensor was developed using a highly lipophilic 1,3-didecyl-2-methylimidazolium cation and a tetraphenylborate antagonist ion. This sensor was inserted into a PVC-membrane that had been plasticized as a sensing component. These sensors exhibited effective sensing applications in biochemical detection.[2] Nikola Sakac *et al.* reported a study of anionic and non-ionic surfactants in disinfectants and personal care products by direct potentiometry using a new surfactant sensor based on 1,3-dihexadecyl-1*H*-benzo[*d*]imidazol-3-ium. Results from direct potentiometric titrations of readily available cleaning products and personal care products that included cationic surfactants were in good agreement with those obtained by employing a surfactant sensor.[10,11] Hui Li *et al.* utilized acetylene black

electrodes enhanced with zwitterionic surfactant and carbon nanotubes to detect triclosan in household products. A brand-new electrochemical sensor based on acetylene black, carbon nanotubes, and cetylsulfonylbetaine was developed to measure triclosan and used as a sensitizing material.[12]

There are many different mechanisms that stabilize surfactants. Use of pH buffers, chelating agents, and anti-foamers are all part of chemical stabilization. Selecting surfactant characteristics like charge, hydrophobicity, and hydrophilicity carefully is the key to achieving physical stabilization. Using surfactants and co-solvents allows microemulsions to be stabilized. The utilization of naturally occurring or biodegradable surfactants allows for the stabilization of biological processes.

Surfactants are molecules with a hydrophilic head that attracts water and a hydrophobic tail that repels it. They are employed in a number of products, including emulsifiers, detergents, and shampoos. The kind of surfactant, the concentration of surfactant, the pH of the solution, the temperature, and the presence of other substances in the solution are all variables that affect how stable a surfactant solution will be. The stability of a surfactant solution is significantly influenced by the type of surfactant used. It is crucial to select the appropriate type of surfactant for the application since some surfactants are more susceptible to degradation than others. Its stability is also influenced by the surfactant's concentration. Generally speaking, more stability will result from higher surfactant concentrations.[13]

A surfactant sensor's lifespan is influenced by the type of sensor used and the application. A surfactant sensor typically has a lifespan of several months to several years. This can be impacted by elements such as surrounding conditions, temperature, and mechanical or chemical stress.

There are many uses for recycled surfactant sensors. They can be used to control the addition of surfactants to industrial process streams, measure the concentration of surfactants in water and wastewater, monitor the effectiveness of surfactant-based treatments of contaminated soils, detection, and tracking the presence of oil and grease in air and water. They can be used in agriculture to identify pesticide presence, track the concentration of surfactants in agricultural runoff, and assess the efficacy of surfactant-based crop disease treatments. They can be used in the medical industry to gauge the amount of pharmaceutical surfactants present and to track how well respiratory disorders are being treated with surfactant-based therapies. They might be utilized in industrial settings to keep an eye out for dangerous surfactants in the streams of industrial process.[14]

This chapter on surfactant sensors focuses more on the design and development of highly stable, enhanced lifespan and reusable sensors for chemical and biochemical detection. Some examples of fascinating research fields that support the field of surfactant sensors include optical, thermal, and surface acoustic wave sensors. Chemical sensor research appears to have undergone a significant shift recently. It is among the most productive, interesting, and interdisciplinary analytical chemistry research topics. In

addition, it seems to be one of the most experimental disciplines right now, where fresh ideas and thoughts have been recently explored.[12]

4.2 Classification of Surfactants

Surfactants are almost identical in nature, and comprise a hydrocarbon chain which can be framed as linear, branched, or aromatic in nature. Fluorocarbon and siloxane surfactants have identical chains and many surfactants consist of polyether chains usually ending with polar anionic groups. These materials enhance the hydrophilic property of the surfactants. Polypropylene oxides contrarily enhance the lipophilic property of a surfactant. The tail comprises the chain formation of the surfactant molecule. Based on their solubility, surfactants are mainly categorized into hydrophilic and hydrophobic, which are soluble in water and lipids respectively. Most ionic surfactants are usually water soluble.[13] Surfactant types and their general applications are shown in Figure 4.2.

Surfactants are classified into four types based on their charge of their polar head group, generally:

1. Anionic surfactants
2. Cationic surfactants
3. Non-ionic surfactants
4. Amphoteric surfactants

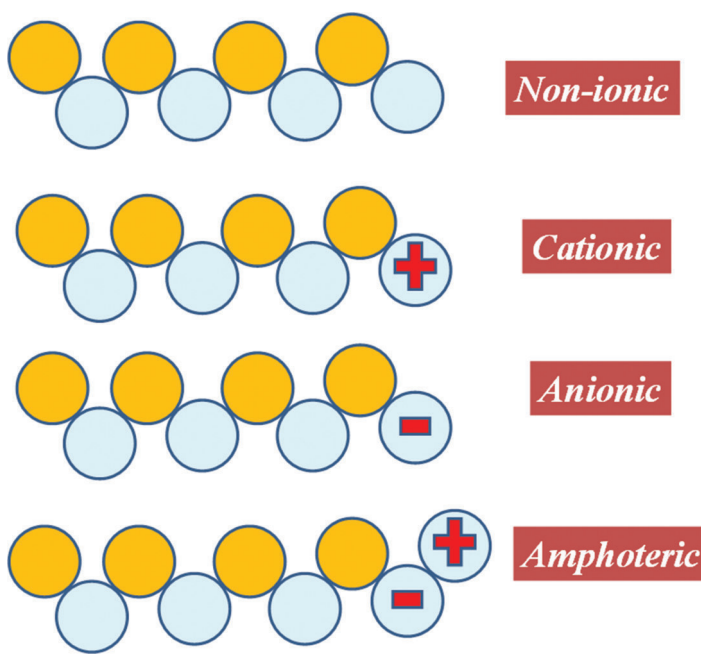

Figure 4.2 Classification of surfactants based on their composition.

4.2.1 Anionic Surfactants

The charge of the head group is generally negative and such a group comprises of sulfates, sulfonates, phosphates, and carboxylates. The most important alkyl sulfates are sodium lauryl sulfate, ammonium lauryl sulfate, sodium myreth sulfate and alkyl ether sulfates.[14] Sodium stearate incorporated in carboxylate salts produces perflorooctanaesulfonate, Doclsate along with special characteristics in sodium lauryl sarcosinate and carboxylate-based fluorosurfactants.[15] The general applications of these surfactants are shampoos and dishwashing liquids. The most common surfactants include alkyl ether sulfates, soaps, alkyl benzene sulfonates, and alkyl sulfates.

4.2.2 Cationic Surfactants

The charge of the head group is generally positive, which exhibits pH-based surfactant properties. Cationic surfactants possess adsorption behavior on charged surfaces. Most cationic surfactants comprise quaternary ammonium compounds. These surfactants can be used in softening agents, hydrophobic agents, and for hydrotropism and antistatic applications.[16]

4.2.3 Non-ionic Surfactants

These surfactants are formed by enclosing the non-charged head group. Formation of a covalent bond between the surfactants leads to a change in its structure. The oxygen-containing hydrophilic groups are covalently bonded to the hydrophobic parent molecule. The water solubility of the surfactant is the direct cause of the formation of hydrogen bonding at a particular temperature. The sensitivity of non-ionic surfactants reduces with hardness of the water. Dissociation of ions in hydrated solutions does not occur with non-ionic surfactants.[17]

4.2.4 Amphoteric (Zwitterionic) Surfactants

The charge on the head group consists of both positive and negative charges. The dual nature of these surfactants arises from both of the charged centers of the same molecule. Cations are formed by primary, secondary and ternary ammonium cations; anions are formed by CHAPS (3-[(3-cholamidopropyl)dimethylammonio]-1-propanesulfonate, sulfonates, and cocamidopropyl. These surfactants have biological applications with the formation of amines such as phospholipids, phosphatidylethanolamine, phosphatidylserine and sphigomyelins.[18]

4.3 Characterization Methods for Surfactants

Surfactants play a crucial function in the mixing of liquids and when they come into contact with solid materials as wetting agents, emulsifiers,

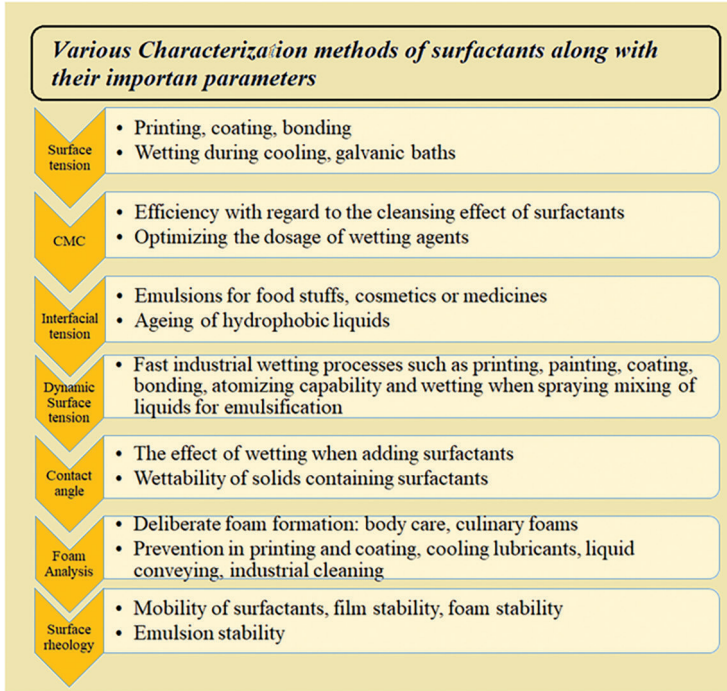

Figure 4.3 Various characterization methods and their uses.

cleansers, or foaming agents. Figure 4.3 shows the various characterization methods for surfactants along with their applications. The creation, optimization, and proper dosage of surfactants are usually thorough analysis of the interface. We can assess the effectiveness and efficiency of surfactants using tensiometers, which measure surface tension. They aid in the construction and optimization of emulsions by precisely measuring the interfacial tension. The knowledge required to use surfactants in quick processes is provided by dynamic tensiometers. The degree of wetness can be accurately determined by analyses performed with contact angle measurement equipment. Furthermore, a foamy product can be optimized or foam avoided with the use of foam analysis tools.[19] The different types of characterization methods for surfactants are:

- Measurement of surface tension.
- Measurement of the critical micelle concentration (CMC).
- Measurement of the interfacial tension between liquids.
- Measurement of dynamic surface tension and interfacial tension.
- Measurement of contact angle.
- Foam analysis.
- Surface rheological investigations.

4.3.1 Measurement of Surface Tension

The high surface tension of water makes it difficult to moisten hydrophobic surfaces and particles. Surfactants reduce surface tension, which helps to moisten solid surfaces and make powders more dispersible. Tensiometers precisely measure the surface tension, in order to calculate the impact of the surfactant. Drop shape analysis equipment uses optical pendant drop measurements to analyze the smallest sample volumes.[20]

4.3.2 Measurement of the Critical Micelle Concentration (CMC)

The level at which all of the surface is covered in surfactant molecules is known as the critical micelle concentration (CMC). Surfactant molecule clusters, or micelles, start to appear in the solution above this concentration. Micelles, which can accept and mobilize hydrophobic molecules, are among the factors that contribute to a surfactant's cleansing action. CMC measurement can be used to determine the surfactant concentration at which the cleansing effect becomes apparent.[21]

4.3.3 Measurement of the Interfacial Tension Between Liquids

Surfactants act as emulsifiers by lowering the interfacial tension between incompatible phases and enhancing mixing. They simultaneously facilitate the formation of tiny droplets and stabilize the emulsion by slowing or preventing droplet fusion. The interfacial tension between a liquid and water determines its hydrophobic nature. The interfacial tension is therefore measured in order to assure the quality of liquids where a phase mixing with water is undesirable.[22]

4.3.4 Measurement of Dynamic Surface Tension and Interfacial Tension

Various applications and manufacturing processes involve the rapid formation of surfaces and interfaces. But the diffusion and adsorption times for surfactants are very particular. Consequently, the surface tension and interfacial tension are influenced by the amount of time that has passed for the development of a new phase boundary. As a result, with dynamic processes, in a steady state, the interfacial tension or surface tension might be significantly larger. The appropriate selection and dosage of a surfactant are substantially impacted by the circumstances. Dynamic surface tension is visible above the surface, using bubble pressure tensiometers. Printing, painting, coating, and bonding are quick industrial wetting processes.

Atomization and its ability to moisten liquid emulsification are possible through mixing.[23]

4.3.5 Measurement of Contact Angle

When a surfactant is added, the wetting of a liquid is improved to a certain extent, which is indicated by the contact angle. Depending on the requirement, the contact angle is measured by drop form analysis tools with a high degree of automation. The conditions of a wetting process can be accurately simulated by measurements at high or low temperatures, under controlled humidity, or with varying dosing dynamics.[24]

4.3.6 Foam Analysis

Surfactants regularly create foams and are frequently employed alone to do so. Specific application areas necessitate varied standards for foamability, foam stability, moisture content, and bubble size. Foam analysis tools measure the foam height with relation to time using repeatable foam generation processes and methods. A conductivity module can measure the amount of moisture in the foam as well as how the height of a foam column changes over time at various heights. For the purpose of specifically optimizing the foam's characteristics, an optical foam structure analysis module estimates the bubble size distribution and its time dependency.[25]

4.3.7 Surface Rheological Investigations

In surface rheology, the rate of change in the interface region is compared to the rate of change in surface tension or interfacial tension. Surface rheology equipment evaluates a number of factors, including the interface viscosity and elasticity. Using these numbers, inferences can be made about the stability of liquid films and droplets in emulsions, as well as the mobility of surfactants. Additionally, the outcomes are typically connected with foam properties like drainage rate and foam bubble stability.[26,28,29]

4.4 Stability of Surfactant Sensors

Surfactants are ''head-and-tail'' molecules that interact with other molecules in a solution. The hydrophobic/hydrophilic balance, head and tail size, charge, and other parameters affect the stability of a surfactant solution. The stability of the solution may be harmed if the surfactant concentration is too high because it may become overly viscous and form an impenetrable layer. The stability of the surfactant is also influenced by the pH of the solution. The majority of surfactants are most stable at a pH of 7. The stability of the solution can be decreased by surfactant molecule breakdown brought on by an excessively high or low pH. Surfactant stability is also influenced by the temperature of the solution, that is, lower

temperatures can result in the surfactants precipitating out of solution, while higher temperatures typically increase stability. The stability of the surfactant may also be impacted by the presence of other compounds in the solution. The surfactant stability can be decreased by interactions with certain chemicals, such as salts. Making sure that all these elements in the solution are compatible with the surfactants is crucial for their stability. Some of them are given below:

1. Balancing between hydrophilic and hydrophobic molecules: the hydrophilic (attracted to water) head of the surfactant molecule and the hydrophobic (repelled by water) tail (not attracted to water). When the equilibrium between hydrophobic and hydrophilic molecules is preserved, a surfactant solution is stable.
2. Size of the head and tail: the solubility of the surfactant in a solution depends on the size of the head and tail. The surfactants with larger heads and tails are more soluble.
3. Charge: the charge of the surfactant molecule has the potential to impact stability. Positively charged surfactants tend to be more stable, whereas negatively charged surfactants are less stable.
4. Temperature: the stability of a surfactant solution can be impacted by temperature. Lower temperatures increase stability.
5. Solvent: the choice of solvent can have an impact on how stable a surfactant solution is. A surfactant's stability is more likely to eteriorate in polar solvents like water than in non-polar solvents like oils.
6. Critical micelle concentration (CMC): the CMC is the amount of surfactant molecules present in a solution that is required for the formation of micelles. Micelles are surfactant molecule aggregations that form a stable, spherical structure that can aid in stabilizing emulsions and raising surface tension.
7. pH: surfactant stability is significantly influenced by the pH of a solution. Surfactants are more soluble and stable at higher pH levels.
8. Additives: surfactant solutions can be supplemented with additives to improve the stability of the surfactant. Electrolytes, alcohols, and polymers are examples of typical additives.
9. Molecular weight: the stability of a surfactant in aqueous solutions is significantly influenced by its molecular weight. Surfactants with a higher molecular weight are typically more stable than those with a lower molecular weight.
10. Chain length: the chain length of a surfactant has a significant impact on its stability in aqueous solutions. Short-chain surfactants are frequently less stable than long-chain surfactants.

4.5 Lifetime of Surfactant Sensors

Depending on the type of sensor, the usage environment, and the frequency of use, the lifespan of surfactant sensors can vary significantly. Surfactant

sensors typically survive up to 10 years, while some can last far longer, depending on the usage circumstances. The lifespan of a surfactant sensor may be impacted by the following factors:

1. Chemical exposure: some substances, such as acids and bases, which can corrode the electrodes, can harm sensors.
2. Temperature: extreme heat will short circuit a surfactant sensor by causing condensation to form on the electrodes; low temperatures will prolong the life of a surfactant sensor.
3. Humidity: excessive humidity can lead to electrode degradation, while low humidity can lead to the sensor drying up and malfunctioning.
4. Electrical interference: electrical interference can affect the sensor readings and lead to the sensor failing before its time.
5. Contamination: the sensor may malfunction or fail if it is contaminated with dust, dirt, oil, or other contaminants.
6. Use frequency: using a sensor frequently might shorten its lifespan by causing it to wear out more quickly than if it is used less frequently.

Surface bubbles are a common occurrence in many natural phenomena and technical applications. There are several theories and some experimental research, but a thorough comprehension of the lifetime phenomenon is still lacking. In view of the simulations and past findings, we will also analyze the trends in the lifetime of bubbles and drops, which have been documented in earlier experimental research.

The lifespan of surfactant sensors can be increased in the following ways:

1. Consistent maintenance: consistent maintenance is necessary to prolong the life of the sensors and ensure that they are functioning properly. Cleaning and part replacement should both be done on a regular basis.
2. Temperature control: keeping temperatures under control can extend the lifespan of surfactant sensors. Keep the temperature within the prescribed range and store the sensors in a cool, dry location.
3. Correct installation: surfactant sensors can be damaged and have their lifespan shortened if they are not installed properly. For the sensors to have the longest possible lifespan, it is crucial to make sure they are installed correctly.
4. Consistent calibration: the sensors must be calibrated consistently in order for them to function accurately and effectively. Their lifespan will be extended as a result of this.
5. Protective coating: to shield the sensors from the elements and lengthen their lifespan, a protective coating can be added.

4.6 Reuse of Surfactant Sensors

Many industries, such as cosmetics, laundry detergents, and cleaning goods, allow the reuse of surfactants. It can be done by employing a variety of

methods, including recycling, centrifugation, distillation, and electrolysis. Used surfactants must be broken down into their component elements in order to be recycled. Surfactants and water or other contaminants are separated using centrifugation. Using evaporation, the process of distillation allows components of a mixture to be separated. An electric current can be used to purify compounds in a process called electrolysis. Reusing surfactants can cut waste and save money by lowering environmental pollution.

When reusing surfactants, however, the following safety measures must be taken:

1. Verify that no dangerous substances are present in the surfactants.
2. When handling surfactants, keep your skin and eyes away from contact, and use protective gear.
3. Ensure that surfactants are stored safely away from heat sources, sparks, and open flames.
4. In compliance with local laws, dispose of any unused or contaminated surfactant.
5. Before reusing a surfactant, familiarize yourself with its risks by consulting safety data sheets (SDSs).

4.7 Chemical Surfactants and Sensing

In order to simulate the function of olfaction, many chemical sensor arrays have been created with the intention of integrating an electronic nose with a range of materials. Figure 4.4 shows chemical surfactants in chemical sensing. Combining pattern recognition techniques with chemical sensor arrays replicates biological sensory recognition techniques. There are electronic nose systems for sale that are used in the food sector to ensure product quality. Current research focuses on the use of consumer-grade wearable electronic devices and commercial equipment to implement the electronic nose principle in environmental monitoring and medicine.

The idea that analytes will interact with various materials in different ways is at the core of chemical sensor arrays. As a result, any type of material may be utilized in sensors.[27] Polyacetylene, polythiophene, and polyaniline are some of the substances that can be chemically doped to make them conductors. The chemical and morphological properties of conductive polymers are affected by monomer identity, polymerization conditions, and device fabrication techniques.

Figure 4.5 shows the structure of surfactants and micelle formation. The ions that surround ionic surfactant micelles in solution, referred to as counterions, are attracted electrostatically. The effects of micelle charge on the structure of the surrounding solvent are visible at substantial distances from the micelle, despite the fact that the closest counterions can partially hide a charged micelle. The electrical conductivity of the mixture is one of the numerous qualities influenced by ionic micelles. Smaller ionic micelles

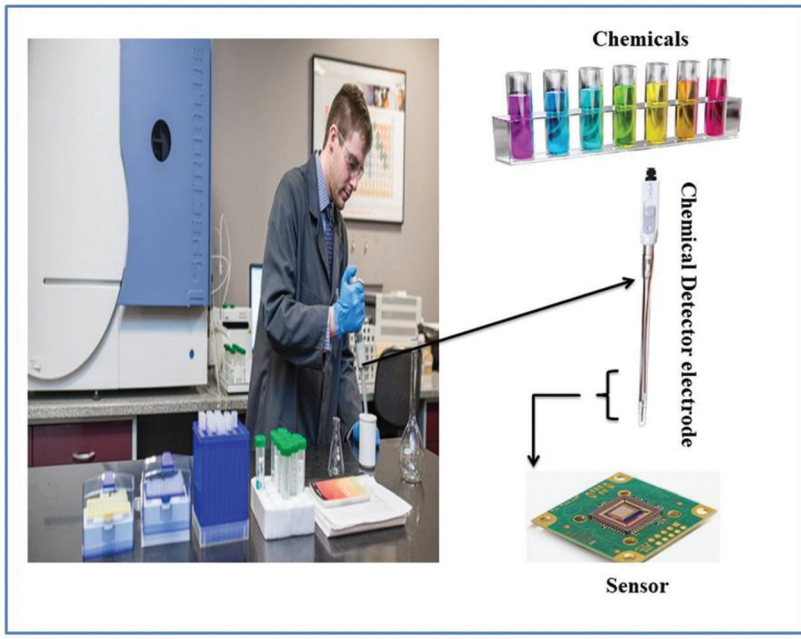

Figure 4.4 Usage of surfactants in chemical detection.

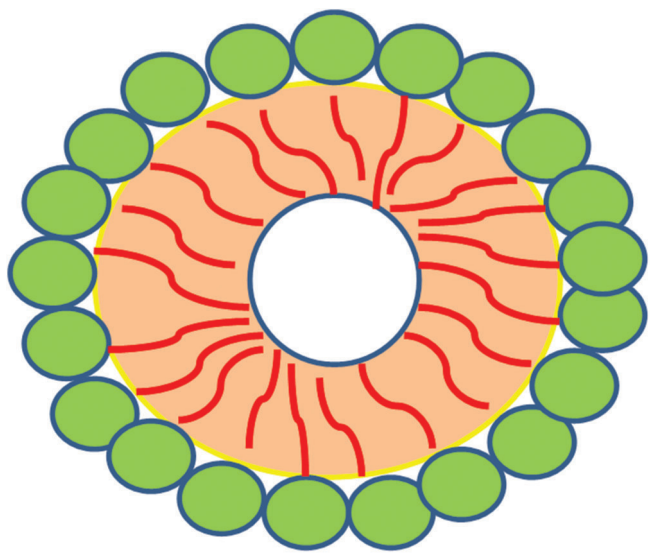

Figure 4.5 Structure of a micelle.

can be generated when salts are added to a colloid containing micelles, weakening the electrostatic connections in the process.

The response from the sensing device is recognized and processed using a known array of data patterns. The identification of signals is analyzed by various processes including the principal component method, neural network method, least square method, and machine learning for designated analysis of certain sequences. Chemical sensors play a major role in the analysis of data pertaining to sensing devices. The investigation of sensing parameters depends on various factors to give information on both qualitative and quantitative aspects of a sensor. Based on the techniques used for sensing properties, chemical sensors are usually classified into four types, namely, electronic chemical sensor, acoustical wave chemical sensor, optical chemical sensor, and electrochemical sensor.

4.7.1 Electronic Chemical Sensors

The modulation of an electronic signal has become of prime importance in these kinds of sensors. These sensors employ semiconducting materials, nanomaterials, and conducting polymers as sensing materials to enhance the sensitivity of the sensor. The basic design of chemical sensor comprises chemiresistors with capacitors and transistors in the architecture of a sensor. The variation in resistance is due to chemisorption or physisorption of the target molecules.[12] Various categories of materials for use of nanoelectronic detection systems have been discovered, notably graphene, carbon nanotubes, and 2D and 3D framework materials. Leading-edge location flaws and surface modification by covalent or non-covalent modifications are utilized as host–guest interaction sites in graphene-based materials, respectively.[30] An example of this involves the alteration of single-walled carbon nanotubes with multiple important protective factors to enable separation of volatile organic compounds.

4.7.2 Optical Chemical Sensors

Optical chemical sensor grids use light to examine chemical relations between an analyte and a sensing material, which distinguishes them from electronic chemical sensing devices. Generally, optical sensors use quantitative approaches like absorbance, diffraction, fluorescence, refraction, and scattering for examining how molecules react to light. Fluorescence sensors typically display better sensitivity than other imaging sensors.[31] The phrase ''optoelectronic nose'' has been utilized to categorize optical chemical sensor devices by constructing thumbprints for particular compounds and using predictive modelling to recognize those components in mixtures.[32] In addition to selectively engaging with solutes, optical sensors require two aspects: a probe material and a fluorophore. The chemical interactions between probes and analytes

should be properly taken into account when developing cross-reactive optical and fluorescent matrices.[33,34]

4.7.3 Acoustic Wave Chemical Sensors

Acoustic wave devices, thickness shear mode resonators (TSM), and quartz crystal microbalances are just a few of the very broad categories of wave device technology. These devices oscillate at fixed frequencies, and variations in the mass of the device modulate particular frequencies. These devices can be modified using a number of the materials that have previously been described as also being suitable for chemical sensor arrays. The broad range of inter-molecular reactivity and specific interactions with such a variety of compounds that each of these materials exhibits, when combined, permits the fingerprint detection of individual compounds in mixtures.[35]

Wave devices can be adapted for various combinations of volatile organic chemicals, hydrogen gas, and mercury vapor. These materials use microfabricated metal-oxide cantilevers that have polymer sheets on top of them. These higher-order sensors use bulk and surface acoustic wave devices, in addition to electrical and optical signaling molecule channels.[11]

4.7.4 Electrochemical Sensors

Electrodes are different classes of material that can be utilized in electrochemical sensing devices. Electronic tongues are a common name for electrochemically based sensors. The surface of an electrode can be altered, which allows the system to target specific molecular interactions. The ability of partially permeable membrane materials to specifically oxidize or reduce targeted particles allows electrodes to be converted into sensors.[37] The ability to monitor the amounts of nitrate, nitrite, and ammonium in an aqueous phase has been demonstrated for a number of selectively permeable membrane sensors built from potentiometric polymers such as poly(vinyl chloride). The technique, which has been pioneered using these voltametric and potentiometric methods, is a popular subject of study since it provides classification of redox products as well as multi-analyte analysis of aqueous solutions such as cerebrospinal fluid.[36]

4.8 Surfactant Sensors in Chemical Detection and Application

4.8.1 Anionic Surfactant Sensors

Anionic surfactant sensors are used in thin films for analyzing conjugated polydiacetylenes based on imidazolium. In recent years, research on polydiacetylenes (PDAs), which are produced by UV irradiating self-assembled diacetylene (DA) supramolecules, has received a lot of attention.

Numerous PDA-based chemosensors have been developed as a result of its stimulus-induced blue-to-red shift. An example of an anionic surfactant-selective sensor based on PDA and an imidazolium polymer exhibited fluorescence amplification and colorimetric alterations in the presence of several anionic surfactants.[37] The conducting nature of poly(3,4-ethylenedioxythiophene) was significantly increased by incorporating anionic surfactants into the polymer solution, producing poly(styrenesulfonate) films. Addition of anionic surfactants to PEDOT:PSS aqueous solution has been suggested as a strategy to improve the conductivity of PEDOT:PSS film. According to the study, TsO anions improved the conductivity of PEDOT:PSS when added to its aqueous solution. The preparation of conducting polymer films involved spin-coating the polymer solution on glass substrates.[38]

Anionic sensors can be employed in cationic–anionic surfactant two-phase systems where temperature-sensitive aqueous surfactants manifest interesting phase behaviors and features. The cationic and anionic surfactant aqueous mixtures are mostly the result of electrostatic interactions between opposing charged head groups.[8,41] These interactions can be tuned to form different microstructures with distinctive geometries ranging from spherical to cylindrical to planar, which have been extensively researched both theoretically and empirically in the literature.[39]

4.8.2 Cationic Surfactant Sensors

A cationic surfactant–liquid crystal sensor platform for detecting thrombin has been developed. Based on the high specificity of aptamer identification, the liquid crystal (LC) sensing platform was shown to be effective. At first, LCs doped with octadecyl-trimethyl ammonium bromide (OTAB), a cationic surfactant, adopted a homeotropic orientation matching a dark optical picture. Thrombin and the matching aptamer were used to build the LC sensing platform.[40] The detection of thrombin by the LC sensing platform exhibited outstanding, consistent performance. A sensitive quinoline yellow sensor based on liquid crystals coated with cationic surfactants exhibited effective results in chemical detection. One of the synthetic colorings widely used in the food business is quinoline yellow (QY). The development of precise and straightforward QY detection procedures is crucial to guarantee food safety. In order to lower risk, it is crucial to effectively detect this food colorant. By using a cationic surfactant-decorated LC interface, an inventive liquid crystal (LC)-based sensor was created for the label-free and ultrasensitive detection of the QY.[41] This work is the first to describe how cetyltrimethylammonium bromide (CTAB) affects the electrochemical behavior of folic acid (FA) on the surface of a carbon paste electrode (CPE) in actual samples. Cyclic voltammetry (CV), chronocoulometry, and differential pulse voltammetry (DPV) were used to conduct the experiments.[45] Creation of a folic acid (FA) sensor based on the CTAB enhancing effect. Various electrochemical analyses of FA in the presence of CTAB have been explored.[42,46]

4.8.3 Non-ionic Surfactant Sensors

Poly ethoxylated non-ionic surfactant determination using a potentiometric sensor has been investigated. Different ethoxylated non-ionic surfactants (EONSs) and polyethylene glycols were examined using a novel liquid membrane surfactant sensor based on a 1,3-didecyl-2-methylimidazolium–tetraphenylborate ion-exchange complex. Amphipathic compounds known as non-ionic surfactants do not ionize in aqueous solution.[43] The potentiometric behavior of various barium-polyethoxylate complexes, including ethylene oxide units, has also been studied because ethoxylates have significant applications as surfactants.[44] The determination of the homologs of polyoxyethylated nonylphenols used arrays of non-selective non-ionic-surfactant sensors. It was shown that polyoxyethylated nonylphenols with various numbers of oxyethyl groups, which are homologs of non-ionic surfactants, may be independently determined using multisensor systems of the electronic tongue type based on non-selective solid-contact potentiometric sensors. A novel barium pseudocationic combination of a strongly ethoxylated fatty alcohol polyglycol ether and tetraphenylborate has been developed as the basis for a liquid membrane non-ionic surfactant-sensitive electrode. The compound has been integrated into a PVC membrane that has been plasticized and employed as a sensing material.[45]

4.8.4 Amphoteric (Zwitterionic) Surfactant Sensors

The effective reusability of a taste sensor with lipid polymer membranes *via* amphoteric surfactant cleaning has shown enhanced results in chemical detection. The purpose of the study was to improve the effectiveness of the cleaning procedure in order to make a taste sensor more reusable. This study used hydrophobic lipid polymer membranes in a surfactant cleaning approach for two different types of bitterness sensors. Four different types of surfactants with various polarities and ionicities were tested for usability in order to choose the best ones for cleaning. Use of both the normal cleaning solution and the LDA acid solution together significantly increased the reusability of an astringency sensor in numerous measurements of black tea. Effects of zwitterionic surface activity wormlike micelles driven by Na^+, ionic liquid, and anionic surfactant. The physicochemical characteristics of a mixed sodium dodecyl sulfate/*N*-alkyl-*N*′-carboxymethylimidazolium inner salt ionic liquid with zwitterionic surface activity has been investigated. The mixture under study displayed a stronger synergism, that is, more negative interaction characteristics, when compared to the mixed zwitterionic betaine surfactant/SDS system. Acetylene black electrodes enhanced with zwitterionic surfactant and carbon nanotubes to detect triclosan in household products have been examined.[11]

4.9 Biochemical Surfactants and Sensing

Figure 4.6 shows surfactants used in biochemical detection. Surfactants have emerged as versatile materials for many biological applications. The search

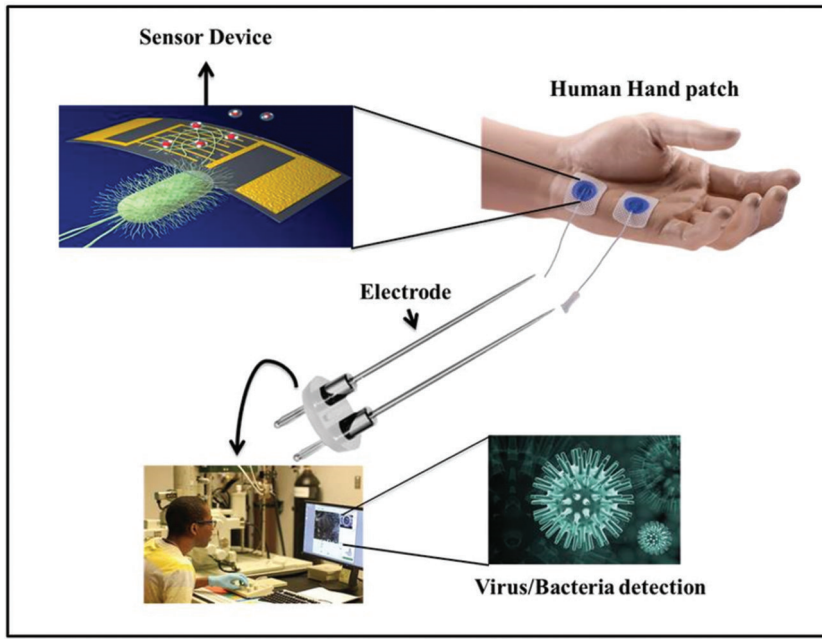

Figure 4.6 Usage of surfactants in biochemical detection.

for new surfactants for the betterment of biological applications is a continuous process, and in this regard bio-surfactants are considered to be favorable compounds. The use of bio-surfactants, bio-transformation and biodegradation has been discussed deliberately. The use of enzymes such as protease and amylase requires bio-technological skills for analysis of enzyme production, isolation, thermal behavior, storage stability, and pH stability. The invention of nanoparticle technology has profound applications in many biological activities with enhanced characteristic properties, such as enzyme encapsulation in spherulites, colloidal gas aphrons using multilayer surfactants, recovery of cells, proteins, biological molecules, and gas transformation in bio-reactors. The recent advancement in high-pressure phase transformation in phospholipid bilayers has become a model system for detection of biomembranes. Surfactant membranes are used in medicine, biotechnology, as an environmental protective shield for isolation of hydrocarbons and gases, and for the separation of metal ions, amino acids, and other suspensions. Sugar surfactants are used in the determination of various properties related to microemulsions.[8]

In order to lower surface tension at the air–liquid interface of the alveolus, pulmonary surfactant, a complex mixture of phospholipids and proteins, is used. The alveolus receives the generated, assembled, transported, and secreted surfactant, where it undergoes degradation and is subsequently recycled. In comparison to adults, babies, particularly premature ones, have a slower metabolism of surfactant. Respiratory distress from a problem with

pulmonary surfactant metabolism is accompanied by morbidity and mortality. This happens because the metabolism of surfactants is impaired due to genetic abnormalities, proteolytic degradation, or rapid breakdown. The management of some of these conditions has been successful with the use of prenatal corticosteroids, surfactant replacement, whole lung lavage, and lung transplantation. Pulmonary surfactants lower surface tension at the alveolus' air–liquid contact, preventing the alveolus from collapsing during end-expiration. Additionally, it takes part in the host's natural defensive mechanism against inhaled infections.[50]

Non-ionic surfactants and organic solvents with low concentrations have enhanced the properties of cholesterol oxydase by increasing the activity of the enzyme. The cationic surfactants in reversed micelles in organic solvents emphasized two hydrolyzing enzyme proteases and amylase on detection of DNA from salmon testes. The evolution of surfactant-based sensors in biochemical detection is evidence of its various applications, which include medical and healthcare, antiviral activity, cyclic lipopeptide antibiotic, and clinical symptoms like irritation, skin dryness, itching, and stinging. In the view of all these, surfactant-based biochemical detection is very much necessary to prevent and to take measures after the serious effects. The most appropriate, simple, and cost-effective surfactant sensors are explored.

Electrochemical surfactant sensors will be described, focusing specifically on developments that have already been published.[51] In accordance with the actual measured value, electrochemical sensors are usually categorized as highly sensitive and selective, amperometric, conductometric, or impedimetric surface sensors.[5] Some of most significant are potentiometric surfactant sensors due to how simple and adaptable they are. There are various amperometric surfactant sensors that are real biosensors and involve living cells and microorganisms.

4.9.1 Potentiometric Surfactant Sensors

Even though several direct potentiometric sensors have been reported, potentiometric surfactant sensors are typically employed as quantitative terminal sensors. Among the most common types of sensor in this category are coated wire-type, liquid membrane, and ISFET (ion-selective field effect transistor) sensors. The sensors can be used to recognize non-ionic as well as ionic (cationic and anionic) surfactants.[6] They can be operated constantly in flow injection analysis (FIA) mode or intermittently in batch mode. Although several direct potentiometric sensors have been described, potentiometric surfactant sensors are typically employed as titration endpoint sensors.[47–49] For sensors designed using liquid membrane surfactants and coated wire it is indeed difficult to distinguish between liquid membrane sensors and coated wire sensors. These variants employ ISE membranes to operate. Since these membranes are generally solid for practical purposes, the term liquid membrane can be misleading. Yet, the smart phone complexing agents known as sites are typically included in a

matrix gel after being dissolved in a suitable solvent.[50] An ion-selective electrode has been described as the end-point titration sensor for determining the concentration of anionic and cationic surfactants *via* titration. It demonstrated that surfactant mixtures and non-ionic surfactants can both be tested using the same electrode. As precisely and easily as the pure surfactant, the concentrations of combinations of anionic and non-ionic surfactants may be calculated.[51]

4.9.2 Impedimetric Surfactant Sensors

Direct affinity sensors have been presented with simple preparation approaches. The oligonucleotide or antibodies were similarly immobilized as a result of the self-consistent introduction of a hydrocarbon chain attached to an oligonucleotide pentadecathymidylate into the hydrophobic region of the surfactant bilayers or as a result of the adsorption of antibodies on the surface of the bilayers. Impedance spectroscopy was utilized to find the responses and antibody–antigen interactions increased the impedance, whereas particular DNA-coupling decreased the actual fraction of the impedance.[52] Easy procedures have been suggested for making direct affinity sensors. The generation of immunosensors is a result of antibodies adhering to bilayer surfaces. Significant alterations in impedance spectra have been seen in both trials. The results are encouraging for the development of impedimetric affinity sensors for use in healthcare or the environment. The lubricating qualities of motor oil can be adversely affected by as little as a few hundred ppm of water. The oil additives (surfactants) and water molecules started interacting right away after the injection, creating an inverse micelle-based water-in-oil emulsion. After emulsification, water in the solution was gradually removed by evaporation and electrolysis. A computer analysis model was created using the literature equations defining these interactions in order to support the experimental findings and demonstrate the kinetics of the water–oil interactions. The model enhanced understanding of the experimental data by illuminating the processes taking place in the water–oil system.

4.9.3 Conductometric Surfactant Sensors

This sort of surfactant sensor for conducting conductivity measurements to track the evolution of a number of particles in the emulsion polymerization has been discussed. The three main phases of the polymerizing latex were assumed to be equally divided among the surfactant in the developed model. A soft-sensor approach was then suggested for counting the amount of polymer particles by fusing the conductivity model with the available conversion, temperature, and conductivity signals (N-P). The major objectives were to watch the evolution of N-P (nucleation/coagulation) in real time under varied reaction scenarios and to validate the conductivity model over a

larger variety of operational settings. Several batch and semi-batch polymerization operations were conducted.[53]

4.9.4 Amperometric Surfactant Sensors

Several real surfactant biosensors using microorganisms or cells are available alongside amperometric surfactant sensors. Numerous modified PVC membranes have been characterized based on their permeability and selectivity for electrochemically active substances. The species were identified using a two-electrode amperometric cell in phosphate buffer solution. The diffusing species were observed to be paracetamol, catechol, ascorbic acid, and hydrogen peroxide. Cationic and non-ionic surfactants were employed as the membrane modifying agents in the research.[54] The detection of anionic surfactants was achieved by building a *Pseudomonas rathonis* T-based amperometric biosensor. Plasmids used in surfactant degradation were found in microorganisms. Sodium dodecyl sulfate and volgonat were quite corrosive to the sensor. The selectivity of PVC membranes plasticized with surfactants and liquid crystals was studied using an amperometric sensor, and the results were presented. The effects of non-ionic surfactants on the electrochemical behavior of the compounds might be studied by including ubiquinone and menaquinone in a carbon paste electrode. Additionally, impacts on the sensitivity of the glucose biosensor were shown when a similar modification was applied to create an enzyme electrode in which the quinone molecule functions as a redox mediator.[55]

4.10 Surfactant Sensors in Biochemical Detection and Applications

4.10.1 Anionic Surfactant Sensors

A microbial sensor for the measurement of anionic surfactants has been investigated. For the purpose of detecting anionic surfactants in an aquatic environment a unique biosensor has been built. Analyzing anionic surfactants was quick and easy, and no hazardous organic reagents were needed.[56] Patients may get anaphylactic shock as a result of ingesting food allergens, particularly buckwheat proteins.[63] There is a need for the creation of an easy and quick screening approach using a field effect transistor biosensor for food allergens in food products. In this investigation, a buckwheat allergenic protein was successfully detected using FET.[57] Sodium dodecyl sulfide (SDS), an anionic surfactant, served as a signal amplifier for FET detection. For the purpose of detecting allergens in industrial domain, the suggested approach attained the desired level of sensitivity. An anionic surfactant-based electrochemical nicotine sensor based on cerium nanoparticles has been explored. The primary alkaloid in tobacco leaves (*Nicotianata bacum* L. Solanaceae) is nicotine, also known as

3-(1-methyl-2-pyrrolidinyl) pyridine. These leaves are more famous for their use in cigarettes than for their therapeutic uses.[17]

4.10.2 Cationic Surfactant Sensors

A glucose-modified carbon paste sensor in the presence of a cationic surfactant for mefenamic acid detection in urine and pharmaceutical samples has been studied. A unique and reliable carbon paste electrode (CPE) modified with glucose was created for the ultrasensitive detection of mefenamic acid (MA).[58,64] Diffusion–adsorption control was visible in the sensing results. The technique displayed a low detection limit and a broader linear dynamic range. Both biological and pharmacological samples of MA were successfully detected by the newly designed sensor.[58] A dangerous analog of glucose called alloxan (AL) selectively kills the pancreatic cells that make insulin, acting as a strong inducer of diabetes. In order to analyze AL in the presence of anthrone, a sensitive and focused carbon paste electrode immobilized with cetyltrimethylammonium bromide (CTAB) was used.[59]

A study of its increased voltammetric determination in cationic surfactant medium employing a boron-doped diamond electrode served as the first electrochemical evaluation of the antiviral drug favipiravir used to treat COVID-19.[60] The lipophilicity affects the membrane resistance, ionophore solubility, ion exchange across the membrane, and ultimately the analytical signal. All of the examined cationic surfactants could be titrated using potentiometric titration, and P1 plasticizer demonstrated exceptional titration performance, rapid reaction time, high signal change, and signal stability.[48]

4.10.3 Non-ionic Surfactant Sensors

A sensitive and specific protein detection method using a non-ionic surfactant-decorated liquid crystal sensor has been developed. In the human body, proteins are in charge of most biochemical processes. The creation of sensitive and focused protein detection techniques is crucial. This study used a liquid crystal-based sensor for highly sensitive and specific lysozyme detection. By employing an LC interface and dodecyl β-D-glucopyranoside, a non-ionic surfactant, concanavalin A and bovine serum albumin were created. *Pseudomonas aeruginosa* proliferation has been studied using a new sensor technique. To investigate how surfactants affect *Pseudomonas aeruginosa* growth in media, a novel sensor technology based on series piezoelectric quartz crystal sensing was developed. The frequency shift curves produced under various growth circumstances were compared with one another. Three kinetic parameters were obtained to explain the growth of microorganisms by fitting frequency shift curves. When it came to bacterial growth, surfactants were a growth inhibitor.[17]

Applications for mesostructured polyaniline in H_2O_2 and glucose sensing have been found utilizing a combination of mixed surfactants, anionic

sodium dodecylsulfate, and non-ionic polymers. Mesostructured polyaniline was made by allowing a mixture of a non-ionic polymeric surfactant and sodium dodecyl sulfate, an anionic surfactant, to self-assemble. The approach used in this study created a novel platform for the creation of high-performance glucose and other biosensors based on polyanilines. Immobilizing the sensing material within the membrane with graphene nanoparticles lowered the electrical resistance and signal noise of the membrane by preventing the leaching of electroactive material from the membrane.[61,62]

4.10.4 Amphoteric (Zwitterionic) Surfactant Sensors

A biosensor based on laccase-halloysite nanotubes and imidazoliumzwitterionic surfactant for determining dopamine has been developed. Improved catalytic activity and stabilities in biosensing are provided by zwitterionic surfactants that integrate nanomaterials and biomolecule architectures.[9] A novel electroanalytical approach for the measurement of dopamine by square-wave voltammetry was created using the biosensor. This review summarizes the most recent developments in membranes, micro-nanocapsules, nano-microgels, as well as multilayered thin films with amphoteric properties. In light of their prospective use in nanotechnology, biotechnology, and medicine, as well as their stimuli responsive behavior, synthetic methods for amphoteric materials and physicochemical characteristics have been described.[51] As a result of their strong propensity for self-organization in aqueous conditions, amphoteric macromolecules with hydrophobic moieties can act as a crude model of biological membranes. For peroxidase immobilization in the creation of biosensors, gold nanoparticles have been disseminated in zwitterionic surfactants.

4.11 Conclusion

This chapter consists of basic information on the stability, life time, and reuse of surfactants, and their applications in chemical and biochemical detection. Here, the impact of surfactants in daily life has been discussed extensively along with their applications. Most of the surfactants are similar in nature, including a hydrocarbon chain which can be framed as linear, branched, or aromatic in nature, which enhances the hydrophilic property of the surfactants. Nonionic surfactants contain both hydrophilic and lipophilic groups. Surfactants are classified into four types, based on the charge of their polar head group: anionic, non-ionic, amphoteric and cationic surfactants. The creation, optimization, and proper dosage of surfactants are carried out through analysis of the interface. We can assess the effectiveness and efficiency of surfactants using tensiometers, which measure surface tension. They aid in the construction and optimization of emulsions by precisely measuring the interfacial tension. Current research focuses on the use of consumer-grade wearable electronic devices and commercial equipment to implement the electronic nose principle in environmental

monitoring and medicine. The idea that analytes will interact with various materials in different ways is at the core of chemical sensor arrays. As a result, any type of material may be utilized in sensors. The use of bio-surfactants, bio-transformation and bio-degradation has been reviewed in this chapter. The use of enzymes such as protease and amylase requires biotechnological skills for analysis of enzyme production, isolation, thermal behavior, storage stability, and pH stability. The invention of nanotechnology has profound applications in many biological activities with enhanced characteristic properties.

Acknowledgements

One of the authors acknowledges the management of Ballari Institute of Technology and Management, Ballari for their support.

References

1. A. V. Kim, N. N. Medvedev and A. Geiger, Molecular dynamics study of the volumetric and hydrophobic properties of the amphiphilic molecule, *J. Mol. Liq.*, 2014, **189**, 74.
2. M. Mobin, R. Aslam and J. Aslam, Non toxic biodegradable cationic gemini surfactants as novel corrosion inhibitor for mild steel in hydrochloric acid medium and synergistic effect of sodium salicylate: Experimental and theoretical approach, *Mater. Chem. Phys.*, 2017, **191**, 151.
3. J. D. York and A. Firoozabadi, Comparing effectiveness of rhamnolipid biosurfactant with a quaternary ammonium salt surfactant for hydrate anti-agglomeration, *J. Phys. Chem. B*, 2008, **112**(3), 845.
4. C. Cowan-Ellsberry, S. Belanger, P. Dorn, S. Dyer, D. Mcavoy and H. Sanderson, Environmental safety of the use of major surfactant classes in North America, *Crit. Rev. Environ. Sci. Technol.*, 2014, **44**(17), 1893.
5. J. Ju and W. Chen, In situ growth of surfactant-free gold nanoparticles on nitrogen-doped graphene quantum dots for electrochemical detection of hydrogen peroxide in biological environments, *Anal. Chem.*, 2015, **87**(3), 1903.
6. G. Ziyatdinova, E. Ziganshina and H. Budnikov, Voltammetric sensing and quantification of eugenol using nonionic surfactant self-organized media, *Anal. Methods*, 2013, **5**(18), 4750.
7. A. A. P. Khan, A. Khan, M. M. Rahman and A. M. Asiri, Conventional surfactant-doped poly(o-anisidine)/GO nanocomposites for benzaldehyde chemical sensor development, *J. Sol–Gel Sci. Technol.*, 2016, **77**(2), 361.
8. G. Tigari and J. G. Manjunatha, Optimized Voltammetric Experiment for the Determination of Phloroglucinol at Surfactant Modified Carbon Nanotube Paste Electrode, *Instrum. Exp. Tech.*, 2020, **63**(5), 750.

9. O. Galovic, M. Samardzic, M. Hajdukovic and M. Sak-Bosnar, A new graphene-based surfactant sensor for the determination of anionic surfactants in real samples, *Sens. Actuators, B*, 2016, **236**, 257.
10. D. Madunic-cacic, M. Sak-Bosnar, O. Galovic, N. Sakac and R. Matesic-Puac, Determination of cationic surfactants in pharmaceutical disinfectants using a new sensitive potentiometric sensor, *Talanta*, 2008, **76**(2), 259.
11. N. Sakac, D. Markovic, B. Šarkanj, D. Madunic-Cacic, K. Hajdek and B. Smoljan, Direct potentiometric study of cationic and nonionic surfactants in disinfectants and personal care products by new surfactant sensor based on 1,3-dihexadecyl-1*H*-benzo[*d*]imidazol-3-ium, *Molecules*, 2021, **26**(5), 1.
12. H. Li, Z. Deng, Q. Tian, L. Lun, P. Zhao and X. Yang, Application of carbon nanotubes and zwitterionic surfactant-modified acetylene black electrode for the determination of triclosan in household commodities, *Int. J. Environ. Anal. Chem.*, 2022, **102**(4), 987.
13. S. Gold, F. J. Ibanez and F. P. Zamborini, Chemiresistive Sensing of Volatile Organic Compounds with Films of Surfactant-Stabilized Gold and Gold Silver Alloy Nanoparticles, *ACS Nano*, 2008, **2**(8), 1543.
14. A. Pastore, D. Badocco and P. Pastore, Talanta Influence of surfactant chain length, counterion and OrMoSil precursors on reversibility and working interval of pH colorimetric sensors, *Talanta*, 2020, **212**, 120739.
15. D. Jadreško and M. Zelić, Square-wave voltammetry of electroinactive surfactants, *Electroanalysis*, 2015, **27**, 1669.
16. S. Sharvelle, R. Lattyak and M. K. Banks, Evaluation of biodegradability and biodegradation kinetics for anionic, nonionic, and amphoteric surfactants, *Water, Air, Soil Pollut.*, 2007, **183**(1–4), 177.
17. A. J. Frend, G. J. Moody, J. D. R. Thomas and B. J. Birch, Flow injection analysis with tubular membrane ion-selective electrodes in the presence of anionic surfactants, *Analyst*, 1983, **108**, 1357.
18. N. Sakač, M. Jozanović, M. Karnaš and M. Sak-Bosnar, New Sensor for Determination of Anionic Surfactants in Detergent Products with Carbon Nanotubes as Solid Contact, *J. Surfactants Deterg.*, 2017, **20**, 881.
19. M. Hajdukovic, M. Samardzic, O. Galovic, A. Szechenyi and M. A. Sak-Bosna, functionalized nanomaterial based, new, solid state cationic-surfactant-selective sensor with fast response and low noise, *Sens. Actuators, B*, 2017, **251**, 795.
20. H. Harma, S. Laakso, S. Pihlasalo and P. Hanninen, A Fluorometric fullerenol sensor for rapid detection of ionic and non-ionic surfactants, *Tenside, Surfactants, Deterg.*, 2010, **47**(1), 40.
21. R. A. Salkar, P. Jeevanandam, G. Kataby, S. T. Aruna, Y. Koltypin and O. Palchik, Elongated Copper Nanoparticles Coated with a Zwitterionic Surfactant, *J. Phys. Chem. B*, 2000, **104**(5), 893.

22. Y. Tian, R. G. Holt and R. E. Apfel, Investigation of liquid surface rheology of surfactant solutions by droplet shape oscillations: Experiments, *J. Colloid Interface Sci.*, 1997, **187**(1), 1.
23. J. Eastoe and J. S. Dalton, Dynamic surface tension and adsorption mechanisms of surfactants at the air–water interface, *Adv. Colloid Interface Sci.*, 2000, **85**(2), 103.
24. A. P. Santos and A. Z. Panagiotopoulos, Determination of the critical micelle concentration in simulations of surfactant systems, *J. Chem. Phys.*, 2016, **144**(4), 044709.
25. D. Rana, G. H. Neale and V. Hornof, Surface tension of mixed surfactant systems: Lignosulfonate and sodium dodecyl sulfate, *Colloid Polym. Sci.*, 2002, **280**(8), 775.
26. D. R. Otis Jr, E. P. Ingnetio, R. D. Kamm and M. Johnson, Dynamic surface tension of surfactant TA: Experiments and theory, *J. Appl. Physiol.*, 1994, **77**(6), 2681–2688.
27. K. Babu, N. Pal, A. Bera, V. K. Saxena and A. Mandal, Studies on interfacial tension and contact angle of synthesized surfactant and polymeric from castor oil for enhanced oil recovery, *Appl. Surf. Sci.*, 2015, **353**, 1126.
28. N. D. Denkov, S. Tcholakova, K. Golemanov and K. P. Ananthpadmanabhan, The role of surfactant type and bubble surface mobility in foam rheology, *Soft Matter*, 2009, **5**(18), 3389–3408.
29. A. Bhattacharyya, F. Monroy, D. Langevin and J. F. Argillier, Surface rheology and foam stability of mixed surfactant-polyelectrolyte solutions, *Langmuir*, 2000, **16**(23), 8727.
30. N. Abramova, Application of Photocured Polymer Ion Selective Membranes for Solid-State Chemical Sensors, *Chemosensors*, 2015, **3**, 190.
31. O. J. DSouza, R. J. Mascarenhas, T. Thomas, B. M. Basavaraja, A. K. Saxena and K. Mukhopadhyay, Platinum decorated multiwalled carbon nanotubes/Triton X-100 modified carbon paste electrode for the sensitive amperometric determination of paracetamol, *J. Electroanal. Chem.*, 2015, **739**, 49.
32. A. K. Dwivedi, M. Pandeeswar and T. Govindaraju, Assembly modulation of PDI derivative as a supramolecular fluorescence switching probe for detection of cationic surfactant and metal ions in aqueous media, *ACS Appl. Mater. Interfaces*, 2014, **6**(23), 21369.
33. R. Kumar and S. R. Raghavan, Photogelling fluids based on light-activated growth of zwitterionic wormlike micelles, *Soft Matter*, 2009, **5**(4), 797.
34. L. Ding, S. Wang, Y. Liu, J. Cao and Y. Fang, Bispyrene/surfactant assemblies as fluorescent sensor platform: Detection and identification of Cu^{2+} and Co^{2+} in aqueous solution, *J. Mater. Chem. A*, 2013, **1**(31), 8866.
35. I. Thivaios, V. Koukoumtzis, J. K. Kallitsis and G. Bokias, Quinoline-labeled poly(N-isopropylacrylamide): A selective polymeric luminescent sensor of cationic surfactants, *Sens. Actuators, B*, 2016, **233**, 127.

36. F. Li, J. H. C. Wang and Q. M. Wang, Thickness shear mode acoustic wave sensors for characterizing the viscoelastic properties of cell monolayer, *Sens. Actuators, B*, 2008, **128**(2), 399.
37. M. M. Charithra and J. G. Manjunatha, Enhanced voltammetric detection of paracetamol by using carbon nanotube modified electrode as an electrochemical sensor, *J. Electrochem. Sci. Eng.*, 2020, **10**(1), 29.
38. V. B. Patil, S. J. Malode, S. M. Tuwar and N. P. Shetti, Graphene sheet-based electrochemical sensor with cationic surfactant for sensitive detection of atorvastatin, *Sens. Int.*, 2022, **3**, 100198.
39. S. Lee, K. M. Lee, M. Lee and J. Yoon, Polydiacetylenes bearing boronic acid groups as colorimetric and fluorescence sensors for cationic surfactants, *ACS Appl. Mater. Interfaces*, 2013, **5**(11), 4521.
40. A. Pasha, S. Khasim, O. A. Al-Hartomy, M. Lakshmi and K. G. Manjunatha, Highly sensitive ethylene glycol-doped PEDOT-PSS organic thin films for LPG sensing, *RSC Adv.*, 2018, **8**(32), 18074.
41. P. A. Pushpanjali, J. G. Manjunatha and M. T. Shreenivas, The Electrochemical Resolution of Ciprofloxacin, Riboflavin and Estriol Using Anionic Surfactant and Polymer-Modified Carbon Paste Electrode, *Anal. Chem.*, 2019, **4**, 13427.
42. A. Sein and J. B. F. Engberts, Micelle to Lamellar Aggregate Transiiion of an Anionic Surfactant in Dilute Aqueous Solution Induced by Alkali Metal Chloride and Tetraalkylammonium Chloride Salts, *Langmuir*, 1995, **11**(2), 455.
43. Y. Wang, Q. Hu, T. Tian, Y. Gao and L. Yu, A nonionic surfactant-decorated liquid crystal sensor for sensitive and selective detection of proteins, *Anal. Chim. Acta*, 2016, **937**, 119.
44. F. S. Mohseni-Shahri, F. Moeinpour and A. Verdian, A cationic surfactant-decorated liquid crystal-based sensor for sensitive detection of quinoline yellow, *Sci. Rep.*, 2021, **11**(1), 1.
45. N. S. Prinith and J. G. Manjunatha, Materials Science for Energy Technologies Surfactant modified electrochemical sensor for determination of Anthrone – A cyclic voltammetry, *Mater. Sci. Energy Technol.*, 2019, **2**(3), 408.
46. M. Behpour, A. M. Attaran, M. M. Sadiany and A. Khoobi, Adsorption effect of a cationic surfactant at carbon paste electrode as a sensitive sensor for study and detection of folic acid, *Measurement*, 2016, **77**, 257.
47. M. Sak-Bosnar, M. Samardzic and O. Galovic, The influence of ethoxylated nonionic surfactants on the potentiometric determination of anionic surfactants, *Int. J. Electrochem. Sci.*, 2011, **6**(3), 561.
48. M. Sak-Bosnar, D. Madunic-Cacic, N. Sakac, O. Galovic, M. Samardzic and Z. Grabaric, Potentiometric sensor for polyethoxylated nonionic surfactant determination, *Electrochim. Acta*, 2009, **55**(2), 528.
49. N. M. Mikhaleva and E. G. Kulapina, Arrays of nonselective nonionic-surfactant sensors for the separate determination of the homologues of polyoxyethylated nonylphenols, *J. Anal. Chem.*, 2005, **60**(6), 646.

50. N. Hareesha and J. G. Manjunatha, Surfactant and polymer layered carbon composite electrochemical sensor for the analysis of estriol with ciprofloxacin, *Mater. Res. Innovations*, 2019, **24**(6), 349–362.
51. C. Raril and J. G. Manjunatha, A simple approach for the electrochemical determination of vanillin at ionic surfactant modified graphene paste electrode, *Microchem. J.*, 2020, **154**, 104575.
52. N. Sakac, D. Markovic, B. Sarkanj, C. Madunic, D. Acic, K. Hajdek, B. Smoljan and M. J. Direct, Potentiometric Study of Cationic and Nonionic Surfactants in Disinfectants and Personal Care Products by New Surfactant Sensor Based on 1,3-Dihexadecyl 1*H*-benzo[*d*]imidazol 3-ium, *Molecules*, 2021, **26**, 1366.
53. O. Fizer, M. Fizer, V. Sidey and Y. Studenyak, Predicting the end point potential break values: A case of potentiometric titration of lipophilic anions with cetylpyridinium chloride, *Microchem. J.*, 2021, **160**, 105758.
54. M. Karnas, N. Sakac, M. Jozanovic, M. Tsakiri, M. Kopriva, E. K. Andrić and M. Sak-Bosnar, The Influence of Plasticisers on Response Characteristics of Anionic Surfactant Potentiometric Sensor, *Int. J. Electrochem. Sci.*, 2017, **12**, 5921.
55. M. Jozanovic, N. Sakac, M. Karnas and M. Medvidovic-Kosanovic, Potentiometric Sensors for the Determination of Anionic Surfactants–A Review, *Crit. Rev. Anal. Chem.*, 2021, **51**(2), 115.
56. J. Sanchez and M. Del Valle, Determination of anionic surfactants employing potentiometric sensors – A review, *Crit. Rev. Anal. Chem.*, 2005, **35**(1), 15.
57. D. Madunic-Cacic, M. Sak-Bosnar, R. Matesic-Puac and M. Samardzic, Potentiometric determination of anionic surfactants in formulations containing cocoamidopropyl betaine, *Int. J. Electrochem. Sci.*, 2012, **7**(1), 875.
58. S. Duval, M. Keddam, M. Sfaira, A. Srhiri and H. Takenouti, Electrochemical Impedance Spectroscopy of Epoxy-Vinyl Coating in Aqueous Medium Analyzed by Dipolar Relaxation of Polymer, *J. Electrochem. Soc.*, 2002, **149**(11), 520.
59. H. M. Naien, S. Dzyadevych, F. Lagarde and N. Jaffrezic-Renault, A Conductometric Sensor Specific for Cationic Surfactants, *Electroanalysis*, 2012, **24**(6), 1441.
60. T. Thomas, R. J. Mascarenhas, O. J. D' Souza, S. Detriche, Z. Mekhalif and P. Martis, Pristine multi-walled carbon nanotubes/SDS modified carbon paste electrode as an amperometric sensor for epinephrine, *Talanta*, 2014, **125**, 352.
61. L. Taranova, I. Semenchuk, T. Manolov, P. Iliasov and A. Reshetilov, Bacteria-degraders as the base of an amperometric biosensor for detection of anionic surfactants, *Biosens. Bioelectron.*, 2002, **17**(8), 635.
62. M. Gao, L. Wang, J. Chen, S. Li, G. Lu and L. Wang, Aggregation-Induced Emission Active Probe for Light-Up Detection of Anionic Surfactants and Wash-Free Bacterial Imaging, *Chem. – Eur. J.*, 2016, **22**(15), 5107.

63. J. G. Manjunatha, A novel voltammetric method for the enhanced detection of the food additive tartrazine using an electrochemical sensor, *Heliyon*, 2018, **4**, e00986.
64. A. B. Monnappa, J. G. Manjunatha and A. S. Bhatt, Design of a sensitive and selective voltammetric sensor based on a cationic surfactant-modified carbon paste electrode for the determination of alloxan, *ACS Omega*, 2020, **5**(36), 23481.

IOP Publishing

Graphene-Based Sensors

Jamballi G Manjunatha

Chapter 5

Graphene-modified electrochemical sensors for estimation of food contaminants

B Chethan, V Prasad, A Sunilkumar and S Thomas

In the present situation, it is essential to detect food pollutants to maintain the excellent health of humanity. In this regard, electrochemical sensors work effectively to sense food contaminants. The primary food contaminants are bio-molecules and food pollutants. Nowadays, two-dimensional (2D) materials are extensively used to fabricate the sensing device. Among these 2D materials, graphene, its derivatives and their composites are highly workable materials. The chapter extensively studies graphene derivatives and their composites-based electrochemical sensors to detect food pollutants. The present chapter focuses on the organic and inorganic pollutants contaminating food. The organic contaminants like food colouring agents, pesticides and drugs, and the inorganic pollutants like metal cations and anions influence contaminating food is deliberately discussed. The use of the nanocomposites and derivatives of graphene to develop sensing material is briefly outlined. In the last section, the challenges faced and the conclusion are sketched.

5.1 Introduction

Food is the primary source of energy for human beings and living organisms. Getting nutrient and pollutant-free food is the fundamental right of every individual [1–11]. Food pollution and adulteration occur naturally and artificially in every food production and processing step. The presence of pollutants damages the health condition of human beings. According to the World Health Organization, contaminated and adulterated food may lead to more than 200 diseases [12–18]. The main reason for food contamination is a polluted ecosystem. Hence, identifying, detecting and controlling food pollutants is challenging. Food security is essential to secure human beings' health and increase the standard of life [19].

doi:10.1088/978-0-7503-5578-0ch5

Today many analytical techniques, namely chromatography, spectrophotometry, and electrochemical techniques, are more popular to estimate and determine food pollution [20–22]. These techniques are precise, sensitive and selective for detecting and determining food pollutants. But these techniques find more disadvantages like high cost, sophisticated instrumentation, miniaturisation not being possible, and multiple pretreatments required [22]. So, the scientific community finds many challenges to fabricating low-cost, reliable, versatile, miniaturised, and accurate methods to detect pollution in food products. With great anticipation, the research community has proposed the electrochemical sensor. Electrochemical sensors have found significant applications in ecosystem monitoring, agriculture, and industrial applications in recent decades [23, 24]. The great interest in electrochemical sensors is due to their trustable sensitivity, timing characteristics, better selectivity and portability.

Electrochemical sensors work on the principle of the redox process to detect the electroactive analyte [25, 26]. The changes in the physical impulse are determined by measuring the changes in the applied potential. Usually, many researchers are working on metals and metal oxide-based sensors, but graphene, a carbon-based material, gives more promising applications than the rest of the other materials because of its astonishing applications, such as rapid timing behaviour, multiple detection ability and over potential. Compared to other 2D materials (carbon nanotubes (CNTs), graphite and fullerene), graphene-based materials have more potential [27]. Usually, in the electrochemical process, graphene nanosheets attach to the graphitic electrodes through a π–π interaction [28]. This interaction negatively affects the sensing ability of the graphene system. Because of these reasons, the research community has increased their studies on graphene oxide (GO) and reduced graphene oxide (RGO) materials. GO and RGO contain hydroxyl, carboxyl and epoxy functional groups, forming a good interaction with the analyte, facilitating the easier hopping of the electrons [29]. The polar functional groups also enhance the interlayer separation between the graphene nanosheets and convert it into a hydrophilic material. With all these efforts, graphene and its derivative-based material synthesise the electrochemical sensors for pollutant detection in food materials.

With these ideas, this chapter focuses on detecting particular types of pollutants. We discuss the graphene-based electrochemical sensor system for detecting organic contaminants like food colourants, drugs, and pesticides and inorganic pollutants like metal cations and anions in food items (figure 5.1). The last part of the chapter consists of the conclusion and the challenges faced in this area of research.

5.2 Graphene and its derivatives-based electrochemical sensors for organic food pollutants

5.2.1 Food colourants and preservatives

The colouring agents and preservatives are added to the food items to attract consumers. The colouring agents include two types, namely, natural and synthetic

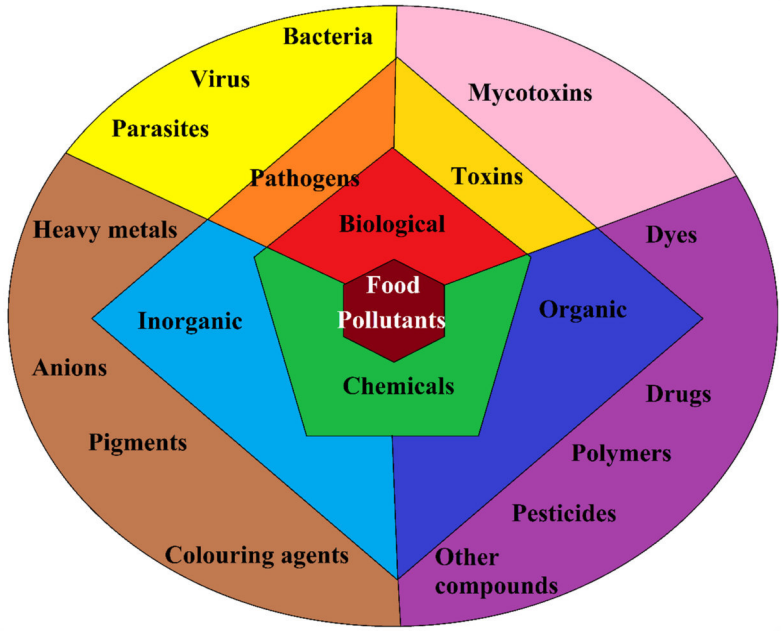

Figure 5.1. Food pollutants classification.

food colours. These artificial colouring agents are added to beverages, bakery items, ice cream and meat products to increase their flavour, colour and perishability [30, 31]. The natural colourants are extracted from plants, vegetables, fruit and animals. Usually, these natural colourants are non-toxic and safe. But the synthetic colouring agents are synthesised in artificial mode and are unrealistic.

5.2.1.1 Pure material for pollutants detection

Jampasa *et al* fabricated an RGO on screen-printed carbon electrode to detect sunset yellow and tartrazine in soft drinks, juice, and energy drink. At particular electrochemical conditions, the fabricated sensor has shown good sensitivity in detecting sunset yellow and tartrazine in food items. The fabricated sensor has seen a sunset yellow in the 0.01–20.0 mM concentration range and tartrazine concentration range from 0.02 to 20.0 mM [32].

5.2.1.2 Nanocomposites for pollutants detection

To enhance the sensitivity and timing behaviour and decrease the detection limit, the graphene-based composites are synthesised by compositing with polymers, metal nanoparticles and metal oxides. Many researchers have fabricated. The graphene-based sensor devices for the detection of pollutants in food products. Some of the reviews are provided in table 5.1.

Table 5.1. Graphene-based nanocomposites for various food pollutants detection.

Material	Dye detected	Detection limit	Food item	Ref.
Ag/graphene/screen-printed carbon electrodes (SPCEs)	Rhodamine B	1.9 μM	Crackers	[33]
Ag/RGO/paper electrode	Sudan I	41.3 nmol	Chilli powder	[34]
RGO/5-amino-1,3,4-thiadiazole-2-thiol/Pt/GCE	Orange II	3.4×10^{-10} M	Ketchup	[35]
NiO/Ag/RGO/GCE	Sunset Yellow	13 nM	Soft drinks	[36]
Poly(diallyldimethylammonium chloride) RGO/GCE	Quinoline Yellow	0.002 μM	soft drink	[37]
Poly(diallyldimethylammonium chloride)–graphene/Ni/GCE	Allura Red	8.0 nmol l^{-1}	Strawberry juice	[38]

5.2.2 Pesticides

Chemicals like insecticides, fungicides, and herbicides are included in the category of pesticides [39]. The primary purposes of their addition to farming areas are to boost crop output and safeguard agricultural products from pests. Extensive use of pesticides in agriculture may result in health hazards such as neurological disorders, respiratory problems, bone marrow disorders, infertility, and carcinogenicity [40]. It has also been generally established that pesticides accumulate in food goods. Pesticides in food goods must be identified for safe food and healthy life.

5.2.2.1 Pure graphene material

Tasaltin *et al* published an article based on a fungicide called propamocarb that can be detected in cucumbers using an RGO/Au electrode. In contrast, this electrode does not respond to cypermethrin, deltamethrin, or malathion and only responds favourably to propamocarb. This electrode has good sensitivity and responds to propamocarb quickly within short intervals [41].

5.2.2.2 Doped graphene materials

Mousavi and Moradian and Hong *et al* have shown that the conductivity of host materials is typically improved by doping with impurity atoms at an ideal concentration [42, 43]. Chen *et al* reported that nitrogen (N)-doped holey graphene, a graphene derivative with nanopores on a basal plane, modified GCE to quantify methyl parathion. This study shows that the *N*-configurations (pyridinic N, pyrrolic N, and graphitic N) play an essential role in detecting methyl parathion (pH = 8). Doped holey graphene containing pyrrolic N exhibits a comprehensive dynamic response (1 ng mL to 150 g mL) and a meager detection limit (3.5 pg mL). This sensor's apple, grape, and cucumber samples exhibit respectable recoveries [44].

5.2.2.3 Graphene-based nanocomposites

Research on nanocomposites based on graphene derivatives as electrode modifying layers has also been found to be generally advantageous in pesticide detection. Nehru *et al* used Ce-doped TiO_2/GO/GCE as an example to detect methyl parathion [44, 45]. Nanocomposite electrode exhibits excellent sensitivity, a small detection limit (0.0016 M), and a broad dynamic range (0.002–48.327 M) for the measurement of methyl parathion. This composite electrode demonstrates excellent selectivity, stability, and real-world applications with positive recoveries. Notably, N-doped holey graphene/GCE has picomolar level sensing capability towards methyl parathion [44].

Wang *et al* built an Ag/RGO/GCE-based pentachlorophenol sensor. This sensor responds to pentachlorophenol gradually in the 0.008–10.0 M range. By using this electrode, pentachlorophenol can be detected down to 0.001 M. With good recoveries (DPV, 94.0%–108.0%), this electrode successfully detects pentachlorophenol in vegetables. High-performance liquid chromatography (96.0%–103.3%) could also be used to verify this result. The appropriate surface area and electron-transfer capability of the Ag/RGO nanocomposite are credited with the improved sensing performance [46].

Ijaz *et al* showed that the insecticide paraquat (C12H14Cl2N2) is another significant one frequently used on crops like cotton and coconuts. However, research on the toxicity of paraquat has also been deliberately discussed [47].

Sant'Anna *et al* have created activated biochar/RGO/CPE for paraquat determination using the DPV approach. With a more excellent cathodic current responsiveness than bare CPE (pH = 6), the one-electron process reduces paraquat on this modified electrode. Oxygen and nitrogen chemical groups make paraquat interact more favourably, which improves detection. The detection limit, linearity, and sensitivity of activated biochar/RGO/CPE are 3.52 AL mol 1, 0.74–9.82 mol l^{-1}, and 23.1 nmol l^{-1}, respectively. This sensor could also be used successfully with honey, coconut water, lemon, and lettuce leaf samples [48].

Q1

5.2.3 Drugs

Antibiotics are examples of drugs that treat illnesses, soothe pain, and safeguard people's lives. However, their incorrect use has adverse effects on both people and animals. For instance, overuse of antibiotics will result in poor taste perception and inadequate nutrition in people [49, 50]. Sensors are being made to assess the presence of antibiotics in food samples [49, 50].

5.2.3.1 Pure graphene derivatives

Pan *et al*, by utilising differential pulse anodic stripping voltammetric methods, presented GO/SPCE for the detection of ciprofloxacin [51]. The complex that forms when ciprofloxacin and Mn^{2+} ions interact is the basis for the sensing technique. This technique has been performed on milk samples with recoveries ranging from 81.4% to 95.4% (1–8 M). In a study by de Faria *et al*, the detection threshold for the ciprofloxacin analysis was shown to be 0.3 M. An RGO/GCE sensor for

chloramphenicol determination was explored in another study. The study's researchers utilised adsorption stripping differential pulse voltammetry as an analytical technique. This electrode's sensitivity is nearly ten times higher than plain GCE. Additionally, RGO/GCE has been used on milk samples (whole and skimmed) and has shown recovery rates of 93%–108% for the measurement of chloramphenicol [52].

5.2.3.2 Graphene derivatives-based nanocomposites

Many binary/ternary nanocomposites made from graphene and its derivatives have been employed as drug sensors. The following are the points derived from the earlier literature.

(a) Sensors with nano-molar detection limits could be easily identified by utilising graphene-based composites.
(b) The analytical performance of composite-modified electrodes is affected by drug structure.
(c) The sensing ability is also affected by the type of working electrodes.
(d) Most of the sensors have been tested in natural water and biological samples. They've also been found in food samples.
(e) Polymers or metal oxides have been discovered to be the best components to be added to graphene or its derivatives for the best sensing capability.

5.2.4 Other compounds

Willson *et al* showed that caffeine, or 1,3,7-trimethyl xanthine, is an active component in food. However, it causes various issues in people. Thus, its presence must be approximated as mandatory in food samples. As a result, a caffeine sensor was created [53]. Further, Shehata *et al* developed GO/reduced glutathione/CPE for the fast detection of caffeine in water. Caffeine was determined using DPV with a linear range of 8–800 M (detection limit = 0.153 M). This caffeine sensor's performance has been tested against black tea, coffee, Nescafe, and Cola with outstanding results [54].

Jose *et al* created a new caffeine sensor by altering the electrode material for GCE with nicotinic acid hydrazide/GO. This composite-modified GCE has a higher peak current for caffeine than bare GCE and a lower detection limit (8.7–10 9 M). This sensor also showed good recoveries for caffeine added to Imol plus and energy beverages. The detection ability of nicotinic acid hydrazine/GO is superior to that of GO/reduced glutathione/CPE [55].

Tian *et al* described a PtFe/graphene-based voltammetric sensor for detecting bisphenol A. De-alloying of PtFeAl ternary alloy results in nanoporous PtFe. Bisphenol A could be calculated linearly using this sensor in the 0.2–96 M range. The lowest concentration of bisphenol A detectable by PtFe/graphene is 0.17 M. Furthermore, a PtFe/graphene sensor was used to detect bisphenol A in natural water samples with high recoveries (96%–101%) [56].

Wang *et al* employed iodine-doped graphene/GCE for bisphenol A measurement. In a simulated solution (10 M bisphenol A in 0.1 M phosphate buffer solution,

pH = 6), this electrode exhibits redox peaks with high peak currents and a lower detection limit (0.02 M). The electrode has been employed for bisphenol A sensing in milk samples with adequate recoveries (95%–110%) [57].

5.3 Electrochemical sensors based on graphene and its derivatives for inorganic food contaminants

5.3.1 Metal ions

Kharazi *et al* metal ions may reach the human body through the nutrient chain and deposit in tissues, producing severe health problems. As a result, graphene derivatives-based electrochemical detectors have been demonstrated to measure traces of metal ions precisely. In most cases, electrochemical build-up followed by a stripping technique will be used to quantify metal ions. The initial procedure is aggregation (or pre-enrichment), during which metal ions become embedded on the outermost layer of the working electrode by applying an appropriate negative voltage. The reduction process will deposit a specified concentration of metals at regular times [58].

The following procedure, stripping, includes oxidising (dissolving) the metal that has been applied as a layer to form equivalent metal ions. The peak current of anodic reactions will be commensurate to the amount of these ions containing metals. Highly dangerous metal cations such as mercury, lead, and cadmium ions were found in diverse food samples.

5.3.1.1 Pure graphene derivatives

Liendo *et al* built antimony (Sb^{3+}) sensors entirely from pristine eRGO. The surface area of the eRGO/GCE is 0.28 cm^2, which is greater than the surface area of the bare GCE (0.11 cm^2). The ideal pH, accumulation period, and voltage potential are 4.3, 150 s, and 1.0 V, respectively. This sensor performs well in determining Sb^{3+} ions in lettuce, celery, and canned drinks [59].

5.3.1.2 Graphene derivative-based nanocomposites

Ma *et al* demonstrated Ag/RGO-modified GCE for sensing Hg^{2+} ions. Hg^{2+} ions were placed for thirty seconds at 1.1 V (pH = 5.0). Exfoliating was done using DPV at possibilities ranging from 0 to +0.4 V. This electrode's wavelength detection limit and dynamic spectrum are 0.018 nM and 0.01–100 μg l^{-1}, respectively. The higher electrochemical surface space (0.13 cm^2) and the enhanced electron-transfer capabilities of the Ag/RGO composite contribute significantly to its sensing performance. With acceptable recoveries, this electrode also identifies Hg^{2+} ions in fish (head, body, and tail section) samples [60].

Wang *et al* discovered that sulphur-doped C_3N_4/graphene composites can detect trace quantities of Hg^{2+}, Cd^{2+}, and Pb^{2+} ions. This redesigned electrode has a detection threshold of 1.17, 0.38, and 0.61 nM for Cd2+, Pb^{2+}, and Hg^{2+} ions, respectively. This electrode's improved detection abilities are due to its multilayer permeable layer framework, distinctive tube bundle topology, and larger active centres [61].

Jeong *et al* recently developed graphene fibre using a laser-assisted technique for the simultaneous measurement of Cd^{2+} and Pb^{2+} ions. As the source and laser, an authorised polyimide film and a CO_2 laser (energy = 46 J cm^{-2}) were employed, respectively. Bismuth might additionally be electrochemically synthesised on graphene fibre. At pH = 4.5, the graphene fibre/Bi electrode exhibits an excellent linear response (1.0–140.0 g l^{-1}) and a meager detection limit (0.4 g l^{-1}) for both Cd^{2+} and Pb^{2+} ions [62].

Guo *et al* in another work investigated the RGO/MoS_2/chitosan/GCE as a Pb^{2+} ion sensor. This system's variable range and threshold for detection have been determined to be 0.005–0.05–2.0 and 0.0016 mM, correspondingly. This research found that this electrode may detect Pb^{2+} ions in tobacco leaves (sensitivity = 31.12 mA mM RGO and MoS_2 nanoflowers enhanced electrical conduction and a particular surface area, respectively [63].

5.3.2 Inorganic anions

Xu *et al* elevated quantities of inorganic anions in food, such as nitrite, sulphite, and others, are also hazardous to living creatures. The subsequent article covers electrochemical detectors for anions. Although a metal–graphene hybrid might improve electrochemical capabilities, current combinations cannot overcome the limitations of their intrinsic properties because metals and graphene are conductors. This paper describes the creation of a ruthenium–graphene quantum dot hybrid by reducing RuCl3 with aspartic acid and arginine-functionalized graphene quantum dots (Asp–Arg–GQDs). Asp–Arg–GQDs are a synthesis reducing agent, stabiliser, linker, and semiconductor. The resulting Ru–Asp–Arg–GQDs have a three-dimensional network structure of tiny Ru nanoparticles and graphene sheets. The suggested technique was effectively employed in the electrochemical detection of carbendazim in strawberries. This research also provides the path for developing a metal–graphene hybrid with good catalytic performance in sensing, energy storage, and catalysis [64].

In work by Qu *et al* it is demonstrated that food contains several chemicals that impact daily life. Food additive safety guidelines currently focus on the toxicity of single additions; however, food additives are frequently combined and may have additive, synergistic, or antagonistic effects. The current study used high content analysis (HCA) to explore the toxicity of dietary additives and damage pathways in HepG2 cells. To assess cell viability, we used the CCK-8 test. They were providing an experimental basis for establishing the safety of food additives. All of the dietary additives tested were found to inhibit the development of HepG2 cells in a dose-dependent manner. Sunset yellow and sodium sulphite had IC50 values of 1.06 and 0.30 g l^{-1} after 24 h, respectively. According to HCA, sunset yellow and sodium sulphite synergistically affected cell number, membrane permeability, mitochondrial membrane potential, intracellular calcium level, oxidative stress, and high-dose group DNA damage [65].

5.3.2.1 Pure graphene

In a study by Zhang *et al* for the measurement of chloride ions, graphene nanosheets incorporating CPE have been developed. The researchers investigated various voltammetry techniques (cyclic voltammetry, DPV, linear sweep voltammetry, and square-wave voltammetry) and discovered that DPV is the most effective approach for determining chloride ions. Considering several chloride ion sources, the typical peak value for chloride ions was determined to be 0.05 V. Graphene/CPE attained a sensitivity of 0.156 A mM cm^2 in 30 s. The degree of linearity and threshold for detecting this sensor are 0.5–1000 and 0.2 mM, respectively. This technological innovation worked well as a chloride sensor in ordinary water but not when applied to food samples. This study additionally discovered that the reaction of CPE and graphene-modified CPE is superior to that of bare GCE [66].

5.3.2.2 Composite-based electrodes

Katabami *et al* and Berardi *et al* state that nitrite ions are a popular food additive; however, in large quantities, they have detrimental effects on people. Surplus nitrite ions can interact with the amines to generate unpleasant nitrosamines. Nitrite gauges have been developed utilising graphene derivatives such as distinctive nanomaterials. The electrochemical detection of nitrite is based on its oxidation, which requires two electrons and two proton reactions [67, 68].

Jian *et al*, for nitrite detection, for instance, described eRGO/Au composite-modified SPCE. The nanoparticles of Au act as nitrite electrocatalytic locations, while the eRGO provides a place for the Au nanoparticles to soak up nitrite ions. This nitrite sensor's sensitivity, linear response, and detection limit are 0.3048 A M^{-1} cm^{-2}, 1–6000 M, and 0.13 M, respectively. Nitrite detection entails the adsorption of nitrite, complex formation, NO_2 creation, and, finally, nitrate formation [69].

In recent years, Yang *et al* developed an amperometric sensor for nitrite measurement using an Au/MoS_2/RGO ternary nanocomposite. The nitrite detection performance of the Au/MoS_2/RGO/GCE sensor depended on the presence of Au nanoparticles. The optimised $Au_{4.5}$/MoS_2/RGO sample has good sensitivity (0.805 A M^{-1} cm^{-2}), linear range (0.2–2600 M), and low detection limit (0.038 M). This sensor could be used to detect nitrites in natural water. Nitrite sensors have been successfully tested in various food samples [70] (table 5.2).

5.4 Conclusions and current challenges

Analytical scientists have devised electrochemical ways for detecting food contaminants using nanotechnology to ensure food safety. Graphene and its derivatives, for illustration, have been extensively researched as electrochemical sensing probes for organic and inorganic food contaminants. Pure graphene, doped graphene, and graphene-based nanocomposites have been developed as electrode components. Graphene-based electrodes were used to determine artificial food colourants, medicines, insecticides, and other chemical substances. Metal ions of mercury, lead, and cadmium have also been precisely selected. Food specimens have also been found to include anions such as nitrite, nitrate, sulphite, and chloride.

Table 5.2. List of research articles published on graphene-based electrochemical drug sensors.

Graphene-based electrode	Drug	Method	Range	Detection limit	Real sample	Reference
Polyaniline/Au/GO/GCE	Azithromycin	DPV	0.3–920.0 nM	0.1 nM	Blood serum	[71]
Ag/polyindole/RGO	Benorilate	DPV	0.06–80 μM	6 nM	Tablets	[72]
Ce-doped WO_3/GO/GCE	Furazolidone	DPV	1–260 μM	0.054 μM	Urine	[73]
Zinc–graphene oxide/ZnO/SPCE	Promethazine	DPV	0.05–177.45 μM	0.3 nM	Human serum, urine, tablet, river water	[74]

The remarkable electrochemical sensing properties of graphene derivatives-based nanomaterials are related to their rapid transfer of electrons ability, various modes of contact, huge electroactive active sites, and stability. The concentration of modifying layers, the unique morphology and nature of the working electrode, the pH of the solution, the electrode surface area, and the structure of the organic pollutant all impact sensing performance. Despite great inspiration for graphene-based electrochemical sensors, obstacles still need to be overcome. The electrodes' operating stability and repeatability are critical concerns. To build a stable sensor, the distinctive morphology of the nanomaterials must be preserved during the redox process. Some graphene-based electrodes could be used in food samples, utilising routine addition procedures.

References

[1] Manjunatha J G 2020 A surfactant enhanced graphene paste electrode as an effective electrochemical sensor for the sensitive and simultaneous determination of catechol and resorcinol *Chem. Data Collect.* **25** 100331

[2] Gleiter H 2000 Nanostructured materials: basic concepts and microstructure *Acta Mater.* **48** 1–29

[3] Pushpanjali P A, Manjunatha J G, Nagarajappa H, D'Souza E S, Charithra M M and Prinith N S 2021 Voltammetric analysis of antihistamine drug cetirizine and paracetamol at poly (L-Leucine) layered carbon nanotube paste electrode *Surf. Interfaces* **24** 101154

[4] Hareesha N, Manjunatha J G, Amrutha B M, Sreeharsha N, Basheeruddin A, Md and Khalid A 2021 A fast and selective electrochemical detection of vanillin in food samples on the surface of poly (glutamic acid) functionalized multiwalled carbon nanotubes and graphite composite paste sensor *Colloids Surf.,* A **626** 127042

[5] Manjunatha J G, Deraman M, Nur Hamizah B and Talib I A 2014 Selective detection of dopamine in the presence of uric acid using polymerized Phthalo blue film modified carbon paste electrode *Adv. Mater. Res.* **895** 447–51

[6] Hareesha N and Manjunatha J G 2021 Electro-oxidation of formoterol fumarate on the surface of novel poly (thiazole yellow-G) layered multi-walled carbon nanotube paste electrode *Sci. Rep.* **11** 12797
[7] Chethan B, RajPrakash H G, Ravikiran Y T, Vijayakumari S C and Thomas S 2019 Polypyyrole based core-shell structured composite based humidity sensor operable at room temperature *Sens. Actuators* B **296** 126639
[8] Tigari G and Manjunatha J G 2019 Electrochemical preparation of poly(arginine)-modified carbon nanotube paste electrode and its application for the determination of pyridoxine in the presence of riboflavin: an electroanalytical approach *J. Anal. Test.* **3** 331
[9] Hareesha N, Manjunatha J G, Pushpanjali P A, Prinith Subbaiah N, Charithra M M, Sreeharsha N, Basheeruddin Asdaq S M and Md Khalid A 2022 Electrochemical sensing of antibiotic drug amoxicillin in the presence of dopamine at simple and selective carbon paste electrode activated with cetyltrimethylammonium bromide surfactant *Monatsh. Chem.* **153** 31–8
[10] Pal S L, Jana U, Manna P K, Mohanta G P and Manavalan R 2011 Nanoparticle: an overview of preparation and characterization *J. Appl. Pharm. Sci.* **06** 228–34
[11] Amrutha B M, Manjunatha J G, Aarti S B and Nagarajappa H 2021 Sensitive and selective electrochemical detection of vanillin at graphene-based poly (methyl orange) modified electrode *J. Sci.: Adv. Mater. Devices* **6** 415–24
[12] Li Z, Zhou J, Dong T, Xu Y and Shang Y 2021 Application of electrochemical methods for detecting abiotic stress biomarkers in plants *Biosens. Bioelectron.* **182** 113105
[13] Rather I A, Koh W Y, Paek W K and Lim J 2017 The sources of chemical contaminants in food and their health implications *Front. Pharmacol.* **8** 830
[14] González N, Marquès M, Nadal M and Domingo J L 2019 Occurrence of environmental pollutants in foodstuffs: a review of organic vs. conventional food *Food Chem. Toxicol.* **125** 370–5
[15] Volschenk C M, Gerber R, Mkhonto M T, Ikenaka Y, Yohannes Y B, Nakayama S, Ishizuka M, Van Vuren J H J, Wepener V and Smit N J 2019 Bioaccumulation of persistent organic pollutants and their trophic transfer through the food web: human health risks to the rural communities reliant on fish from South Africa's largest floodplain *Sci. Total Environ.* **685** 1116–26
[16] Wang Z, Li Y, Kong F, Li M, Xi M and Yu Z 2021 How do trophic magnification factors (TMFs) and biomagnification factors (BMFs) perform on toxic pollutant bioaccumulation estimation in coastal and marine food webs *Reg. Stud. Mar. Sci.* **44** 101797
[17] WHO 2020*Fact sheet on food safety* https://who.int/en/news-room/fact-sheets/detail/food-safety
[18] Poma G, Fujii Y, Lievens S, Bombeke J, Gao B, Jeong Y, McGrath T J and Covaci A 2021 Occurrence, patterns, and sources of hazardous organic chemicals in edible insects and insect-based food from the Japanese market *Food Chem. Toxicol.* **154** 112311
[19] Medina D A V, Borsatto J V B, Maciel E V S and Lanças F M 2021 Current role of modern chromatography and mass spectrometry in the analysis of mycotoxins in food *TrAC Trends Anal. Chem.* **135** 116156
[20] Wang K, Li Z, Li J and Lin H 2021 Raman spectroscopic techniques for nondestructive analysis of agri-foods: a state-of-the-art review *Trends Food Sci. Technol.* **118** 490–504

[21] Zhang K, Gan N, Shen Z, Cao J, Hu F and Li T 2019 Microchip electrophoresis based aptasensor for multiplexed detection of antibiotics in foods via a stir-bar assisted multi-arm junctions recycling for signal amplification *Biosens. Bioelectron.* **130** 139–46
[22] Villamil C, Calderon M N, Arias M M and Leguizamon J E 2020 Validation of droplet digital polymerase chain reaction for *Salmonella* spp. quantification *Front. Microbiol.* **11** 1512
[23] Joshi P, Riley P, Goud K Y, Mishra R K and Narayan R 2022 Recent advances of boron-doped diamond electrochemical sensors toward environmental applications *Curr. Opin. Electrochem.* **32** 100920
[24] Park J, Kim J W, Kim H and Yoon W 2021 An electrochemical hydrogen peroxide sensor for applications in nuclear industry *Nucl. Eng. Technol.* **53** 142–7
[25] Amali R K A, Lim H N, Ibrahim I, Huang N M, Zainal Z and Ahmad S A A 2021 Significance of nanomaterials in electrochemical sensors for nitrate detection: a review *Trends Environ. Anal. Chem.* **31** e00135
[26] Karimi-Maleh H, Tahernejad-Javazmi F, Daryanavard M, Hadadzadeh H, Ensafi A A and Abbasghorbani M 2014 Electrocatalytic and simultaneous determination of ascorbic acid, nicotinamide adenine dinucleotide and folic acid at ruthenium(II) complex-ZnO/CNTs nanocomposite modified carbon paste electrode *Electroanalysis* **26** 962–70
[27] Wu L, Fu X, Liu H, Li J and Song Y 2014 Comparative study of graphene nanosheet- and multiwall carbon nanotube-based electrochemical sensor for the sensitive detection of cadmium *Anal. Chim. Acta* **851** 43–8
[28] Baig N, Waheed A, Sajid M, Khan I, Kawde A N and Sohail M 2021 Porous graphene-based electrodes: advances in electrochemical sensing of environmental contaminants *Trends Environ. Anal. Chem.* **30** e00120
[29] Monnappa A B, Manjunatha J G G, Bhatt A S and Nagarajappa H 2021 Sensitive and selective electrochemical detection of vanillin at graphene based poly (methyl orange) modified electrode *J. Sci.: Adv. Mater. Devices* **6** 415–24
[30] Dey S and Nagababu B H 2022 Applications of food colour and bio-preservatives in the food and its effect on the human health *Food Chem. Adv.* **1** 100019
[31] Spence C 2019 On the changing colour of food & drink *Int. J. Gastron. Food Sci.* **17** 100161
[32] Jampasa S, Siangproh W, Duangmal K and Chailapakul O 2016 Electrochemically reduced graphene oxide-modified screen-printed carbon electrodes for a simple and highly sensitive electrochemical detection of synthetic colourants in beverages *Talanta* **160** 113–24
[33] Kartika A E, Setiyanto H, Manurung R V, Jenie S N A and Saraswaty V 2021 Silver nanoparticles coupled with graphene nanoplatelets modified screen-printed carbon electrodes for rhodamine B detection in food products *ACS Omega* **6** 31477–84
[34] Meng F, Qin Y, Zhang W, Chen F, Zheng L, Xing J, Aihaiti A and Zhang M 2022 Amplified electrochemical sensor employing Ag NPs functionalized graphene paper electrode for high sensitive analysis of Sudan I *Food Chem.* **371** 131204
[35] Yun M, Choe J E, You J M, Ahmed M S, Lee K, Üstündag Z and Jeon S 2015 High catalytic activity of electrochemically reduced graphene composite toward electrochemical sensing of Orange II *Food Chem.* **169** 114–9
[36] Lv G, Shi B, Huang H, Chen H, Feng H, Zhou P P, Ye W, Zhang Z and Yang Z 2021 Ternary NiO/Ag/reduced graphene oxide nanocomposites as, a sensitive electrochemical sensor for nanomolarity detection of sunset yellow in soft drinks *J. Food Compos. Anal.* **104** 104136

[37] Fu L, Zheng Y, Wang A, Cai W and Lin H 2015 Sensitive determination of Quinoline yellow using poly(diallyldimethylammonium chloride) functionalized reduced graphene oxide modified grassy carbon electrode *Food Chem.* **181** 127–32
[38] Yu L, Shi M, Yue X and Qu L 2016 Detection of Allura red based on the composite of poly (diallyldimethylammonium chloride) functionalized graphene and nickel nanoparticles modified electrode *Sens. Actuators B Chem.* **225** 398–404
[39] Ajiboye T O, Oladoye P O, Olanrewaju C A and Akinsola G O 2022 Organophosphorus pesticides: impacts, detection and removal strategies *Environ. Nanotechnol. Monit. Manag.* **17** 100655
[40] Dhananjayan V and Ravichandran B 2018 Occupational health risk of farmers exposed to pesticides in agricultural activities *Curr. Opin. Environ. Sci. Health* **4** 31–7
[41] Tasaltın N, Karakus S, Tasaltın C and Baytemir G 2022 Highly sensitive and selective rGO based non-enzymatic electrochemical sensor for propamocarb fungicide pesticide detection *Food Chem.* **372** 131267
[42] Mousavi H and Moradian R 2011 Nitrogen and boron doping effects on the electrical conductivity of graphene and nanotube *Solid State Sci.* **13** 1459–64
[43] Hong S *et al* 2021 Carbon nanotube fibers with high specific electrical conductivity: synergistic effect of heteroatom doping and densification *Carbon* **184** 207–13
[44] Chen Z, Zhang Y, Yang Y, Shi X, Zhang L and Jia G 2021 Hierarchical nitrogen-doped holey graphene as sensitive electrochemical sensor for methyl parathion detection *Sens. Actuator. B Chem.* **336** 129721
[45] Nehru R, Hsu Y F and Wang S F *et al* 2021 Graphene oxide@Ce-doped TiO2 nanoparticles as electrocatalyst materials for voltammetric detection of hazardous methyl parathion *Microchim. Acta* **188** 216
[46] Wang L, Li X, Yang R, Li J and Qu L B 2020 A highly sensitive and selective electrochemical sensor for pentachlorophenol based *Food Anal. Methods* **13** 2050–8
[47] Ijaz M U, Batool M, Ashraf A, Al-Ghanim K A, Shahzadi S, Samad A, Al-Misned F, Mruthinti S S and Mahboob S 2022 A study on the curative effect of nobiletin on paraquat induced toxicity in rat *J. King Saud Univ. Sci.* **34** 101673
[48] Sant'Anna M V S, de Oliveira S. Silva J, Gevaerd A, Lima L S, Monteiro M D S, Carregosa I S C, Wisniewski A, Marcolino-Junior L H, Bergamini M F and Sussuchi E M 2022 Selective carbonaceous-based (nano)composite sensors for electrochemical determination of paraquat in food samples *Food Chem.* **373** 131521
[49] Kan Y, Nagai J and Uesawa Y 2021 Evaluation of antibiotic-induced taste and smell disorders using the FDA adverse event reporting system database *Sci. Rep.* **11** 9625
[50] Liu D, Xu Y Y, Junaid M, Zhu Y G and Wang J 2022 Distribution, transfer, ecological and human health risks of antibiotics in bay ecosystems *Environ. Int.* **158** 106949
[51] Pan M, Guo P, Liu H, Lu J and Xie Q 2021 Graphene oxide modified screen-printed electrode for highly sensitive and selective electrochemical detection of ciprofloxacin residues in milk *J. Anal. Sci. Technol.* **12** 55
[52] de Faria L V, Lisboa T P, Alves G F, Matos M A C, Muñoz R A A and Matos R C 2021 Adsorptive stripping voltammetric determination of chloramphenicol residues in milk samples using reduced graphene oxide sensor *Anal. Methods* **13** 5711
[53] Willson C 2018 The clinical toxicology of caffeine: a review and case study *Toxicol. Rep.* **5** 1140–52

[54] Shehata M, Azab S M and Fekry A M 2019 May glutathione and graphene oxide enhance the electrochemical detection of caffeine on carbon paste sensor in aqueous and surfactant media for beverages analysis *Synth. Met.* **256** 116122
[55] Jose J, Subramanian V, Shaji S and Sreeja P B 2021 An electrochemical sensor for nanomolar detection of caffeine based on nicotinic acid hydrazide anchored on graphene oxide (NAHGO) *Sci. Rep.* **11** 11662
[56] Tian C, Chen D, Lu N, Li Y, Cui R, Han Z and Zhang G 2018 Electrochemical bisphenol A sensor based on nanoporous PtFe alloy and graphene modified glassy carbon electrode *J. Electroanal. Chem.* 830–1 27–33
[57] Wang K P, Hu J M and Zhang X 2022 Sensitive electrochemical detection of endocrine disruptor bisphenol A (BPA) in milk based on iodine-doped graphene *Microchem. J.* **173** 107047
[58] Kharazi A, Leili M, Khazaei M, Alikhani M Y and Shokoohi R 2021 Human health risk assessment of heavy metals in agricultural soil and food crops in Hamadan, Iran *J. Food Compos. Anal.* **100** 103890
[59] Liendo F, de la Vega A P, Aguirre M J, Godoy F, Martí A A, Flores E, Pizarro J and Segura R 2022 A simple graphene modified electrode for the determination of antimony (III) in edible plants and beverage *Food Chem.* **367** 130676
[60] Ma S, Zhang Q, Zhu J, Shi H, Zhang K and Shen Y 2021 Rational engineering of Ag-doped reduced graphene oxide as electrochemical sensor for trace mercury ions monitoring *Sens. Actuators B Chem.* **345** 130383
[61] Wang J, Yu P, Kan K, Lv H, Liu Z, Sun B, Bai X, Chen J, Zhang Y and Shi K 2021 Efficient ultra-trace electrochemical detection of Cd^{2+}, Pb^{2+} and Hg^{2+} based on hierarchical porous S-doped C_3N_4 tube bundles/graphene nanosheets composite *Chem. Eng. J.* **420** 130317
[62] Jeong S E, Kim S, Han J H and Pak J J 2022 Simple laser-induced graphene fibre electrode fabrication for high-performance heavy-metal sensing *Microchem. J.* **172** 106950
[63] Guo C, Wang C, Sun H, Dai D and Gao H 2021 A simple electrochemical sensor based on rGO/MoS_2/CS modified GCE for highly sensitive detection of Pb(II) in tobacco leaves *RSC Adv.* **11** 29590–7
[64] Xu J, Wang M, Liu Q, Lin X, Pu K and He Z 2022 Gut microbiota mediated the toxicity of high concentration of dietary nitrite in C57BL/6 mice *Ecotoxicol. Environ. Saf.* **231** 113224
[65] Qu D, Gu Y, Feng L and Han J 2017 High Content Analysis technology for evaluating the joint toxicity of sunset yellow and sodium sulfite *in vitro Food Chem.* **233** 135–43
[66] Zhang M, Wang C, Zhang Z, Ye J and Fang P 2019 A novel carbon paste electrode for sensitive, selective and rapid electrochemical determination of chloride ion based on three-dimensional graphene *Sens. Actuators B Chem.* **299** 126951
[67] Katabami K, Hayakawa M and Gando S 2016 Severe methemoglobinemia due to sodium nitrite poisoning *Case Rep. Emerg. Med.* **2016** 9013816
[68] Berardi G, Albenzio M, Marino R, D'Amore T, Taranto A D, Vita V and Iammarino M 2021 Different use of nitrite and nitrate in meats: a survey on typical and commercial Italian products as a contribution to risk assessment *LWT – Food Sci. Technol. (Lebensm. Wiss. Technol.)* **150** 112004
[69] Jian J M, Fu L, Ji J, Lin L, Guo X and Ren T L 2018 Electrochemically reduced graphene oxide/gold nanoparticles composite modified screen-printed carbon electrode for effective electrocatalytic analysis of nitrite in foods *Sens. Actuators B Chem.* **262** 125–36

[70] Yang Y, Lei Q, Li J, Hong C, Zhao Z, Xu H and Hu J 2022 Synthesis and enhanced electrochemical properties of AuNPs@MoS_2/rGO hybrid structures for highly sensitive nitrite detection *Microchem. J.* **172** 106904

[71] Jafari S, Dehghani M, Nasirizadeh N and Azimzadeh M 2018 An azithromycin electrochemical sensor based on an aniline MIP film electropolymerized on a gold nano urchins/graphene oxide modified glassy carbon electrode *J. Electroanal. Chem.* **829** 27–34

[72] Li R F, Zhang S F, Kong F Y, Wang Z X, Fang H L and Wang W 2021 Highly sensitive determination of benorilate using silver nanoparticles/polyindole/reduced graphene oxide nanocomposite modified electrode *J. Electroanal. Chem.* **903** 115771

[73] Ramadhass K D, Ganesan M, Chen T W, Chen S M, Hao Q, Lei W and Gopalakrishnan G 2021 Porous-coral-like cerium doped tungsten oxide/graphene oxide micro balls: a robust electrochemical sensing platform for the detection of antibiotic residue *Colloids Surf. A Physicochem. Eng. Aspects* **628** 127275

[74] Sebastian N, Yu W C, Hu Y C, Balram D and Yu Y H 2021 Morphological evolution of, nanosheets-stacked spherical ZnO for GO-Zn/ZnO ternary nanocomposite preparation a novel electrochemical platform for nanomolar detection of antihistamine promethazine hydrochloride *J. Alloys Compd.* **890** 161768

QUERY FORM

BOOK TITLE: Graphene-Based Sensors

AUTHOR: Jamballi G Manjunatha

CHAPTER TITLE: Graphene-modified electrochemical sensors for estimation of food contaminants

Page 5

Q1
Please check value '3.52 AL mol 1' for correctness.

Page 9

Q2
Please check the value '0.156 A mM cm²' for correctness.

Page 9

Q3
Table 5.2 was not cited in the text. Please confirm that the citation added is in the appropriate place or amend as necessary.